STUDIES ON THE HOMOGENEOUS NUCLEATION OF CRYSTALLINE SOLIDS FROM LYOTROPIC LIQUID CRYSTALLINE SOLUTIONS

To

MY PARENTS

with thanks for "taking the chance"

and to

IRENE

STUDIES ON THE HOMOGENEOUS NUCLEATION OF CRYSTALLINE SOLIDS FROM LYOTROPIC LIQUID CRYSTALLINE SOLUTIONS

By

RAYMOND JAMES PRIME, B. Sc.

A Thesis

Submitted to the Faculty of Graduate Studies

in Partial Fulfilment of the Requirements

for the Degree

Doctor of Philosophy

McMASTER UNIVERSITY

December 1972

© Raymond James Prime 1973

DOCTOR OF PHILOSOPHY (1972)
(Chemistry)

McMASTER UNIVERSITY
Hamilton, Ontario

TITLE: Studies on the Homogeneous Nucleation of Crystalline Solids From Lyotropic Liquid Crystalline Solutions

AUTHOR: Raymond James Prime, B. Sc. (McMaster University, Hamilton)

SUPERVISOR: Dr. O. E. Hileman, Jr.

NUMBER OF PAGES: xi, 137

SCOPE AND CONTENTS:

The results of a study on the homogeneous nucleation of liquid crystalline solutions are reported.

We report the synthesis and some properties of four new esters of sulfoacetic acid and note the observation of the liquid crystalline properties of their aqueous solutions. The existence of these mesophases is interpreted in terms of the micelle structures offerred elsewhere for the similar case of sulfonic acid soap solutions. Also the metastability of some mesophase transitions is reported.

Some significant nucleation parameters are derived from the application of classical nucleation theory to the liquid crystal-solid phase transition. Discrepencies between these values and the literature results for other compounds are interpreted in terms of the extensive pre-nucleation ordering in the liquid phase.

ACKNOWLEDGEMENTS

The author sincerely thanks Dr. O. E. Hileman, Jr. for his help and his friendship both during the course of this work and especially during the two years before, which made it possible.

Also, he wishes to thank Dr. Bell and Dr. Hoffman for their advice and, the latter, for providing the derivation given in Appendix 2.

The other members of our research group are acknowledged for their part in relieving the moments of frustration and for the lasting friendships that have resulted from our association.

Financial assistance provided by the Province of Ontario and McMaster University is also acknowledged.

TABLE OF CONTENTS

LIST OF TABLES

LIST OF FIGURES

SYMBOLS AND NOTATION

a	activity of a solute
c	concentration of a solute
c_o	equilibrium solubility of a solute
k	Boltzmann constant = 1.38×10^{-16} ergs/deg
m	number of available monomers
m_s	mole· of solute
n	number of molecules involved in a phase transformation†
r	radius of the spherical aggregate †
t	time
v	the molecular volume; or, the volume of a droplet
A	the pre-exponential factor in the nucleation rate equation
A	surface area of the spherical aggregate†
D	droplet diameter after time, t
D_o	initial droplet diameter
G	the "neat phase" of aliphatic soap solutions
ΔG	change in Gibbs free energy†
ΔG_a	free energy of activation for diffusion
J	rate of nucleation
N	concentration of molecules available for reaction
M_1	the "middle phase" of aliphatic soap solutions
M_2	the "inverse middle phase" of aliphatic soap solutions
P	probability of finding a crystallized droplet at any time, or the fraction of droplets crystallized
PFHS	precipitation from homogeneous solution
S	supersaturation, the ratio of the actual concentration to the equilibrium molar solubility†

---

† an asterisk (*) associated with this symbol denotes a critical parameter.

T	absolute temperature
V	volume of an aggregate
V_1	the "viscous isotropic" phase of aliphatic soap solutions
V_2	the "inverse viscous isotropic" phase of aliphatic soap solutions
Z	Zeldovich factor
β	frequency of capture of a monomer
μ	chemical potential
σ	excess surface free energy

INTRODUCTION

I.A. HISTORICAL BACKGROUND

It has been recognized since the beginnings of science that matter may exist in three fundamental states of aggregation: solid, isotropic liquid and gas. Transitions between these states have long occupied the curiosity of scientists. This work is a result of such curiosity.

Nucleation is the process whereby a new phase is generated from an unstable initial phase. When this process is spontaneous (ie. not effected by external factors) it is termed homogeneous nucleation; otherwise, it is heterogeneous nucleation.

Any circumstance involving a phase change is governed by a nucleation process, thus nucleation is of interest to researchers engaged in many branches of science, engineering and biophysical science. In particular, analytical chemists are concerned with the fundamental role of nucleation in determining the morphology and purity of analytical precipitates. Furthermore, manufacturing chemistry invariably involves the separation of materials through crystallization. Thus any study leading to a better understanding of the crystallization process has considerable value.

I.A.1. CONCEPT OF NUCLEATION

In spite of its very long use as a purification process, there had been very little progress in the understanding of crystallization phenomena until the work of Ostwald near the end of the last century. That it was possible to exceed the normal solubility of a substance in

solution was recognized as early as 1775 by Lowitz (1) and he drew the analogy with Fahrenheit's (2) earlier discovery of the supercooling of water.

By the middle of the 19th. century scientists had discovered that the atmosphere contained sub-microscopic particles many of which could act as foreign crystal growth centres in supersaturated solutions. Control of this type of contamination led to the observation of higher supersaturations† and it became clear that spontaneous nucleation occurred only when a solution was highly supersaturated.

Ostwald (3) realized that before a crystal could grow spontaneously to a stable new phase, its initial fragment must achieve a minimum size. He performed some empirical experiments to estimate this minimum size, but recognized that his estimates represented upper limits. Ostwald classified solutions according to their degree of supersaturation (see Figure 1), these being: a stable solution from which crystallization could never occur, a meta-stable solution of higher concentration which would not crystallize unless induced to do so, and at still higher concentration a labile solution from which homogeneous nucleation was possible after a limited time. It remains one of the objectives of a nucleation study to determine this metastable limit. Von Weimarn (4) showed that a marked decrease in size and increase in number of crystals formed accompanied an increase in the relative supersaturation of the system.

From these early observations it was evident that there were two steps involved in the crystallization process, and that there was a significant energy barrier to the first step, the formation of a nucleus.

---

† For the purpose of this thesis, supersaturation will be used in the sense of the ratio of the actual concentration to the equilibrium molar solubility.

Figure 1. Ostwald's classification of solutions.

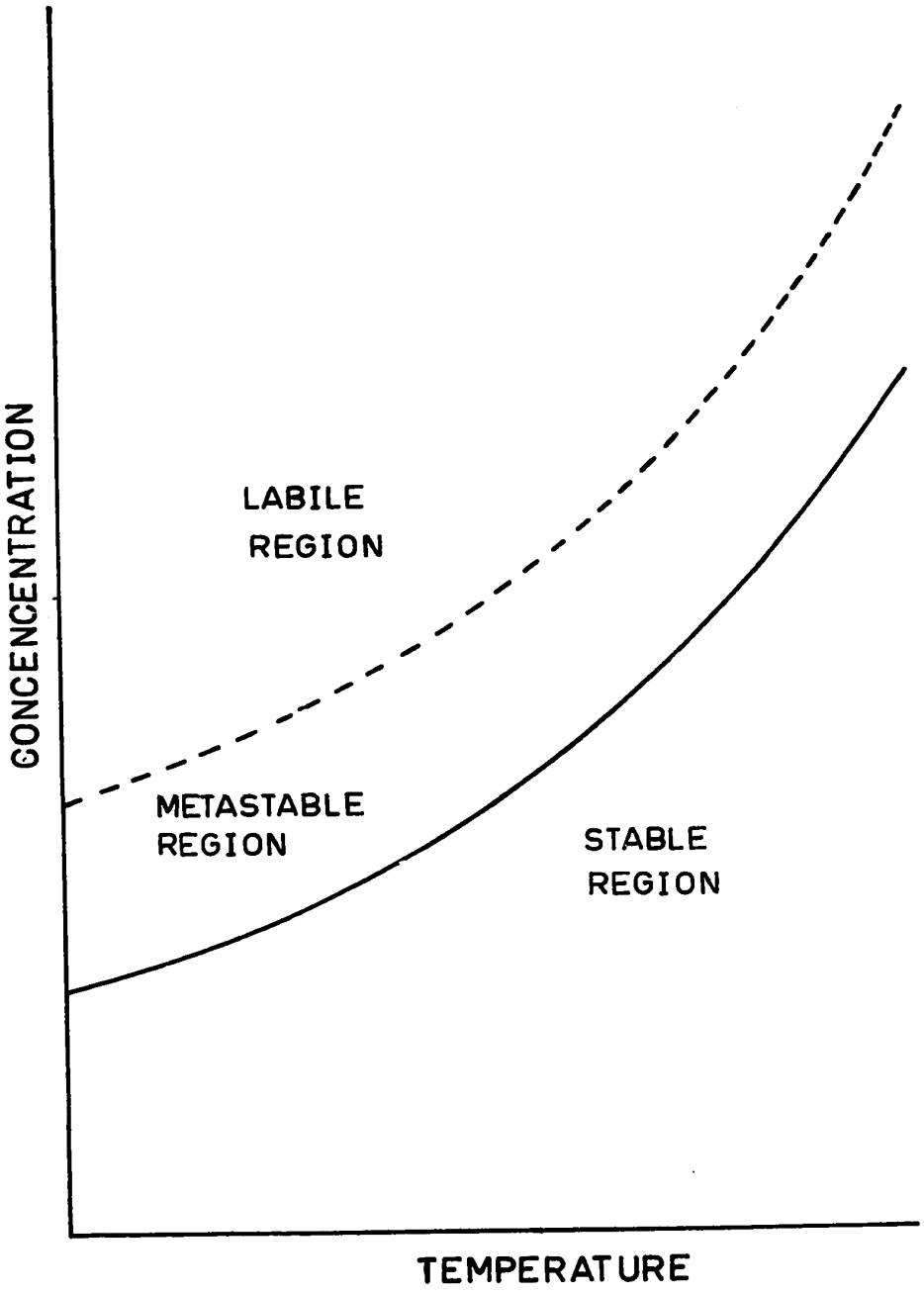
CONCENTRATION
LABILE
REGION
METASTABLE
REGION
STABLE
REGION
TEMPERATURE

This barrier was dependent upon the degree of supersaturation and on the cleanness of the solution. The second step, crystal growth, was assumed to be free of any significant energy barrier compared to the first step. With the recognition of two separate steps to the crystallization process, attention was directed towards the investigation of the nucleation step.

In the middle 1800's, several workers observed that the extent of supercooling was much greater for a decreased sample size. Dufour (5) was one of the first to suspend drops of water in an immiscible liquid; when he cooled these droplets he found that the smaller droplets required more undercooling than the larger ones to cause crystallization. Turnbull (6), proposing that foreign nuclei were sequestered in a small number of individual droplets, adopted this droplet idea as a method of studying the kinetics of nucleation. He applied the droplet technique successfully to the nucleation of supercooled mercury droplets (7). The droplet technique has since gained widespread acceptance as a tool for the study of homogeneous nucleation of solids from melts and from solutions.

The early attempts to apply the droplet technique to solutions followed the pattern established for the study of melts in that hot aqueous solutions were cooled. Among the first to apply this technique to solutions were White and Frost (8) who studied the homogeneous nucleation of potassium nitrate from water. The technique had several difficulties of which the main drawback was the requirement of a high temperature-coefficient of solubility. A more sophisticated technique was that recently employed by Velazquez and Hileman (9) who combined the technique of precipitation from homogeneous solution (PFHS) with the droplet technique to study the nucleation of analytically important metal chelates by the *in situ* generation of the insoluble metal chelate from soluble precursors.

I.A.2. DISCOVERY OF LIQUID CRYSTALLINE BEHAVIOUR

Besides the three fundamental states of matter it is now known that intermediate phases (mesophases) are stable. The first suggestion of their existence came near the end of the last century from the work of Reinitzer (10) and Lehmann (11). Independently they recorded some interesting observations on the properties of a new class of compounds. These compounds, now termed liquid crystals, exhibited optical properties of a crystal while possessing the mechanical properties of a liquid. Numerous examples of this behaviour followed its discovery.

The early rationales due to Tamman, Nernest, and Quincke (12) described these phenomena as stemming from the colloidal effect of small crystals suspended in an isotropic liquid, or from the presence of impurities giving an emulsion of two liquids. Later, when it was found that these mesophases gave a clear field of view in the ultramicroscope and that transitions between the crystal and the mesophase, and between the mesophase and the isotropic liquid were perfectly well-defined and reproducible, they became accepted as a true state of matter, intermediate between the solid and isotropic liquid. Since the early studies on liquid crystals, the use of modern techniques, particularly X-ray diffraction, has shown them to possess extensive ordering in the liquid state and has confirmed their existence as true states of matter.

I.B. CLASSICAL THEORY OF HOMOGENEOUS NUCLEATION FROM SOLUTION

Historically the classical theory of homogeneous nucleation from the melt and from solution has evolved from the earlier theories of vapour condensation (13, 14, 15) which had been successfully verified by experiment. The qualitative concepts of nucleation theory when extended to melts and solutions have gained widespread acceptance, although quantitatively the theory leaves much for discussion (Section I.B.3). There is, however, enough agreement between the theory and the experimental observations, to justify its continued use (in the absence of a viable alternative) by experimentalists.

There are several books (16 - 19), and excellent reviews (20 - 23) dealing with the subject of nucleation. The following is intended to give only a brief outline of classical nucleation theory and to develop a few equations pertinent to this thesis.

I.B.1. THERMODYNAMIC BASIS OF NUCLEATION THEORY

A successful theory of nucleation must account for the experimental observations; namely, the existence of an energy barrier to the nucleation process manifested in the existence of a supersaturation, and the critical dependence of the rate of crystal formation on this supersaturation. To achieve this, classical nucleation theory has developed from an unusual coupling of equilibrium thermodynamics and kinetics.

The crystallization event can be represented by the equation

$$nX \rightarrow X_n$$

in which 'n' molecules of solute X give a bulk crystal X_n. This process of crystallization can be divided further into two stages - nucleation and growth.

Nucleation is believed to occur through the formation of clusters or aggregates by a series of bimolecular collisions between these aggregates and single molecules as illustrated by the sequence:

$$X + X \rightleftarrows X_2$$

$$X_2 + X \rightleftarrows X_3$$

$$X_3 + X \rightleftarrows X_4$$

$$\vdots$$

$$X_{i-1} + X \rightleftarrows X_i \text{ (nucleus)}$$

$$X_i + X \rightleftarrows X_{i+1}$$

$$X_{i+1} + X \rightarrow \text{crystal growth}$$

The contribution to the formation of clusters by other processes such as multi-molecular collision and combination of aggregates themselves is assumed to be negligible. There exists a critical sized aggregate, X_i, designated the critical nucleus which can either decompose to smaller clusters or grow spontaneously into a crystal. Clusters smaller than the critical nucleus are referred to as embryos, while those larger are nuclei. It is generally assumed that once an aggregate has passed the critical size it cannot decompose to embryos.

In the classical concept, nucleation is considered as being controlled by two factors: change in free energy in going from the unstable homogeneous phase to the stable heterogeneous phase, and the energy required to form the interface between the two new phases. The former is the driving force dependent upon the number of molecules(n) being transformed to the new phase and predominates at large values of n, while the latter is the barrier to nucleation and is dependent upon the number of surface mole-

cules and dominates at low values of n. It is the purpose of nucleation theory to determine the critical parameters resulting from a balance of these two factors.

When 'n' molecules of a substance are transformed from one phase where its chemical potential is μ_1, to another phase of chemical potential μ_2, the change in Gibbs free energy for the system is

$$\Delta G = -(\mu_1 - \mu_2)n + \sigma A. \qquad (1)$$

σ is the excess of surface energy/unit area. The term $(\mu_1 - \mu_2)$ represents the change in Gibbs free energy between two phases of infinite volume referred to one molecule and σA represents the free energy of formation of the new interface. Since A is proportional to the number of molecules transformed then

$$\Delta G = - \Delta\mu n + Kn^{2/3}\sigma. \qquad (1a)$$

Figure 2 shows the behaviour of ΔG as the size of the embryo increases. It is clear from the figure that, for solutions which are not supersaturated, ΔG will increase steadily with increasing n, while the plot for supersaturated solutions exhibits a maximum value of ΔG resulting from a balance of the driving force and the impeding force to nucleation. This maximum represents the critical-sized nucleus. Either growth or decomposition of the nucleus results in a decrease in the free energy. This point represents a metastable equilibrium since $\frac{\partial \Delta G}{\partial n} = 0$, but a slight change in either direction causes a shift from equilibrium with no tendency to return.

Differentiation of equation (1a) with respect to n and imposition of the equilibrium conditions gives:

$$\Delta\mu = \frac{2}{3} \quad \frac{\sigma A}{n^*}$$

Figure 2. The dependence of the Gibbs free energy of formation, ΔG on the size of the aggregate.

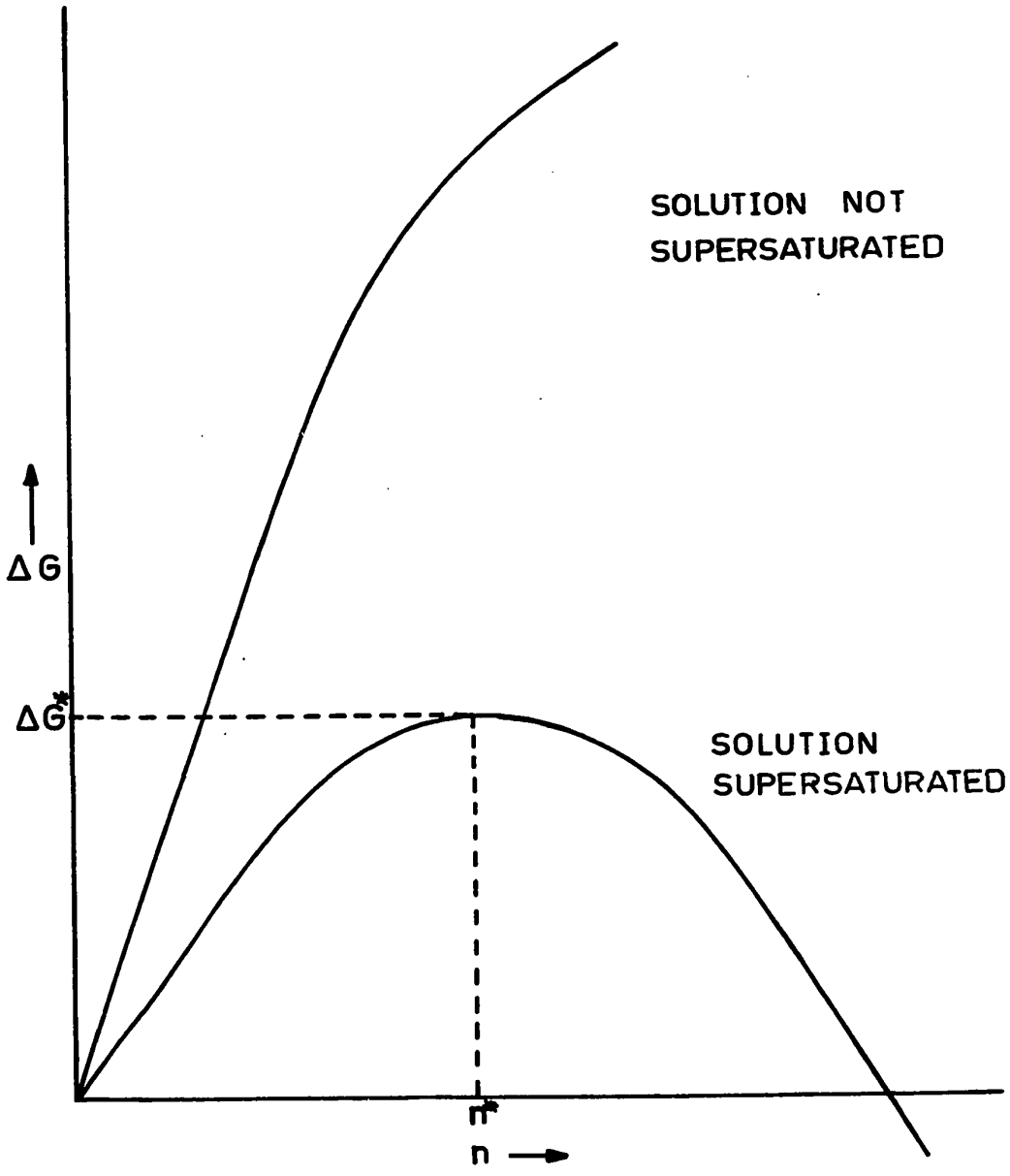
SOLUTION NOT
SUPERSATURATED
ΔG
ΔG*
SOLUTION
SUPERSATURATED
n*
n

Therefore, $\Delta G^* = \frac{1}{3}\sigma A^*$ (2)†

This relationship is what Gibbs called the work of formation of a "fluid of different phase within any homogeneous fluid" and is referred to by La Mer (21) as "the master key to the problem of nucleation". It can be used to determine the important nucleation parameters at the critical point.

Knowing that $\mu = \mu_o + kT\ln a$, where 'a' represents the activity of the solute and is normally approximated by the known value 'c', the concentration, we can write

$$\Delta\mu = kT \ln c - kT \ln c_o$$

$$= kT \ln S. \qquad (3)$$

Where $S = c/c_o$ is the supersaturation. Assuming spherical nuclei of radius 'r' we can write

$$A = \frac{3nv}{r} .$$

'v' is the molecular volume assuming no "dead space" ie. $v = V/n$. Now, using equations (1), (2) and (3) we can define all of the critical values of interest from

$$\Delta G^* = -nkT \ln S^* + \sigma\left[\frac{3n^*v}{r^*}\right] = \frac{1}{3}\sigma\left[\frac{3n^*v}{r^*}\right] .$$

Therefore, $r^* = \frac{2\sigma v}{kT \ln S^*}$. (4)

Then, $n^* = \frac{V}{v} = \frac{32\pi\sigma^3 v^2}{3(kT \ln S^*)^3}$, and (5)

$$\Delta G^* = \frac{1}{3}\sigma A^* = \frac{16\pi\sigma^3 v^2}{3(kT \ln S^*)^2} . \qquad (6)$$

---

† Throughout the text an asterisk denotes a "critical" parameter.

Since the supersaturation is experimentally measurable and the other parameters (except σ) are known, the solution to each of the above equations depends on the evaluation of the interfacial energy.

I.B.2. KINETICS OF NUCLEATION

The process of nucleation has been likened to a chemical reaction and the metastability of a supersaturated phase has been recognized as a problem of kinetics; however, unlike a chemical reaction the activation energy (assumed to be the free energy of formation of a nucleus) for the process of nucleation is not constant but varies sharply with supersaturation. The treatment of the rate of nucleation in solution has evolved by modification of the corresponding treatment for vapour condensation.

It is generally agreed that embryos grow by the addition of monomers to aggregates according to the scheme of Farkas (24) given in Section I.B.1. Thus, by calculating the difference between the rate of growth by monomer impingement on the critical-sized aggregate and the rate of dissolution by loss of a monomer, an expression for the rate of nucleation can be obtained. In order to apply the equilibrium thermodynamic conditions of Section I.B.1., a steady state must be assumed in which clusters above a certain size are considered to be removed and replaced by an equivalent number of monomers. This then allows a steady flux of clusters through the system while the reactions leading to embryo formation can be considered to be in a steady state equilibrium. This flux is taken to be the rate of nucleation.

Before the proposal of the steady state approximation, Volmer and Weber (25) found that the frequency of formation of critical nuclei was proportional to $\exp(-\Delta G^*/kT)$. Application of the steady state approximation and other correction factors from the treatments of Becker and

Doring (26), Zeldovich (27) and others results in the following equation for the classical rate of nucleation for vapour condensation.

$$J = Z\beta m \exp[\frac{-\Delta G^*}{kT}]$$

where Z is the Zeldovich factor (of the order 10^{-2}),

β is the frequency of capture of a monomer,

m is the number of available monomers.

The Zeldovich factor, Z, is a correction term attempting to account for two facts (28):

1. that the number of critical clusters in a steady state system is smaller than the equilibrium number of such clusters,

2. that a cluster of size greater than the critical nucleus can in fact return to smaller than critical size.

A similar expression for condensed phases was derived by Turnbull and Fisher (29) who applied Eyring's theory of absolute reaction rates to the following step of the Farkas model (see Section I.B.1.)

$$X_i + X \rightleftarrows X_{i+1}$$

They obtained an equation for the rate of nucleation of the form

$$J = \frac{NkT}{n} \exp[\frac{-\Delta G_a}{kT}] \exp[\frac{-\Delta G^*}{kT}]$$

where ΔG_a is the free energy of activation for short-range diffusion of the transferring component (usually a constant) and N is the concentration of X units available for reaction. The working form of the rate equation, substituting for ΔG^* from equation (6) then, is given by

$$J = A \exp[\frac{16\pi\sigma^3\mu^2}{3(kT)^3(\ln S)^2}] . \qquad (7a)$$

The pre-exponential factor, A, is a constant and differs slightly from the Turnbull and Fisher value above by the inclusion of the Zeldovich factor. Calculated values of this pre-exponential term have ranged from 10^{17} to

10^{35} but are usually of the order $10^{30\pm3}$.

Qualitatively equation (7) describes the experimental results. The exponential term is a critical function of supersaturation, consequently, at some characteristic value of S for a given system it increases dramatically. The rate of nucleation is very small until this critical value is reached, then it becomes very high. This explosive increase in the nucleation rate explains the sudden collapse of a supersaturated system at the Ostwald metastable limit (Figure 1).

I.B.3. LIMITATIONS OF CLASSICAL NUCLEATION THEORY

There has been a great deal of controversy in the literature concerning the validity of classical nucleation theory. Much of its early success was attributed to fortuitous agreement. The experimentalists who use this simplified theory readily concede that its shortcomings are numerous; however, in spite of them, it continues to serve as a qualitative description of the nucleation process and a quantitative basis for data comparison.

Theoreticians have attempted for many years to develop a statistical mechanical description of nucleation. This approach is showing promise when applied to vapour condensation but the behaviour of condensed systems is presently beyond its scope. The further complications encountered in concentrated solutions will further delay progress in theoretical interpretation. It is only through the development of new instrumental techniques (eg. Raman spectroscopy) that interest has been renewed in the study of the nature of concentrated aqueous solutions (30). Even here the findings show only the degree of hydration and association of single ions, and the study of aggregates of the complexity of a critical nucleus continue to be beyond its scope.

The major difficulty with the classical theory of nucleation arises from the description of the nucleus in terms of macroscopic thermodynamic functions. That is, can one discuss surface tension, a bulk-average concept, when describing a nucleus which at best is only a few hundred molecules in size? Also, in the event of a small nucleus, as those reported for $BaSO_4$ (31), then the differentiation between surface and interior molecules becomes impossible. This appears to be the weakest point of the theory since such small clusters probably cannot be realistically expected to conform to bulk thermodynamics. This observation has prompted Melia (20) to comment that "real progress in extending the theory will not be achieved until macroscopic quantities like the interfacial free energy . . . are replaced by parameters which take due account of the molecular processes involved in nucleus formation."

Accepting the applicability of surface tension then leads to the question of the definition of the surface of a nucleus. It may be expected, especially for melts and solutions of highly soluble substances, that the change from the solution to an actual solid-like embryo would be gradual. Thus the precise definition of a surface of tension comes in doubt. Some reports of low values for the interfacial energy term have been interpreted in terms of the high degree of solvation (32). It is well known that a greater interaction between the solvent and solution results in a lower interfacial evergy (33).

The critical nucleus is usually assigned a spherical shape. This is a matter of convenience based on the fact that a spherical shape will result in a lower energy barrier to the nucleation event. If necessary, correction for shape can be made to give an average interfacial energy for a nucleus of any regular configuration. Unless there is strong evidence

for a particular shape inferred from the geometry of the resulting crystal the nucleus is assumed to be spherical.

The applicability of the assumption of an equilibrium shape was questioned by Binsbergen (34, 35) who performed a computer simulation of the growth of a nucleus. By considering all the possible ways of addition of monomers to a Kossel crystal model, he has shown that an equilibrium shape for the nucleus does not exist. From this he draws the provocative conclusion that "nuclei do not exist". His suggestion that the rate of nucleation does not depend on the thermodynamic stability of a particular configuration, but upon the kinetic probability of reaching certain configurations, may provide a useful basis for an alternative theory of nucleation. The classical theory does not account for differing configurational arrangements.

The present nucleation theory applies only to a stationary nucleus. Additional corrections for rotational and translational motion of a nucleus, factors not considered in the early theories, have recently been attempted (36). It appears that except for the case of vapour condensation the neglect of these terms is not important.

Statistical thermodynamic theories have provided a means of correcting some of the difficulties of the classical theory, however, since they retain essentially the same model of the nucleation process they are subject to some of the same limitations. Also none have been applied rigorously to condensed systems.

Classical nucleation theory does not take proper account of the specific liquid structure and the nature of the crystallizing species. Chemical association, solution viscosity and solvation effects influence the nucleation process. These effects are reflected in the pre-exponen-

tial kinetic factor of the classical rate equation. Often experimental values of the order of 10^3 - 10^6, instead of 10^{30} are reported (see for example Melia and Moffitt (36)). Such low values may also arise from a more fundamental restriction to the theory. It was mentioned in Section I.B.2. that in order to obtain a rate equation the dynamic process of embryo growth resulting in a continuous depletion of monomers was replaced by a steady-state approximation. Corrections for this assumption were included in the kinetic constant and their improper evaluation would lead to discrepencies in this term.

Recently, Daee et al (38) have shown for the case of water condensation that the free energy of formation of clusters was not a smoothly increasing function of the number of molecules. They proposed a clathrate-like structure for the pre-nucleation clusters and found that the concentration of clusters of certain sizes was higher than others. This contradicts the basic thermodynamic principles of classical nucleation theory and thus casts further doubt on certain fundamental assumptions. In their study Daee et al used a molecular model approach with statistical mechanics which did not require the use of bulk thermodynamic properties.

In view of these serious limitations classical nucleation theory must be used with reservation. However, the agreement between its predicted functional relationships and experimental observations is far from discouraging. Nevertheless, because of the serious conflicts involved we must disagree with Binsbergen (35) when he states "we will have a hard time to change the generally accepted concepts of the nucleation theory as it stands today". Classical nucleation theory is indeed in need of revision!

I.C. EXPERIMENTAL METHODS USED FOR THE STUDY OF NUCLEATION

The lack of a proper understanding of the nucleation process had resulted in part from the size of the critical nucleus. Being less than 100 Å in diameter it is impossible to observe a nucleus directly. Thus, the nature of the nucleus must be elucidated from observations made on bulk crystals. This in turn introduces other difficulties arising from crystal growth, dissolution and agglomeration. In addition, because of the explosive increase which occurs in the nucleation rate at a particular supersaturation, it becomes extremely difficult to measure this rate. To compound the problem even further, homogeneous nucleation is not the normal process of initiation of phase change in bulk samples. Usually, the presence of sub-microscopic dust particles (motes) of the order of 10^{-7} cm diameter and defects on container walls serve to lower the energy barrier to crystallization and result in heterogeneous nucleation. Nucleation experiments are thus directed toward the elimination of the effect of these motes and the measurement of the rate of nucleation as a function of supersaturation, by means of some physical characteristic of the macroscopic crystals which result from the nucleation event.

The total number of motes in a solution is considered to be about 10^6 particles ml^{-1}; however, with extreme difficulty, by careful distillation and filtration, this number in some cases (water), can be reduced to the order of a few hundred per ml. Even so, for nucleation experiments the presence of a single effective mote in a supersaturated solution will cause its collapse. There are two separate paths to follow for the elimination of the effect of motes. That used in direct mixing experiments is to increase suddenly the supersaturation to such an extent that it cannot be relieved by growth on heterogeneous centres. This technique has been popularized by Nielson (39). Another method due to Vonnegut (40) is

the droplet technique. In this case a portion of the solution of interest is subdivided into tiny, non-communicating droplets whose number greatly exceeds the number of motes in the system.

The direct mixing technique has several worthwhile advantages; namely, it is isothermal, it utilizes a constant supersaturation at the time of the nucleation burst and the initial supersaturation can be easily varied by changing the starting conditions. A variety of detection methods are available including visual observation, microscopy, conductivity and light-scattering methods. It is, however, limited to the study of sparingly soluble compounds and it does require a great deal of sophistication to overcome the problems of local concentration inhomogeneities during mixing. Also the very high rate of nucleation is difficult to measure. This technique has been used extensively by Nielson (39) who has determined a critical supersaturation of 1000 for $BaSO_4$. This extremly high value has since received wide-spread acceptance. Recently, he has applied this technique to the unusual case of the nucleation of a liquid from solution (41). Hanna and Hileman (42, 43) have used the technique with a particle counter-multichannal analyzer as the detector for the study of some analytically important metal chelates and have found good agreement with the results for the same compounds studied with the droplet technique.†

Many authors have referred to the droplet technique as an "ingeneous" device for the study of homogeneous nucleation. Since its introduction 25 years ago for the study of the solidification of molton metal droplets (see for example Turnbull (44)) it has found much wider applica-

---

† There have been few comparisons of different experimental techniques used for the study of nucleation. It is satisfying to find agreement between the results of two widely different methods.

tion. Presently, the droplet technique is being expanded to include crystal nucleation from solution, while its use in the study of solidification of pure substances (in particular, the freezing of water) is continually receiving refinements in data interpretation.

With solutions containing 10^6 motes ml^{-1} it can be shown that for a population of 100 droplets of diameter 25 microns, only one drop will contain a mote and will be subject to heterogeneous nucleation. This illustrates the great advantage of the droplet technique for the preparation of mote-free solutions. Also, droplet study allows observations to be made on a great number of separate experiments simultaneously, thus giving the results statistical significance. Furthermore, the rate of nucleation can be obtained from the rate of appearance of crystals in the droplets by photographically recording the observations at regular time intervals.

In the initial applications of the droplet technique to solutions, the supersaturation was generated by cooling hot saturated aqueous solutions dispersed in mineral oil (see for example, Melia and Moffitt (45)). This method, however, restricted the selection of compounds to those which had a highly temperature-dependent solubility. Velazquez and Hileman (9) extended its applicability to sparingly soluble substances when they reported the combination of the droplet technique with a PFHS method for the generation of metal chelates. Velazquez and Hileman (46) also described a complimentary technique to that of PFHS for the isothermal build-up of supersaturation in solutions of soluble compounds. This new technique takes advantage of the selective extraction of the solvent into the supporting medium to achieve supersaturation. They illustrated the new technique for salts such as $K_2Cr_2O_7$ and NH_4NO_3. Very recently, Bempah and Hileman (47) have employed this droplet contraction method in the study of

a family cyanoplatinates.

The technique of droplet contraction has a very wide application and for this reason was selected for the purposes of this thesis. Its advantages and limitations will be discussed further in Section III.B.

I.D. INTERPRETATION OF THE EXPERIMENTAL DATA

In the droplet contraction technique the supersaturation within the droplet is continuously built-up as the solvent diffuses into the surrounding medium. The calculation of this supersaturation can be carried out exactly only if the density of the solution is known. Since this cannot be measured, it was assumed that the solution behaved ideally.

A relationship between droplet diameter D, and time can be shown (see Appendix 2) to be

$$D^2 = D_o^2 - k_2 t \ . \qquad (8)$$

where D_o is the initial droplet diameter and k_2 is a constant. This equation results from the assumption of physical transfer of one component from a spherical droplet of an ideal solution with the following restrictions:

1. The concentration of the transferring component (water) in the bulk phase remains constant (ie. small amounts of transferring component involved).
2. The concentration at the droplet-bulk interface corresponds to equilibrium conditions.
3. The solute concentration is uniform within the droplet.
4. The equilibrium concentration for the transferring component is independent of the concentration of non-transferring component in the droplet (this will be true for small concentration changes).

These assumptions are reasonable for the experimental conditions except that a small local increase in the concentration of water in the oil medium is to be expected.

If equation (8) is found to hold experimentally then this model satisfactorily predicts the concentration of the solute within each droplet as a function of time. The result at any time, t is

$$C_s = C_{s_o} + \frac{6m_s}{\pi}\left[\frac{1}{(D_o^2 - k_2 t)^{3/2}} - \frac{1}{D_o^3}\right] . \qquad (9)$$

Here, C_s, C_{s_o} are solute concentrations, m_s is the number of moles of solute. Equation (9) predicts that the concentration of solute in droplets of different initial diameter will not be equal after a time interval has elapsed. This problem will be discussed further in Section III.B.

It is shown in Appendix 2 that the degree of supersaturation from equation (9) reduces to

$$S = \frac{C_s}{C_{s_o}} = \left[\frac{D_o}{D}\right]^3 . \qquad (10)$$

That is, the supersaturation can be written simply as the ratio of the initial to the final volume.

The rate of nucleation is obtainable from the results of a droplet experiment by use of the following expression due to Turnbull (44):

$$J = \frac{1}{v}\frac{1}{(1-P)}\left(\frac{dP}{dt}\right), \text{ where} \qquad (11)$$

P is the fraction of droplets solidified after a time, t. The same expression was obtained from the statistical studies by Bigg (48) and Carte (49).

Having expressions for the calculation of the rate of nucleation and the degree of supersaturation from the experimental data, the nucleation rate equation (7a) can be solved. Taking the logarithm of equation (7a) we have

$$\log J = \log A - \frac{16\pi\sigma^3 v^2}{3(2.303kT)^3(\log S)^2} . \qquad (7b)$$

Thus from the slope of the plot of (log J) vs $(\log S)^{-2}$ we can calculate the only unknown parameter, σ. With this we can then solve equations (4, 5, and 6).

I.E. LIQUID CRYSTALS

I.E.1. CLASSIFICATION OF LIQUID CRYSTALS

When certain solid organic compounds are heated, they do not pass directly to the isotropic liquid state. Although they melt quite sharply, the melt will remain definitely opaque in an intermediate state which is both birefringent and fluid. At higher temperatures this mesophase transforms to the isotropic liquid.. Compounds displaying this temperature dependent phenomenon are termed thermotropic liquid crystals.

Solutions of some compounds often display a liquid crystalline character. In particular, our interests are in those molecules which are water soluble, and amphiphilic, ie. those containing a hydrophilic polar group while the rest of the molecule is hydrophobic. These systems are termed lyotropic liquid crystals.

There are three clearly distinguishable types of liquid crystal phase:

1. The smectic mesophase which is turbid and somewhat viscous. This phase has a stratified structure with the long axis of the molecules normal to the layers.

2. The nematic mesophase which is turbid and mobile with the molecules arranged parallel but unstratified.

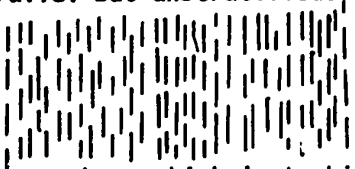

3. The cholesteric mesophase which is turbid and mobile but displays some unique optical properties resulting from optical activity due

to its twisted nematic structure.

A substance may exhibit more than one of these mesophases, the smectic always occurring at the lower temperature, since it has the higher degree of order and is thus more allied to the crystalline state.

I.E.2. MOLECULAR STRUCTURE AND NATURE OF INTERMOLECULAR FORCES

The reason for the existence of the mesomorphic state is suggested by the molecular structures of the compounds which assume it. They have molecules which are very much elongated, and often flattened as well, and they possess at least one polar group. The shape of the molecules causes them to adopt an arrangement in which they are parallel to one another. In the crystalline state they are arranged in the same way and are held together by local attachments due to the electrostatic attractions of the polar groups and van der Waal's forces.

Almost any organic compound with elongated molecules will give rise to a liquid crystalline state (50). Usually substitution in the para-position favours mesomorphism while ortho- and meta- substituents (which could "broaden" the molecule) can cause a loss of this characteristic.

The intermolecular forces operative in these systems are of two types: electrostatic and electrokinetic (51). The electrostatic interactions pertain to the hydrophilic groups and arise from charged ions or dipoles. These attractive interactions tend to be destroyed by the thermal motion of the molecules and will decrease at higher temperatures.

The electrokinetic interactions arise through the motion of electrons within the molecules. When in phase they produce attractive forces between molecules. This type of interaction is almost wholly responsible for the interactions resulting in lipophilic character.

Thus, thermotropic liquid crystals result from the breaking of the

weaker linkages in the crystalline solid, leaving the molecules some freedom of relative movement before they have acquired sufficient thermal energy to overcome the tendency to lie parallel to one another and achieve the random arrangement of an isotropic liquid. Thus, the medium acquires the ability to flow but remains birefringent owing to the preferred orientation of the molecules.

In lyotropic systems the cohesion between molecules is diminished both by thermal agitation (lyotropic systems are also thermotropic), and by dissolution in the solvent (usually water) of the hydrophilic region of the molecule. Amphiphiles which best display liquid crystalline properties are those in which the opposing tendencies are strong and equally balanced. Typical polar groups include the salts of carboxylic and sulfonic acids and the lipophilic group is generally a long chain hydrocarbon (> 8).

I.E.3. SOLUTIONS OF AMPHIPHILES

Much of the early work in the field of lyotropic liquid crystals was done by researchers in the soap industry. The "neat phase", the end-product of the soap boiling operation has been known since late in the 19th century (52) and the "middle phase", occurring with higher water content, has been recognized for almost 50 years (53). Now other phases are known to be stable: the "inverse middle phase" at a lower water content than the neat phase, and two isotropic phases which are stable at concentrations intermediate between each of the above phases.

These mesophases will be referred to by the following commonly used designation:

G - neat phase

V_1 - viscous isotropic phase

M_1 - middle phase

V_2 - inverse viscous isotropic

M_2 - inverse middle

S - isotropic solution

If all these mesophases were to occur at a given temperature then the order of appearance with increasing amphiphile concentration would be (54)

$$S \rightarrow M_1 \rightarrow V_1 \rightarrow G \rightarrow V_2 \rightarrow M_2 \cdot$$

The complete series has not been observed for any one system. Generally M_1, V_1, G or G, V_2, M_2 in the above sequence are observed for a single system.

I.E.4. STRUCTURE OF LIQUID CRYSTALLINE SOLUTIONS.

In an ideal solution of non-polar liquids all molecules interact with each other equally and symmetrically and under the influence of thermal motion a random arrangement of molecules arises. However, in a real solution containing polar molecules a random arrangement no longer occurs and local groupings of molecules arise. In aqueous solutions of amphiphiles there is a tendency for such groupings, called micelles, to arise in which like is associated with like. Thus for soaps, the non-polar paraffin chains tend to associate in a fluid arrangement leaving the polar groups in association with the water molecules. For dilute solutions this results in an isotropic spherical micelle (55) as illustrated in Figure 3a. These micelles are statistical in character and will fluctuate in size and shape under the influence of thermal motion and will be in equilibrium with neighboring molecules.

In liquid crystals, however, micellar groupings show marked persistence and long-range intermicellar order. This grouping of amphiphiles results in various mesophases as the amphiphile to water ratio is changed.

Figure 3. Schematic representation of various micelle structures. (reproduced from Hartshorne and Stuart (52) with the permission of Edward Arnold, London.)

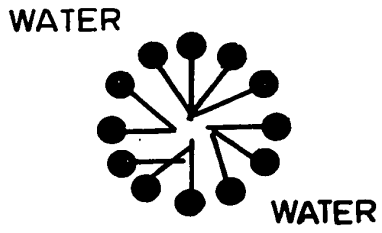

(a) Spherical micelle (diametral section)

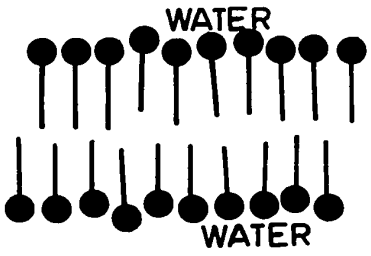

(b) Smectic layer in neat phase (G)

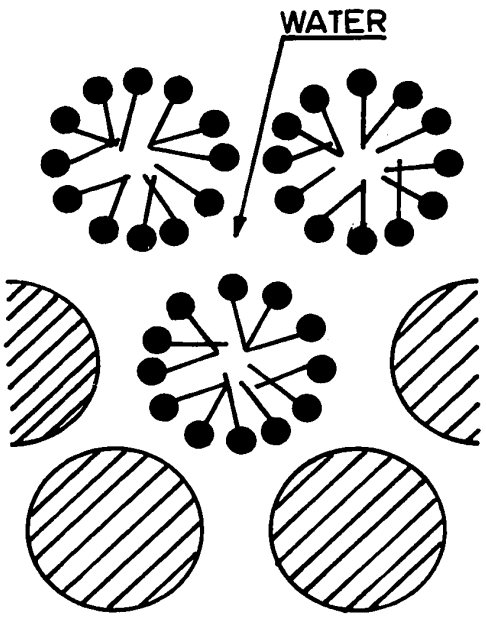

(c) Middle phase (M_1) showing cross section of micellar rods (according to Luzatti)

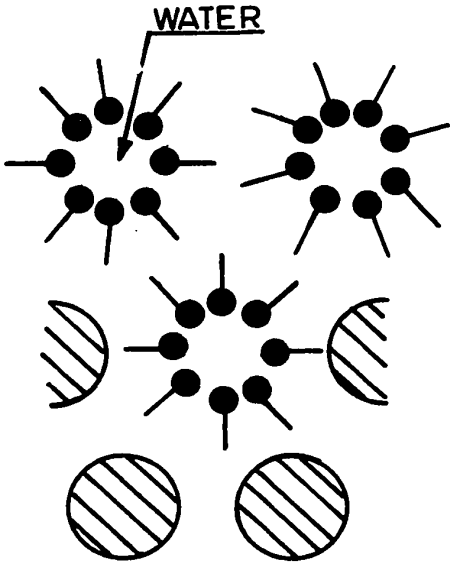

(d) Inverse middle phase (M_2) showing cross section of micellar rods (according to Luzatti)

It is believed that in these phases the structure is determined primarily by the polar groups while the lipophilic parts of the molecules remain in liquid-like association. This has been proven by Clunie et al (56) and others. In spite of the persistence of long range order Winsor (51) points out that any local change in conditions (temperature, concentration, shearing) will immediately alter the micelle structure.

The observation that the addition of more solvent to lyotropic mesophases transformed them into isotropic micellar solutions possessing no structural order led Ostwald (57) to suggest common constitutive units for the micellar and lyotropic mesomorphic states. While this is not true for all cases, there is some contention that the Hartley micelle (spherical micelle, Figure 3a) is a building block for some mesophases. Now, additional micellar structures have been proposed to explain these different mesophases.

I.E.5. TYPES OF MICELLES

The 'G' phase is associated with the smectic state and has a lamellar structure consisting of extensive micellar sheets. The amphiphile molecules form a double layer structure and the sheets are separated by layers of water. This is illustrated in Figure 3b. This structure has gained general acceptance on the basis of conclusive X-ray diffraction studies (56, 58).

The V_1 phase on the other hand is the subject of much controversy and confusion, much of it stemming from the experimental difficulties involved in the isolation of this phase from the G and M_1 phases. Also the model for this phase depends on that structure proposed for the M_1 phase which itself is in debate (see below).

Luzzati and Husson (59) first proposed that the V_1 phase was made

up of spherical micelles in a face centred cubic lattice. This configuration accounted for its isotropic character and suited their X-ray diffraction results. They later suggested a body-centred cubic lattice.

Even more serious now, is the question of the structure of the actual micelles involved. First suggestions that the constituents of the V_1 phase were Hartley micelles, were changed to a similar micelle but with "inverse" structure; ie., the polar heads and water forming the inner core and the lipophilic chains the fluid. Neither of these models accounts for the observed birefringence of the V_1 phase when subjected to a shearing force.

Luzzati's present view (60) is that the micelles are rods of finite length similar to those of the M_1 phase (see below) and that these are held together in a three-dimensional array. Another suggestion put forward by Winsor (61) is that the V_1 phase consists of a stable interdispersion of micro-units of the G and M_1 structures. It seems that the subject of the structure of this phase will be debated until more conclusive results are obtained.

There are presently two models proposed for the structure of the 'M_1' phase: a fibrous structure supported by Luzzati et al (58) and a string-of-spheres constitution supported by Clunie et al (56). In the fibrous model the micelles are depicted as being long rods of indefinite length which are arranged in a hexagonal pattern with water forming the medium between the rods. Within each rod the amphiphiles are arranged radially about the rod axis with the polar groups on the outside. This is illustrated in Figure 3c.

The string-of-spheres model arose from the observation by Clunie, Corkhill and Goodman (56) that the calculated average rod diameter (from

X-ray and density measurements) was not consistent with those calculated for the G and V_1 mesophases. They proposed a model having linear chains of spherical micelles.

Gilchrist et al (61) present evidence against this model based partially on the fact that the string-of-spheres model does not account for the marked birefringence of the M_1 phase since it is made up of isotropic units. They contend that the fibrous model is correct and support a revision of the V_1 model as discussed above.

The most popular concept for the M_1 mesophase is that it is somewhat more organized than the nematic state, but not smectic, and is made up of indefinitely long rod-like micelles arranged in hexagonal array.

The V_2 and M_2 phases have received less attention and are usually assumed to be the inverse of the V_1 and M_1 structure respectively. Luzzati has shown the M_2 mesophase to have a structure as illustrated in Figure 3d, with micellar rods having an inner polar core with the medium between the rods being lipophilic.

For a more detailed account of liquid crystals several excellent books and reviews are available to the reader (50, 51, 54, 62 - 64).

I.F. STATEMENT OF THE PROBLEM

The aim of this project is the study of the nucleation of organic compounds from aqueous solution using the droplet technique. Reports of other studies of nucleation in organic systems are rare and involve only the supercooling of bulk solutions or droplets of a melt, so that investigations relating to the homogeneous nucleation of organic compounds from aqueous solution are in order.

To this end, our intention was to synthesize water soluble organic compounds which could be used to generate _in situ_, an insoluble product. With such compounds in hand, we then hoped to develop a precipitation from homogeneous solution reaction which could be used in combination with the droplet technique to observe the homogeneous nucleation of an insoluble organic product. At the same time, we considered the prospect of a nucleation study on the water-soluble precursers. The very intriguing observation of optical birefringence of the supersaturated solutions of our starting materials led us to investigate its cause and resulted in an expansion of our main interest to liquid crystalline compounds.

It is the purpose of this thesis to report the results of our study of the homogeneous nucleation of crystalline solids from a liquid crystalline solution and of the phase transformations between several lyotropic mesophases. The classical theory of homogeneous nucleation is used to calculate some pertinent parameters relevant to the nucleation event.

EXPERIMENTAL

II.A. PREPARATION OF ORGANIC REAGENTS

One of the aims of this project was the preparation of organic compounds which would have a fairly high water solubility and which could be used to generate an insoluble material *in situ*. Furthermore it was essential that these compounds would be stable in neutral aqueous solution. Esters prepared from sulfoacetic acid are compounds which could offer these characteristics. Variations in the properties of the esters could arise from differing alcohol moieties. To avoid the auto-catalytic effect of the strongly acidic sulfonic acid group, and keeping in mind the need for water solubility, a method was selected which involved the reaction of the neutralized acid salt in aqueous ethanol.

II.A.1. SYNTHESIS OF ESTERS

A solution was prepared by dissolving 31 g (0.2 moles) of sulfoacetic acid (Eastman, practical grade) in 40 ml of water. This was neutralized by the careful addition of 15.5 g $LiOH.H_2O$ (Baker, reagent). The solution was made just acidic to litmus, then transferred to a 500-ml round-bottom flask containing 0.2 moles of the appropriate bromide [α-bromo-p-nitrotoluene (Aldrich), α-bromo-p-nitroacetophenone (Eastman), α,p-dibromotoluene (Aldrich), α,p-dibromoacetophenone (Eastman)] and 120 ml of ethanol. The mixture was refluxed with stirring for 2 - 3 hours with alcohol or water being added if necessary to bring about solution.

While hot, the solution was transferred to a 600-ml beaker,

diluted with 100-200 ml of alcohol and left to cool slowly. The ester separated as large plates and was easily collected on a Buchner funnel.

The esters were purified by recrystallization from hot aqueous ethanol.

Note: The lithium p-bromobenzylsulfoacetate would not separate using the above procedure. In this case, the cooled reaction mixture was extracted twice with large portions of ether to remove the organic residues and most of the alcohol. Further cooling of this concentrate in ice caused precipitation.

II.A.2. ANALYSIS OF ESTERS FOR PURITY

II.A.2.a. Analysis By Hydrolysis

The lithium p-nitrobenzylsulfoacetate and lithium p-bromophenacylsulfoacetate were analyzed by hydrolysis with excess standard sodium hydroxide followed by back-titration of the excess base with standard hydrochloric acid using the following procedure.

A sample of the recrystallized ester was dried for 1 hour at 110°C. Portions of 0.4 to 0.5 milliequivalents of ester were weighed into 50-ml erlenmeyer flasks and dissolved in 5 ml of water, then 10.0 ml of standard 0.1N NaOH were added. This was allowed to react for at least 15 minutes then the excess NaOH was back-titrated with standard 0.1N HCl using 3 drops of cresol red-thymol blue mixed indicator.

II.A.2.b. Analysis By Ashing

The lithium p-nitrophenacylsulfoacetate and the lithium p-bromo-

benzylsulfoacetate were analyzed by converting them to lithium sulfate. Samples of each ester were charred with sulfuric acid. The char was removed by ignition, then the final traces of carbon were oxidized by digestion with nitric acid and then sulfuric acid.

The ester was dried for 1 hour at 110°C, then 0.2 g portions were weighed into tared platinum crucibles. The ester was charred by the addition of 25 drops of conc. H_2SO_4. Ten drops of conc. HNO_3 were added and the acids were gently fumed away. When dry, the carbon char was removed by heating for 3 hours at 550°C in a muffle furnace. The residue was digested with 10 drops HNO_3, then 10 drops H_2SO_4 on a Meker burner. The crucibles were brought to constant weight by heating with the burner.

II.A.2.c. Elemental Analysis for C, H, S

Samples of each ester were sent out for an independent analysis for carbon, hydrogen and sulfur.

II.A.3. SOLUBILITY OF ESTERS

II.A.3.a. Determination By Hydrolysis

The solubility of lithium p-nitrobenzylsulfoacetate and lithium p-bromophenacylsulfoacetate were determined by hydrolysis of their saturated solutions.

Portions of saturated ester solutions were measured in 1.0-ml volumetric flasks, then transferred quantitatively to 50-ml erlenmeyer flasks. These solutions were reacted with 10.0 ml of standard 0.1N NaOH solution and left to stand for at least 15 minutes. The excess base was back titrated with standard 0.1N HCl using cresol red-thymol blue mixed indicator.

II.A.3.b. Determination By Lyophilization

The solubility of lithium p-nitrophenacylsulfoacetate and lithium p-bromobenzylsulfoacetate were determined by lyophilizing their saturated solutions and weighing the resulting precipitates.

A 1.0 ml portion of a saturated solution of the appropriate ester was quantitatively transferred to a tared platinum crucible and frozen in liquid nitrogen. The crucible was immediately put in a vacuum desicator, connected to a vacuum pump and left for 20 hours. After removal the crucible was heated 1 hour at 110°C and on cooling, weighed.

II.A.4. DENSITY MEASUREMENTS

The density of a saturated solution of each ester was determined by weighing a portion of the appropriate solution in a tared 1.0-ml volumetric flask.

The density of each ester was measured by transferring a carefully weighed portion (approximately 1 g) of the appropriate ester into a 10.0-ml portion of chloroform in a calibrated tube. The tube was centrifuged to remove trapped air bubbles then the volume change was recorded.

For comparison, the density of KBr was determined by this procedure.

II.B. NUCLEATION STUDIES

In the droplet technique a drop of the solution of interest is physically broken up into millions of non-communicating, micron-sized droplets in a suitable oil. This produces a population of droplets most of which are free of crystallization catalysts, and ensures that they remain free of contamination from air-borne catalysts and fragments that could be ejected from neighbouring droplets during the solidification process. In order to study the rate of crystallization within the collection of droplets, it is necessary that each droplet remain stationary in the field of view throughout the experiment. This can be achieved by centrifuging a sample of the dispersion in a hydrophobic, flat-bottomed container so that all droplets come to rest on the container bottom. It is then a simple matter to photographically record the size of each droplet and the phase changes within it.

II.B.1. REAGENTS

Silicone fluids of the 200 series (Dow Corning, Toronto) of various viscosities were used as the supporting medium.

The esters were prepared as described in Section II.A.

The saturated ester solutions were prepared by stirring overnight excess ester in water then allowing the solution to stand for one day in contact with the solid. The excess solid was removed by pressure filtration.

The under-saturated solution of lithium p-bromophenacylsulfoacetate was prepared by suitable dilution of the saturated solution with filtered water.

II.B.2. APPARATUS

Filtration Apparatus

The solutions were filtered before use through a 0.3 μ PVC filter (Gelman Instruments, Michigan) in a pressure filter holder supplied by the Millipore Co. (Montreal).

Dispersion Apparatus

The solution was dispersed in the silicone oil by stirring 1 or 2 drops (1 drop = 0.03 ml) in a 6-ml accessory flask by means of a Virtis micro-homogenizer (Fisher Scientific, Toronto). Centrifugation was done with an International Clinical centrifuge (Boston).

Glassware

The initial centrifugation required standard 15-ml centrifuge tubes.

The specially prepared observation cups were made by fusing 28 mm diameter, flat Pyrex discs (Lab Glass, New Jersey) onto Pyrex glass tubing 28 mm x 25 mm. The resulting container had a flat bottom which not only improved its optical properties but also allowed the preparation of more uniformly populated dispersions than the previously used Nessler cups(46). These containers were made hydrophobic by coating them with Drifilm SC-87† (Pierce Chemical Co., Rockford, Illinois).

Microscope

The microscope used in this work was a Vickers M15 polarizing microscope (Vickers Instruments, Toronto), with a magnification of 75 x (5X

---

† Drifilm was found to be superior to the previously used silicone grease (D.C. 200 - 2 million C.S.) because there was no problem of distortion during centrifugation. Also since it is untouched by cleaning solvents each treatment lasted several weeks.

objective, 10X eyepiece, 1-1/2 analyser). This was built on an optical bench (Spindler and Hoyer, W. Germany) and set up for Kohler illumination using a 500-watt super-high pressure mercury vapour lamp (Philips Electronics, Toronto). Both the lamp and the primary condensor of the microscope were housed in water-cooled jackets, and the polarizer was protected by two heat-absorbing filters (Wild Scientific). The microscope was equipped with a micrometer stage (Vickers Instruments) and a removable cell holder for the observation cup. An accurate micrometer dial (Mitutoyo, Japan) having a range 0.01 to 20 mm was mounted on this stage; this allowed the sequential observation of several fields of view and ensured precise re-alignment of each field. The droplet size changes and phase changes were recorded photomicrographically using an Autowind 35-mm camera (Vickers Instruments) and Anscochrome D-500 colour reversal film (G.A.F., Toronto) processed by Benjamin Labs (Toronto). The Autoexposure unit J-35 (Vickers Instruments) was modified to allow control of the shutter speed for the dark field exposures.

A dry atmosphere was maintained by mounting four drawn-polyethylene tubes around the objective lens of the microscope so that a stream of dry compressed-air could be directed into the observation cup. The compressed-air was cleaned and dried by passing it first through an oil and dust filter, then bubbling it through concentrated sulfuric acid. Before being directed into the observation cup it was passed through a mist trap and a column of Ascarite (Arthur H. Thomas, Philadelphia) to remove the sulfuric acid mist, then finally through a dust trap.

The film slides were viewed with a Pradovit projector (Lietz, W. Germany) equipped with a 150-mm lens and a projection screen ruled in millimeters.

II.B.3. PROCEDURE

One or two drops of the appropriate ester solution† were stirred in 5 ml of D.C. 200-20 c.s. oil for 5 seconds at 25000 r.p.m., then transferred to a standard centrifuge tube containing 9 ml of D.C. 200-100 c.s. oil. The tube was centrifuged for 1 minute at 4000 r.p.m., then 2-3 ml were removed with an eye dropper from the middle of the tube and poured onto a thin film of the same oil in an observation cup. This was centrifuged for 30-60 seconds. The supernant oil was decanted, replaced with fresh D.C. 200-100 c.s. oil to a depth of 3 mm and then centrifuged for 30 seconds.

The observation cup was inserted into the cell holder and fitted on the microscope stage and a suitable region selected for observation. Usually 5 or 6 adjacent fields of view were recorded, each being less than 3 mm away from the central field of view.

After processing and sorting, the slides were projected in turn on the ruled screen. The individual droplet diameters were measured, the time of the transition to the liquid crystal phase and the time of the crystallization event were both recorded. All of this information was then punched on cards for processing by a CDC 6400 computer.

The droplet diameters were converted to microns using a scale factor determined by calibrating the ruled screen with a photomicrograph of a millimeter slide taken at the same magnification factor.

---

† In all cases except lithium p-bromophenacylsulfacetate saturated solutions were used. This solution was 90% saturated.

Note: To record the liquid crystal phase change and the crystallization events within the droplet population photomicrographs (crossed polars) were taken at 1 minute intervals using a 10% N.D. filter and 1/2-second exposure. To record the change of droplet size within the population, photomicrographs were taken using transmitted light at regular intervals (usually 5 minutes) using a 0.1% N.D. filter with 1/2-second exposure.

RESULTS AND DISCUSSION

III.A. PREPARATION OF ORGANIC REAGENTS

As discussed in detail in Appendix 5, one of the aims of this project was the development of a method for the generation within an aqueous solution of an insoluble organic compound suitable for nucleation studies using the droplet technique. To this end water-soluble esters of sulfoacetic acid were prepared using the following moieties: p-bromobenzyl alcohol, p-nitrobenzyl alcohol, p-bromophenacyl alcohol and p-nitrophenacyl alcohol.

The esters were first prepared as their sodium salts, but these were not soluble enough for the proposed PFHS reaction. It was found that the lithium salts of the esters were much more soluble although the yield of product was drastically reduced.

To the best of our knowledge these esters are new compounds, so that a more detailed description of their preparation, analysis and properties than would ctherwise be necessary is warranted.

III.A.1. PROPERTIES OF THE ORGANIC REAGENTS

The method of preparation was adapted from that described by Shriner, Fuson and Curtin (65) for the identification of carboxylic acids. The chemical reaction involved is

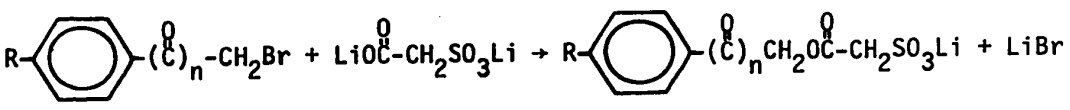

where n = 0 or 1, and R = NO_2 or Br.

The products were obtained as pure shiny crystalline plates. No attempt was made to improve the low yields of these preparations (see Table 1), although the amount of water used and the total solvent volume were kept to a minimum to avoid solubility losses to the solvent. Attempts to collect a second crop of crystals proved impractical as a means of increasing the yield due to the deposition of gummy polymeric material.

The physical properties of the esters and the results of Section II.A. are tabulated in Table 1. The analytical methods used to determine the purity have an experimental error of 1% so that the esters can be considered to be pure. This was confirmed independently by elemental analysis. Spectral data for these compounds were recorded and the characterizing U.V.-visible, infra-red and NMR spectra are included in Appendix 1.

The solutions of the lithium salts of p-nitrobenzylsulfoacetate, p-bromobenzylsulfoacetate and p-bromophenacylsulfoacetate were found to be stable for several months at room temperature. The solutions of lithium p-nitrophenacylsulfoacetate were stable for up to four weeks. Nevertheless, freshly prepared solutions were used throughout this work.

TABLE 1

Properties of the Esters

Property / compound		1	2	3	4
molecular weight		315	281	343	309
colour		pure white	pale beige	pure white	pale yellow
yield (%)		24	32	80	38
purity (%)		99.4	99.3	99.5	99.0
elemental analysis†	%C	34.4(34.3)	38.7(38.4)	35.1(35.0)	38.7(38.8)
	%H	2.7(2.5)	3.1(2.9)	2.5(2.3)	2.7(2.6)
	%S	10.1(10.2)	11.0(11.4)	9.4(9.3)	10.4(10.4)
solubility (moles/l)		2.03	1.92	0.75	2.42
density†† (g/ml)		1.99	1.84	1.94	1.89
density of sat'd solution (g/ml)		1.291	1.186	1.145	1.182
melting point		255(dec)	270(dec)	260(dec)	270(dec)

KEY:
1 lithium p-bromobenzylsulfoacetate
2 lithium p-nitrobenzylsulfoacetate
3 lithium p-bromophenacylsulfoacetate
4 lithium p-nitrophenacylsulfoacetate

---

† Brackets denote expected value
†† KBr density by this method is 2.70; expected value 2.75

III.B. LIQUID CRYSTALLINE CHARACTER OF THESE COMPOUNDS

In the course of some preliminary work, droplet contraction studies using the sodium salt of p-nitrobenzylsulfoacetate showed that the droplets reached a stage in which they became strikingly birefringent and displayed clearly a Maltese cross. Even when the dispersions were left for several days, the droplets remained unchanged; however, when the dispersion was left for several hours over P_2O_5, the droplets transformed to ordinary crystalline masses of irregular shape. For dispersions of a few readily available, similar compounds [p-sulfobenzoic acid, K^+ salt; m-sulfobenzoic acid, Na^+-salt; sulfosalicylic acid] the droplets remained isotropic until the point of crystallization. The unusual behaviour of our ester led to the question of what was causing the intermediate phase and interested us in a more detailed study.

III.B.1. QUALITATIVE OBSERVATIONS OF THE PHASE CHANGES INVOLVED

In the discussion which follows, the experimental observations for the phase changes within the droplets will be illustrated for the case of lithium p-bromobenzylsulfoacetate. Differences for the other esters will be noted later.

Droplets of a saturated solution of lithium p-bromobenzylsulfoacetate dispersed in a silicone fluid were observed to go through a series of phase changes as the concentration of the ester increased through extraction of water. Photomicrographs of the droplets illustrating these phases are included in Figure 4. Each frame represents the same field of view at increasing degrees of supersaturation.

Initially the droplets are clear and isotropic to polarized light (not shown), then with only a slight increase in supersaturation they transform to the first birefringent phase. This phase is evident in Figure

Figure 4. Photomicrographs illustrating the three liquid crystalline phases of the lithium p-bromobenzylsulfoacetate solution under crossed polars.

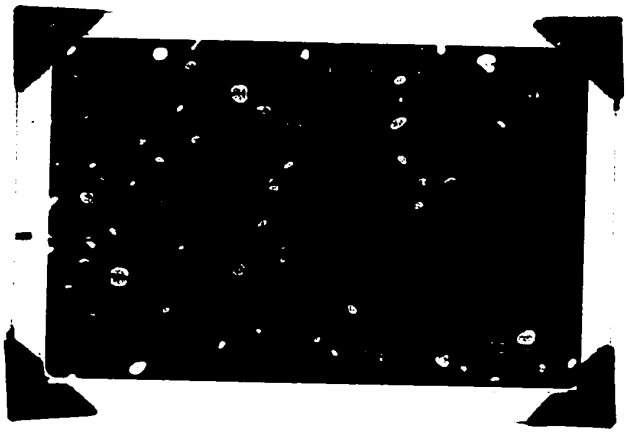

(a)

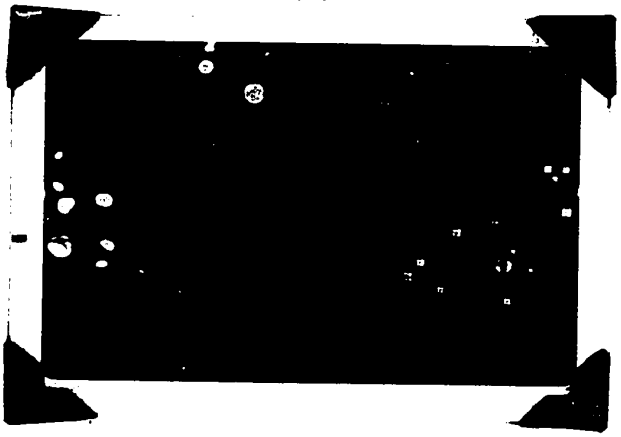

(b)

(c)

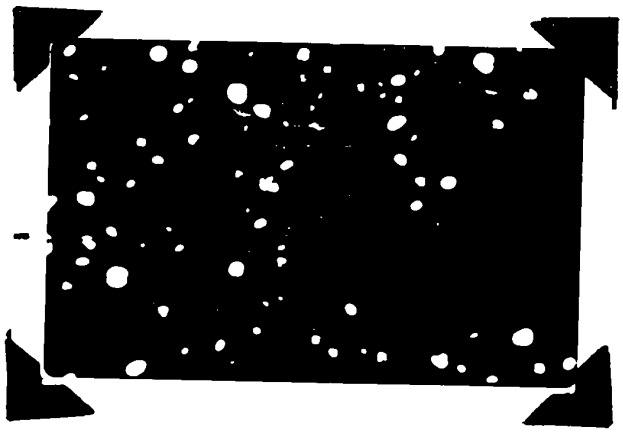

(a)

(b)

(c)

4a which shows that the droplets shine brightly and exhibit random interference patterns. As the supersaturation increases, the droplets extinguish and again become isotropic, this is apparent in some regions of each frame in Figure 4. It is evident that in the case illustrated, there is a gradient of increasing concentration from left to right in the field of view. As the concentration increases, the droplets become birefringent again, but in this case, each droplet displays the same interference figure, the Maltese cross, as seen in Figure 4c. Further increase in supersaturation leads to the instantaneous collapse of the droplet into an irregular mass of crystals (not illustrated).

Under transmitted light the droplets remain completely clear until the moment of crystallization. This is illustrated for the same field of view in Figure 5. Figure 5a is the first of a series of photomicrographs which were used to measure the rate of change in supersaturation. Most of the droplets in this frame, if viewed with polarized light, would exhibit the birefringence effects shown in Figure 4a. Figure 5b corresponds to Figure 4b, being taken one minute later. It is seen that while the droplets were distinguishable under polarized light, they are not under transmitted light. Figure 5c shows the droplet at a later time when crystallization has begun. The crystallized droplets are clearly distinguishable as dark masses. Those droplets which remain uncrystallized, although clear to transmitted light, would under crossed polars display the Maltese cross of Figure 4c. Comparison of Figures 5a and 5c shows the overall change in droplet diameter during the course of the experiment.

In the case of lithium p-nitrobenzylsulfoacetate and lithium p-nitrophenacylsulfoacetate, only one phase was observed prior to crystallization. The droplets transformed directly from the isotropic liquid to

Figure 5. Photomicrographs of the lithium p-bromobenzylsulfoacetate droplets under transmitted light at the start, midway and near the end of an experiment.

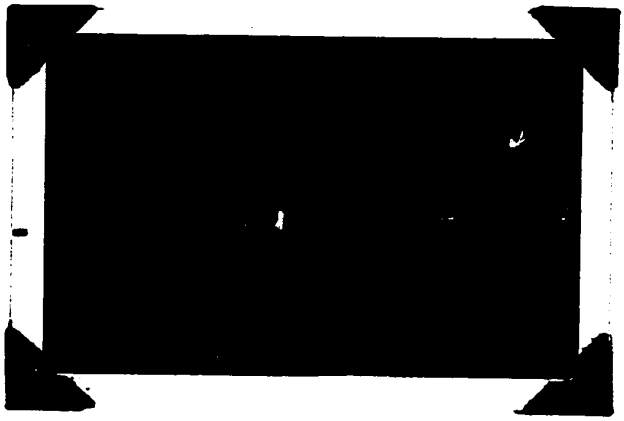

(a)

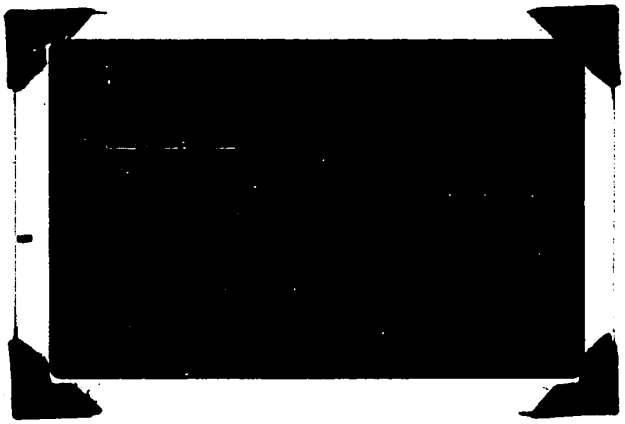

(b)

(c)

(a)

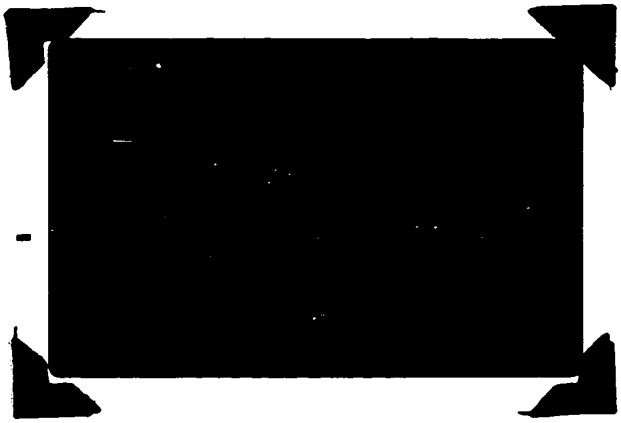

(b)

(c)

the anisotropic phase displaying the Maltese cross. For lithium p-bromophenacysulfoacetate two birefringent mesophases formed which were not separated by an isotropic phase. The two birefringent phases appeared in the same order and showed the same interference patterns as those of lithium p-bromobenzylsulfoacetate.

III.B.2. EXPLANATION OF THE BIREFRINGENCE PATTERNS

Most descriptions of lyotropic mesophases in aqueous systems involve long-chain aliphatic sulfonic acids, while studies on thermotropic systems utilize compounds having more structural complexity with the molecules usually possessing one or more aromatic rings. The molecules described in this thesis are allied structurally to the latter type but they display lyotropic liquid crystalline characteristics. Although apparently less common, this situation is not unique since a number of well known dyes, such as methyl orange, are known to exhibit lyotropic mesophases. The various birefringence effects of the mesophases described in Section III.B.1. can be explained in terms of the micelle structures proposed for aliphatic soaps (Section I.E.5.) .

Birefringence results when a beam of convergent plane-polarized light is passed through an anisotropic medium. In such cases the refractive index is different in two directions and the beam is split into two components vibrating at right-angles to each other. Because of the different refractive indices one beam is retarded relative to the other resulting in interference when the beam is re-combined. The resultant interference pattern can be related to the structure of the system under observation.

The Maltese cross is the characteristic interference pattern of a uniaxial crystal aligned with the line of view coincident with its optic axis. Such a pattern is well known for spherulites (66) in which a spherical crystal is built-up in concentric layers. In this case any diameter

of the sphere corresponds to a normal to the layers and would be an optic axis. Thus, for the liquid crystalline phase displaying this cross an onion-like arrangement of micellar layers of the type shown in Figure 3b would account for the observed interference pattern. This mesophase then, is analagous to the "neat" phase of aliphatic soap systems. Having established this reference point the other phases observed for lithium p-bromobenzylsulfoacetate and lithium p-bromophenacylsulfoacetate can be assigned according to the scheme presented in Section I.E.3. That is, the first birefringent phase observed, which occurs at the lowest concentration, would correspond to the M_1 phase and the isotropic intermediate mesophase to the V_1 phase.

An arrangement of parallel micellar rods would result in the interference patterns associated with a uniaxial crystal. If the optic axis was coincident with the microscope axis, then an interference pattern resembling the Maltese cross would be observed. Any other alignment would result in other interference patterns. In a few cases a Maltese cross was evident, in some others the droplets shone uniformly, but in most cases the pattern displayed was hyperbolic, similar to the seams on a tennis ball. Thus the first birefringent phase is M_1-type. The intermediate phase is isotropic consistent with the expectations for the V_1 phase.

The existence of both M_1-type and G-type phases for two of the esters but only the G-type phase for the others can be explained in terms of the different nature of the molecules. The absence of the M_1-type phase for lithium p-nitrobenzylsulfoacetate and lithium p-nitrophenacylsulfoacetate is most probably due to the electrostatic repulsion of the nitro-groups which retain a higher electron density than bromo-substituents because of their conjugation with benzene ring. Thus, the micellar rods of

the M_1 phase would be unstable because they require a closer packing of the lipophilic chains than the lamellar micelle of the G phase.

It should be mentioned that the existence of these phases could not be confirmed by observing their characteristic textures using conventional methods because they exist only at concentrations higher than the equilibrium solubility of the solid. Thus when attempting to observe the sequence of phases by the usual method of peripheral evaporation of a thin film of solution, crystals formed at the boundary and simply acted as heterogeneous nucleation centres and prevented the required build-up of supersaturation. The droplet technique, by removing the effect of heterogeneous catalysts (Section I.C. and III.C.1.) thus enabled these phases to form under conditions which would not otherwise be possible.

III.B.3. TRANSFORMATIONS TO THE MESOPHASES

Transformation between thermotropic liquid crystalline phases usually occur at the same well-defined temperature whether the sample is heated or cooled. In some cases, however, a slight degree of supercooling has been observed. This has usually been attributed to the different textures involved. Recently, Mocadlo (67) has applied the droplet technique to the study of some cholesteric liquid crystals and found the transition temperature for the isotropic liquid to mesophase to be up to 10°C lower than for the reverse transition. For the case of lyotropic systems Winsor (51) reported that for the $G \rightarrow V_1$ transition with the N,N,N,-trimethylaminododecanoimide - water system, supercoolings of up to 9°C can be observed. Such observations suggest that a nucleation barrier to the transition does exist.

Generally, by analogy to the crystallization of a solid, a metastability of the initial phase relative to the new mesophase might be an-

ticipated. In this study there is a problem of how this metastability should be defined. As has been stated above, the saturated solutions of these compounds do not exhibit liquid crystalline character, only the unstable supersaturated solution is mesomorphic. Thus, the problem is how to decide in the absence of an equilibrium reference concentration, whether or not there is any metastability prior to liquid crystal transformations. For the case of crystal nucleation from solution, a distribution of the number of droplets crystallized as a function of concentration is obtained (as in Section III.C.) because the transformation is a stochastic process. Thus, if within the droplet population there is a distribution of the number of droplets transformed to the mesophase as a function concentration, then it can be reasoned, by analogy, that the initial phase is metastable with respect to this mesophase.

The results for the transformation to various mesophases for the case of lithium p-nitrophenacylsulfoacetate and lithium p-bromobenzylsulfoacetate are presented in Table 2. For the range of supersaturation† over which these transitions occurred the experimental error is about 0.1 units. Thus, there is some doubt in the case of lithium p-nitrophenacylsulfoacetate that the spread of values over the narrow supersaturation range is in fact a distribution due to metastability of the isotropic solution. The significance of the distribution for both the $M_1 \rightarrow V_1$ and the $V_1 \rightarrow G$ transformations in the case of lithium p-bromobenzylsulfoacetate is less doubtful. Here the spread of supersaturation values for the transitions

---

† Here supersaturation still refers to the equilibrium solubility of the solid, since the equilibrium concentration for the existence of the mesophase is unknown.

TABLE 2

Supersaturations at which Transitions to the Liquid Crystalline Phase Occurred

Droplet Size Range 10-20 μ

Compound	1	2	
Supersaturation/Transition	S → G	$M_1 \rightarrow V_1$	$V_1 \rightarrow G$
1.0	0	0	
1.1	189	2	
1.2	145	70	0
1.3	16	176	24
1.4	2	175	150
1.5		43	202
1.6		8	70
1.7		2	22
1.8		0	5
1.9			3
total number of droplets examined	352	477	477

TABLE 2
(continued)

Droplet Size Range 20-30 μ

Compound	1	2	
Supersaturation/Transition	S → G	$M_1 \rightarrow V_1$	$V_1 \rightarrow G$
1.0	0	0	
1.1	87	0	
1.2	123	2	
1.3	8	42	3
1.4	1	82	29
1.5	0	53	72
1.6		18	60
1.7		1	28
1.8		1	6
1.9		0	1
total number of droplets examined	219	200	200

KEY 1. lithium p-nitrophenacylsulfoacetate
2. lithium p-bromobenzylsulfoacetate

is greater than the breadth of the experimental error, so that we can confidently conclude that these mesophases exhibit metastability prior to transformation. It should be noted for the latter compound that the transition S → M_1 had begun in many droplets before the first observations were made so that this transition could not be completely recorded. The very slight degree of metastability observed is consistent with that reported by Mocadlo (67), who found supercoolings of up to 10°C for the isotropic to mesophase transition. These values were much lower than her findings of supercoolings of up to 50°C for the solidification process.

The energy changes involved in the development of long-range order prior to solidification must result in a lowering of the nucleation barrier for the crystallization process. It may be possible, in the future, to evaluate this lowering of the energy barrier through the energy changes associated with the metastability of the mesomorphic states.

III.C. RESULTS OF THE NUCLEATION STUDIES

III.C.1. COMMENTS ON THE DROPLET TECHNIQUE

The droplet contraction technique takes advantage of the selective extraction of water from a solution thus offering a unique way of building up the concentration of solute in a droplet immersed within it. This has several advantages over other droplet techniques (see Section I.C.). It applies to a wider variety of compounds than supercooling methods because it is not restricted to those compounds which have a high temperature dependence of solubility; also it is isothermal. The technique does not involve unnecessary bi-products, as in PFHS methods, which have an undetermined effect on the nucleation process. It also avoids the complex chemical problems which can arise with a PFHS method. Furthermore, the rate of change in supersaturation is slow and comparable to that of supercooling experiments, whereas, in situ generation is usually rapid. In addition, the rate of reaction in the supersaturated droplet may differ from that in the bulk.

For the droplet contraction method to be useful a means of accurately determining the concentration of the solution is necessary. It was pointed out in Section I.D. that the supersaturation could be calculated as the ratio of the initial to the final volume.

In order to gain confidence in this approximation it is necessary to show that the boundary conditions outlined in Section I.D. were upheld. Thus plots of the diameter squared against time were constructed for 50 randomly selected droplets for the case of lithium p-nitrobenzylsulfoacetate. These plots were of the form illustrated in Figure 6. It is clear that for the early part of the experiment the plot is linear as predicted by equation (8) but tends to level off near the end. This levelling is a result of the increase in the concentration of water in the silicone oil

Figure 6. Plot of $\underline{D^2}$ vs. time for lithium p-nitrobenzylsulfoacetate (selected for illustration from a sample of 50 similar plots)

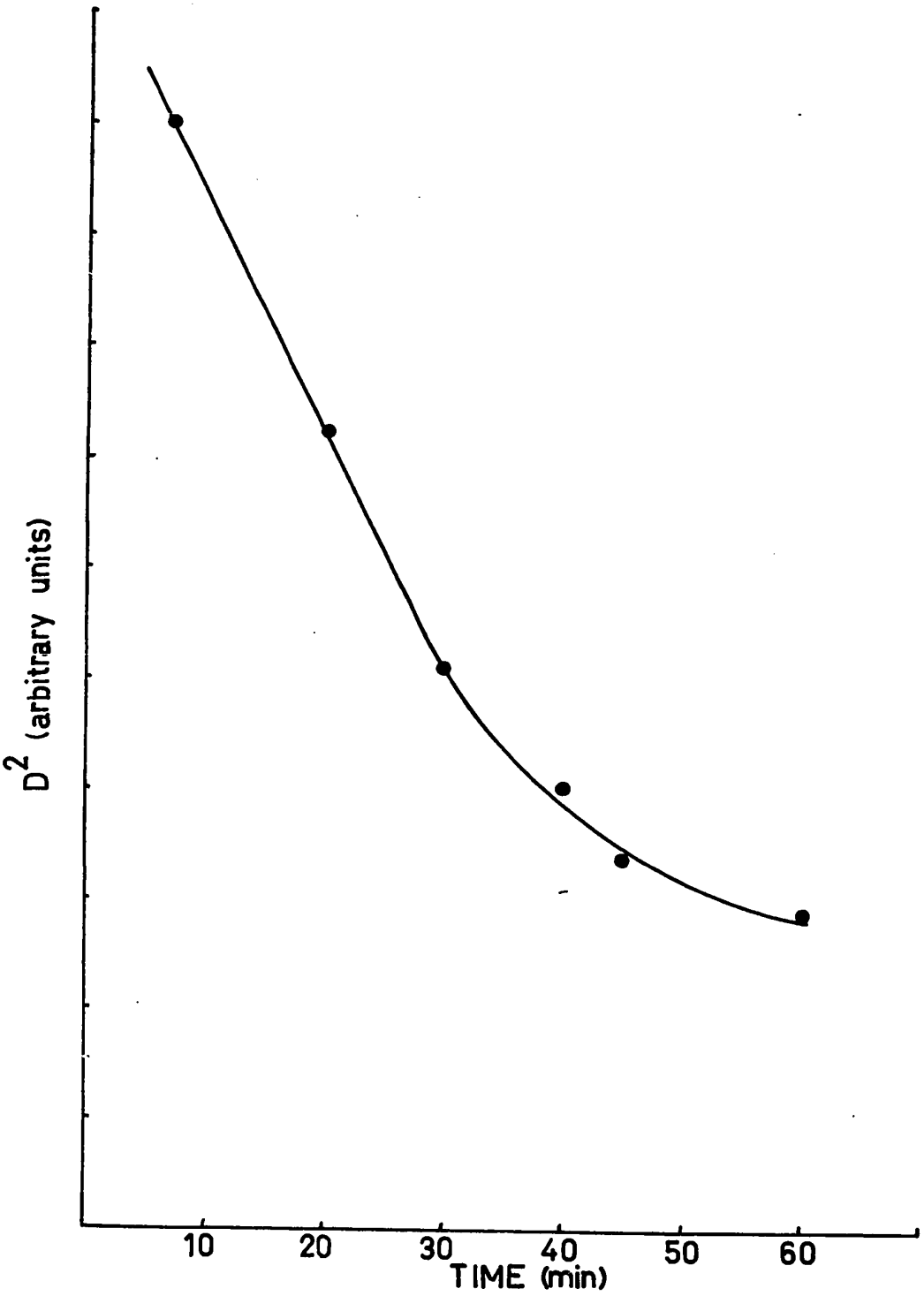
D^2 (arbitrary units)
10
20
30
40
50
60
TIME (min)

in violation of condition (1). That the problem is due to the increasing water concentration is evident from the fact that the amount of levelling depends on the population density of the droplets. Also as discussed in detail below, without some mechanism for the removal of water, the droplets reach a limiting diameter. If the water could be effectively removed so that condition (1) was not violated the system should continue to behave ideally.

The violation of condition (1) explains the failure of equation (9) to predict the concentration as a function of time. However, unless the other conditions are violated, equation (10) serves as a suitable though more tedious means of calculating the supersaturation.

One main problem associated with the droplet contraction technique is that the rate of contraction of the droplets is dependent upon the local concentration of water in the oil. Thus for regions with a high density of droplets the rate of change in concentration is slower and the supersaturation lags behind that for sparsely populated regions. Also, since the rate of loss of water depends on the extent of the surface area (see Section I.D.) then droplets of greatly different size will have different rates of change of supersaturation. This means that since the supersaturation is not the same in each droplet at any instant of time, time in laboratory coordinates cannot be used to determine the rate of nucleation for reasons outside those related to the nucleation process. The latter problems can be overcome by simply restricting the size range studied to those droplets having diameters which do not differ greatly. The first problem is more serious.

Velazquez (68) took a representative sample of droplets and measured an average rate of change of supersaturation with time. From this and the

time of crystallization, he calculated the supersaturation at the time of crystallization. This means that the most important parameter of the nucleation study is derived, not experimentally measured. Furthermore, a few randomly selected droplets may not necessarily reflect a true description of the experiment. Bempah (32) found that the supersaturation in his systems reached a constant value before crystallization began; this allowed the selection of a zero-time relative to which the time for crystallization could be measured at constant supersaturation. This, however, is a special case peculiar to his family of compounds. Neither of these solutions seemed suitable for the purpose of this study.

In this study, it was found that although the rate of change in supersaturation was irregular over much of the droplet contraction experiment it became linear, or nearly linear, in most cases just prior to the crystallization event. Thus, for a 30 minute time interval immediately before crystallization, the rate of change of supersaturation for each individual droplet was approximated by a straight line (method of least squares). Having obtained a value for the rate of change of supersaturation with time for each droplet in the population, then the most representative rate for the population was selected to correlate supersaturation with time. The actual supersaturation was experimentally measured, so that in effect this calculation is substituting an average value for time (instead of an average value of S, as Velazquez used) which then allows the subsequent calculation of the nucleation parameters to be performed with the experimental value for the supersaturation.

In a droplet contraction experiment it is desirable to obtain all of the data for a particular system from one set of observations. This then avoids the problem of large differences in the rate of shrinking of droplets

in unrelated populations. Experimentally it is convenient to photograph up to five adjacent fields of view. This means that in order to get a statistically significant number of droplets from one experiment, the field of view must contain 100-200 droplets. With such a high population of droplets, the chemical potential of the water in the silicone oil becomes so high that the droplets stop shrinking before crystallization occurs and are stable for several days. To speed up the extraction of water, Velazquez (68) placed his observation cup in a desicator over P_2O_5. This technique however, results in a discontinuous rate of change in supersaturation because the container must be removed periodically for observation; also, since the changes cannot be monitored while the container is in the desicator, the start of crystallization may be missed rendering the experiment useless. More important, when the container is finally removed from the desicator in order to record the phase changes an abrupt decrease in the rate of change of supersaturation occurs and this new rate cannot be determined.

In order to solve these problems the same principle was adopted by making the observation cup into a "mini-desicator" by sweeping dried air through it. This was effective in allowing a controlled rate of change in supersaturation thus bringing about crystallization within a reasonable amount of time. There was no danger of contamination of the droplets by foreign particles from the air stream because the droplets were covered by a 3-mm layer of silicone oil.

In the application of the droplet technique to nucleation studies one question which commonly arises is what effect, if any, the droplet-oil interface has on the nucleation events. Usually the experiments can be repeated in a different medium and then, if no difference in the median

crystallization time is observed, it is concluded that the interface has no effect. In this work we were restricted in that only one type of oil could be used to extract water from the droplets. A change from D.C.200-100 cs oil to D.C.200-200 cs oil showed no qualitative difference; however, since the chemical nature of the two oils is so similar this could not be used as a suitable criterion. We have to rely on the conclusive evidence in the literature (48, 68, 69) that the nucleation process is not affected by the droplet-oil interface.

III.C.2. CALCULATION OF THE RATE OF NUCLEATION

III.C.2.a. Relation of the Rate of Nucleation to Probability

With the restriction of one nucleation event per droplet the following expression used by Turnbull (44) can be used to calculate the rate of nucleation, J.

$$J = \frac{1}{1-P} \frac{1}{v} \left[\frac{dP}{dt}\right] \qquad (11a)$$

where 'v' is the volume of the droplet and P is the probability of finding a crystal (ie. a crystallized droplet) after a time t. J is the rate of nucleation in number of nuclei-cm^{-3}-sec^{-1}. This expression has been derived by Carte (49) and others also. For the supercooling of water at a controlled rate of change of temperature with time, Kuhns and Mason (70) used

$$J = \frac{1}{1-P} \frac{1}{v} \left[\frac{dT}{dt}\right]\left[\frac{dP}{dT}\right]$$

where $\frac{dT}{dt}$ represents the rate of change in temperature with time and P is measured as the fraction of droplets crystallized at any temperature. By analogy we can write

$$J = \frac{1}{1-P} \frac{1}{v} \left[\frac{dS}{dt}\right]\left[\frac{dP}{dS}\right] \qquad (11b)$$

here $\frac{dS}{dt}$ is the rate of change of supersaturation with time and P is the

fraction of droplets crystallized at any supersaturation.

III.C.2.b. Flow of Calculations

The raw data were collected and punched on computer cards so that the complete history of each individual droplet was recorded on a separate card. Thus, a card contained a series of values for the droplet diameter (in arbitrary units, mm) for specific times, and a series of columns tabulating: final droplet diameter, time of each liquid crystal transition, time of detection of a crystal, and the field of view identifying the population. The time was represented by a slide number.

The sequence of calculations was as follows:

1. The diameters were read and checked for processing errors, the times were converted from slide number to actual time in minutes. A new data deck was punched with these actual times, which was subsequently sorted and arranged according to increasing final diameter.
2. The final diameter in mm was multiplied by a scale factor to change it to the actual value in microns then the number of droplets in each size range was determined. The size groups were:

   0 - 10 μ,
   10 - 20 μ,
   20 - 30 μ, and
   30 - 40 μ.

3. The supersaturations corresponding to each value of the diameter for each droplet were calculated and punched on a separate deck including as well times of phase transition and the field of view.
4. The number crystallized as a function of final supersaturation for each size group was determined. From this the

relative frequency of crystallization and the probability of crystallization were calculated.

5. Plots of S vs t were prepared for randomly selected droplets.
6. A least squares fit of the last four points for S vs t was performed for each droplet. A punched output for the slope of the S vs t plot was provided.
7. Using the output from 6, the best slope of the S vs t plot was selected by plotting the number of droplets having each particular slope.
8. The median value for the diameter was obtained from the number of times a particular diameter appeared within a population.

Copies of the programs used for the above calculations for the case of lithium p-bromobenzylsulfoacetate are included in Appendix 3.

Plots of relative frequency of crystallization as a function of supersaturation were constructed and the best curve drawn through these points. From this curve the probability of crystallization as a function of time was constructed and used to obtain values of P and $\frac{dP}{dS}$ to calculate J.

III.C.3. QUANTITATIVE RESULTS FOR CRYSTAL NUCLEATION

In applying the methods of Section I.D. and Section III.C.2. to the interpretation of the experimental results it is necessary to make a few approximations. The data will be presented and discussed for lithium p-bromobenzylsulfoacetate, then the results for other esters will be presented for comparison. The discussion will also be restricted to the common size group 10-20 microns. Figures and Tables for the other size ranges

are compiled in Appendix 4. The raw data from which these results were obtained can be consulted in Appendix 6.

To calculate the rate of nucleation, J from equation (11b),

$$J = \frac{1}{v}\frac{1}{1-P}\left[\frac{dS}{dt}\right]\left[\frac{dP}{dS}\right] , \qquad (11b)$$

suitable choices for v and dS/dt must be calculated which best represent the droplet population.

One of the limitations resulting from the use of a microhomogenizer-centrifuge combination for the preparation of the dispersions (see Section III.B.1.) is that it is not possible to produce a statistically significant number of mono-sized droplets. Thus the droplet populations so produced were divided into several size groups in such a way that there was a fairly uniform distribution of droplet sizes within each group. The median diameter was then selected to calculate the appropriate volume for use in equation (11). Unless there is a large difference in the size of the droplets within a group the effect on the solution to the nucleation rate equation (7b) is small.

Usually a dispersion contained droplets ranging from 5 microns to 60 microns final diameter, however, because of the large increase in relative error in the measurement of small droplets those below 10 microns† were not counted. There were only a few droplets greater than 40 microns and these usually crystallized early in the experiment, presumably heterogeneously, thus they were discarded in the analysis. The size group, 30 - 40 microns, was included for lithium p-nitrophenacylsulfoacetate and lithium p-bromobenzylsulfoacetate but the number of droplets (about 60) was not statistically significant so that no conclusion could be drawn from the data. The relative frequency plots (see

† For the case of lithium p-nitrobenzylsulfoacetate droplets greater than 8 microns were included.

below) are, however, included in Appendix 4.

As pointed out in Section III.C.1. the rate of change in supersaturation was calculated for each droplet and the most representative value was used for dS/dt in the rate equation.

From the number of droplets crystallized at any supersaturation, plots of relative frequency of crystallization as a function of time were constructed. The best curve was drawn through these points as illustrated in Figure 7. From this plot the fraction of droplets crystallized up to a particular supersaturation was determined. These data were plotted on probability paper and the results shown in Figure 8. Using increments of S equal to 0.1, $\frac{\Delta P}{\Delta S}$ was calculated for various values of P, from Figure 8.

As discussed in Section I.D. equation (7b)

$$\log J = \log A - \frac{16\pi\sigma^3 v^2}{3(2.303kT)^3} (\log S)^{-2} \qquad (7b)$$

can be used to evaluate the interfacial energy, σ.

Figure 9 shows the plots of log J vs $(\log S)^{-2}$ for both size ranges studied for lithium p-bromobenzylsulfoacetate. As predicted by equation (7b) a linear relationship was obtained. The least squares fit of this data then gave an intercept of 7.2, the value of log A, and a slope from which σ was calculated to be 4.8. The value of the critical supersaturation was found by substituting log J = 0 (by tradition) into equation (7b). This gave S* = 1.4.

The corresponding data for the three other compounds are presented in Figures 10 to 18. They each showed a similar relative frequency distribution with no pronounced skewing so that the probability of crystallization as a function of supersaturation is a straight line on pro-

Figure 7. Plot of Relative Frequency of Crystallization vs Supersaturation for lithium p-bromobenzylsulfoacetate. Size range 10 - 20μ. 477 droplets.

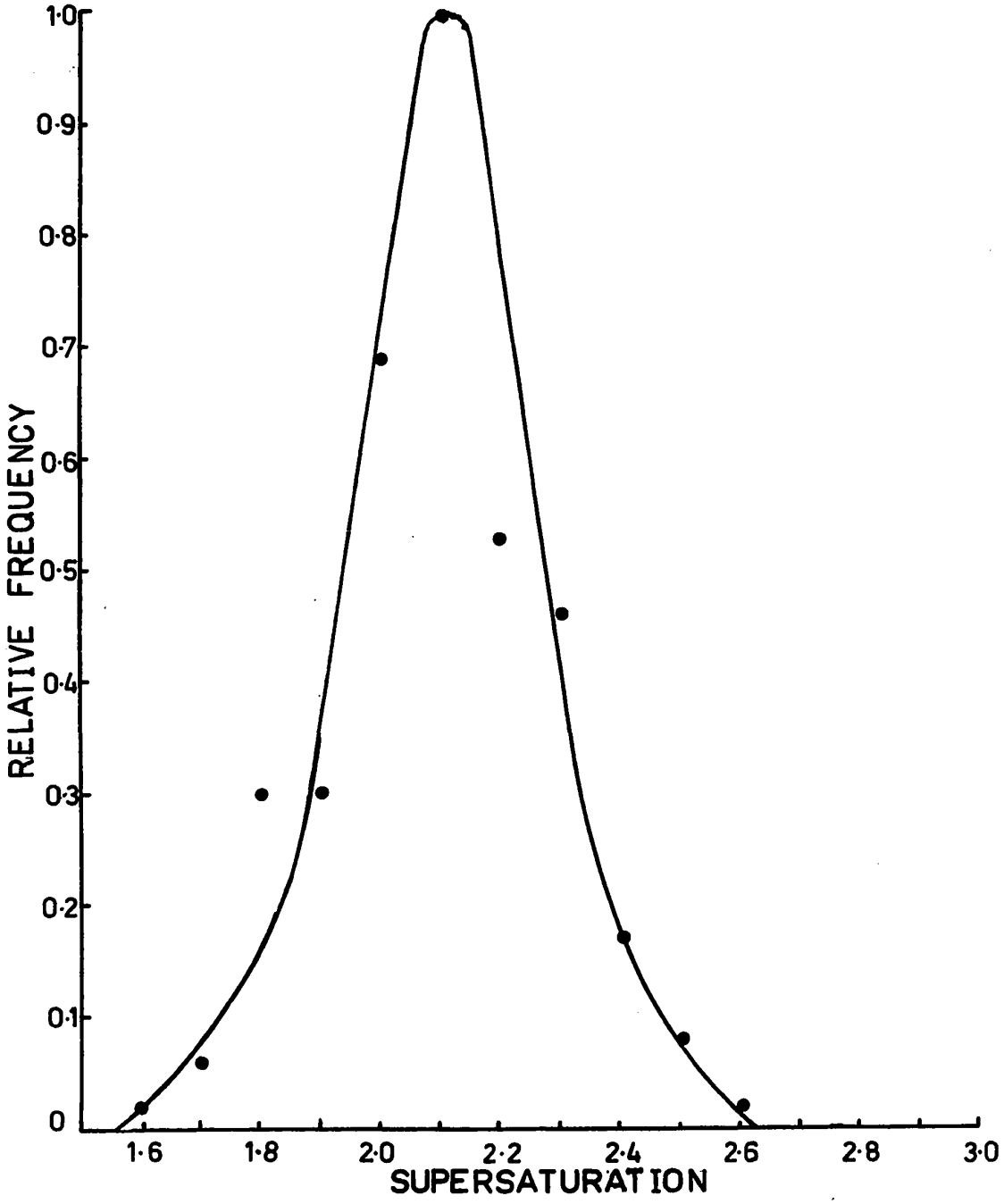
RELATIVE FREQUENCY
1·0
0·9
0·8
0·7
0·6
0·5
0·4
0·3
0·2
0·1
0
1·6
1·8
2·0
2·2
2·4
2·6
2·8
3·0
SUPERSATURATION

Figure 8. Plot of Probability of Crystallization vs Supersaturation for lithium p-bromobenzylsulfoacetate. Size range 10 - 20μ 477 droplets.

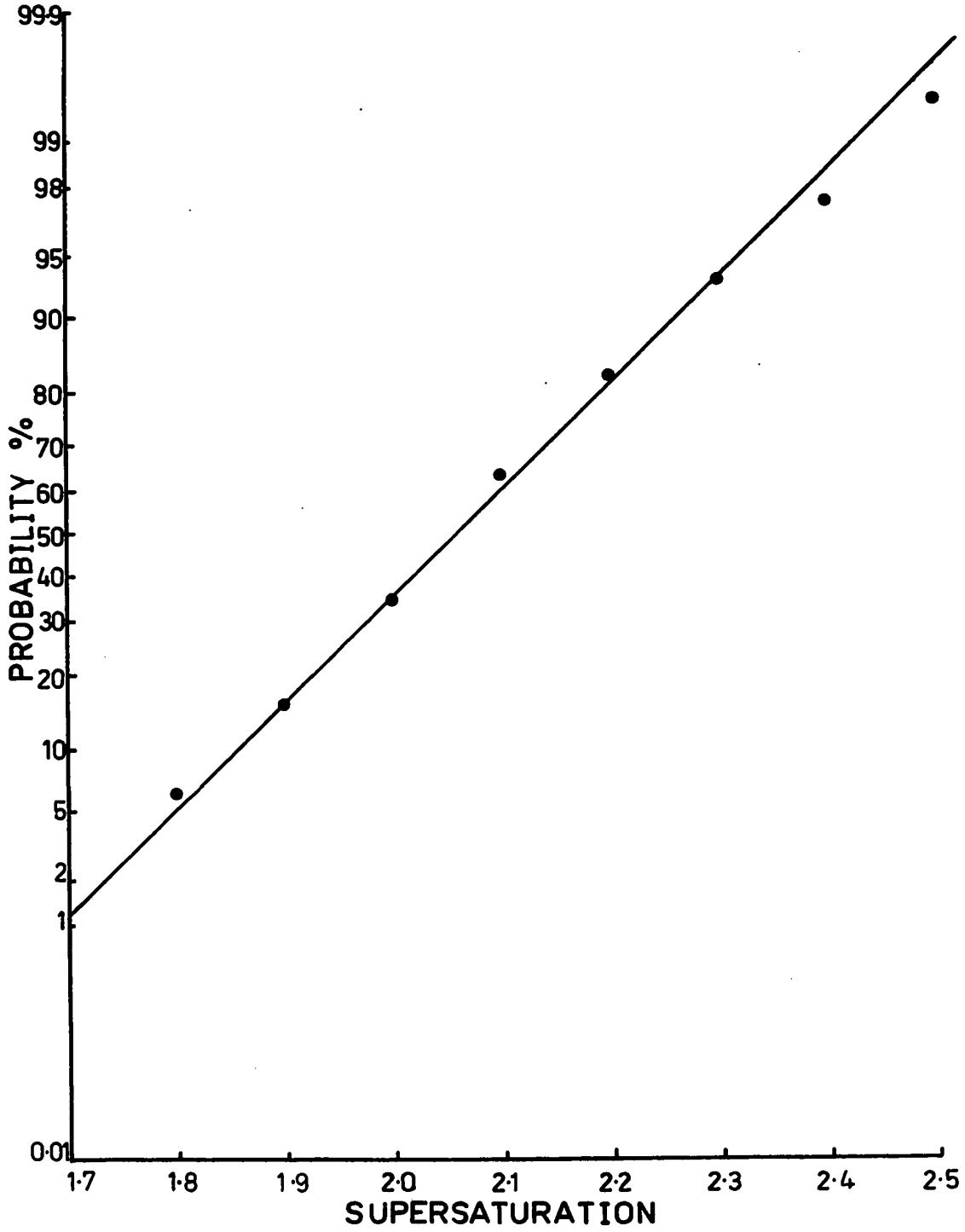
PROBABILITY %
99·9
99
98
95
90
80
70
60
50
40
30
20
10
5
2
1
0·01
1·7
1·8
1·9
2·0
2·1
2·2
2·3
2·4
2·5
SUPERSATURATION

Figure 9. Plots of $\underline{\log J}$ vs $\underline{(\log S)^{-2}}$ for lithium p-bromobenzylsulfoacetate.

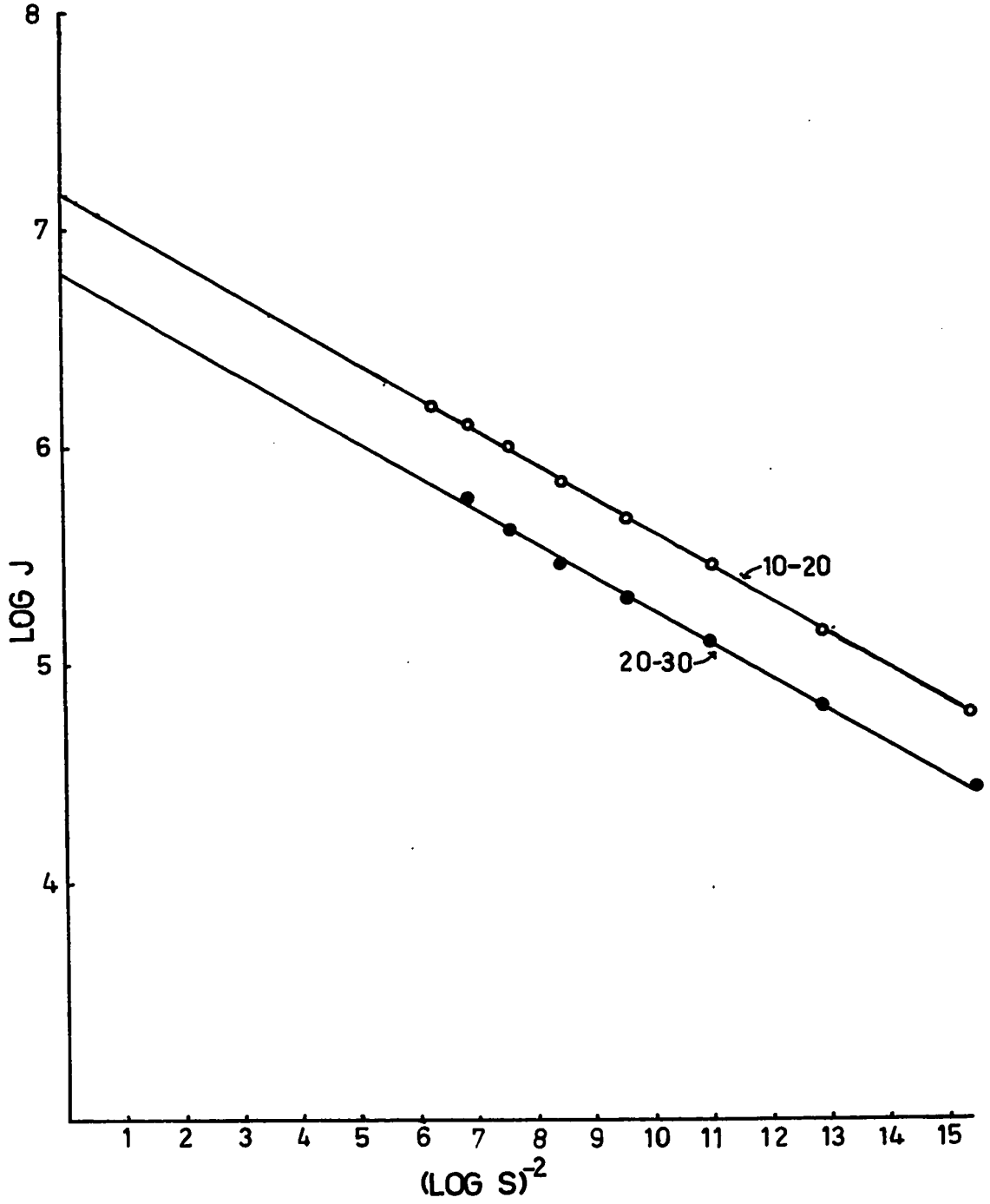
8
7
6
5
4
LOG J
10-20
20-30
1 2 3 4 5 6 7 8 9 10 11 12 13 14 15
(LOG S)$^{-2}$

Figure 10. Plot of Relative Frequency of Crystallization vs Supersaturation for lithium p-nitrophenacylsulfoacetate. Size range 10 - 20 μ. 356 droplets.

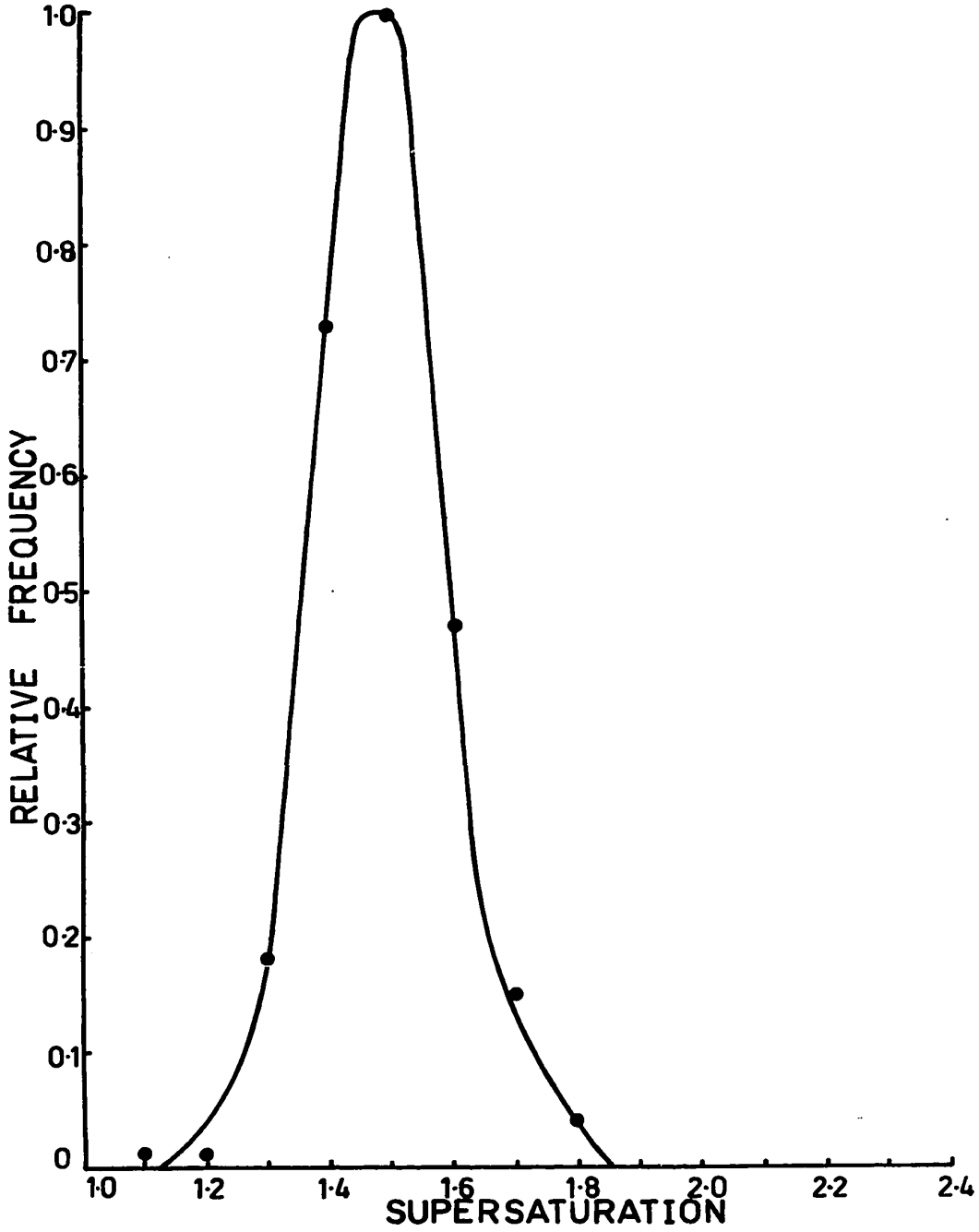
1·0
0·9
0·8
0·7
0·6
0·5
0·4
0·3
0·2
0·1
0
RELATIVE FREQUENCY
1·0
1·2
1·4
1·6
1·8
2·0
2·2
2·4
SUPERSATURATION

Figure 11. Plot of Probability of Crystallization vs Supersaturation for lithium p-nitrophenacylsulfoacetate. Size range 10 - 20 μ. 356 droplets.

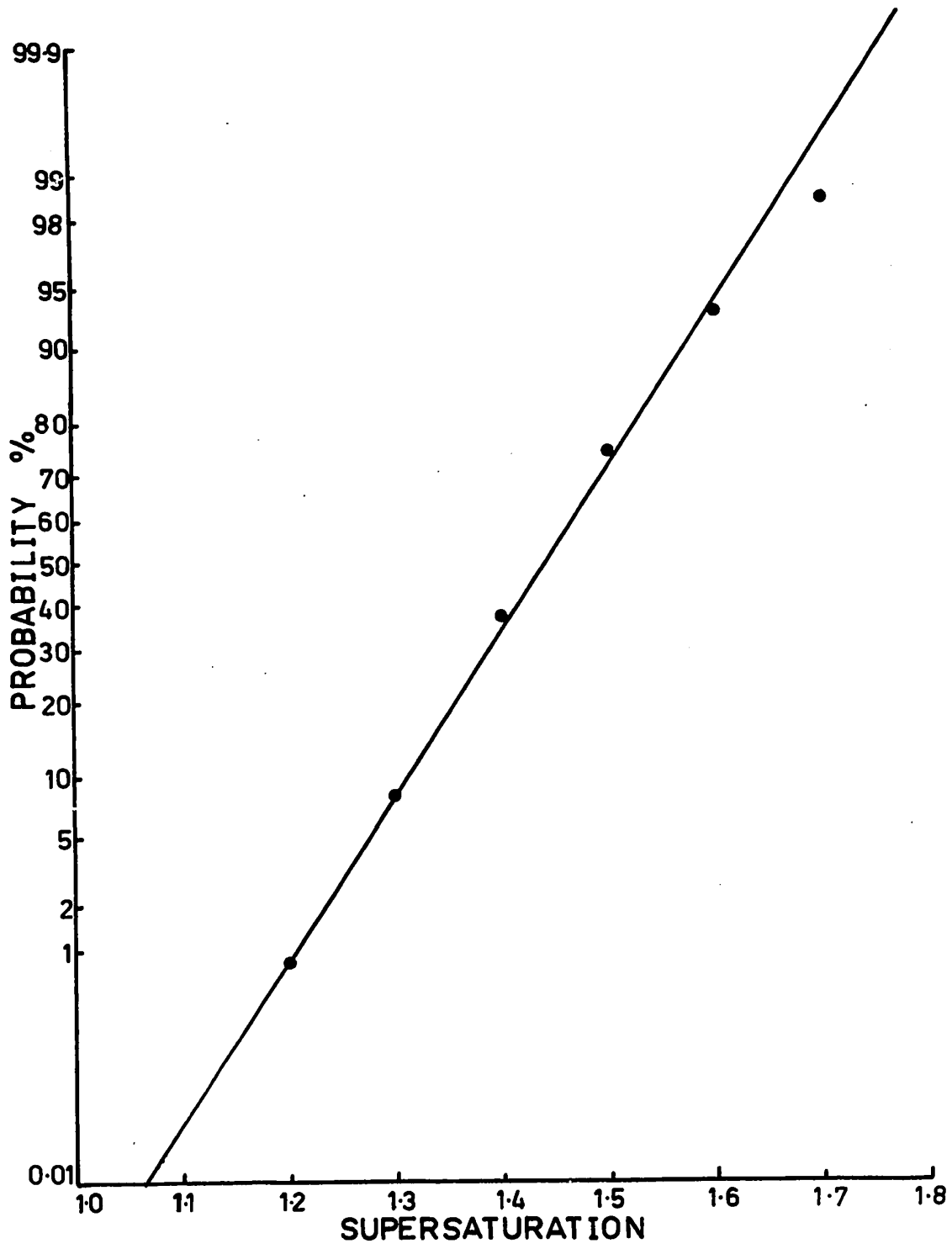
99·9
99
98
95
90
80
70
60
50
40
30
20
10
5
2
1
0·01
PROBABILITY %
1·0
1·1
1·2
1·3
1·4
1·5
1·6
1·7
1·8
SUPERSATURATION

Figure 12. Plots of $\underline{\log J}$ vs $\underline{(\log S)^{-2}}$ for lithium p-nitrophenacylsulfoacetate.

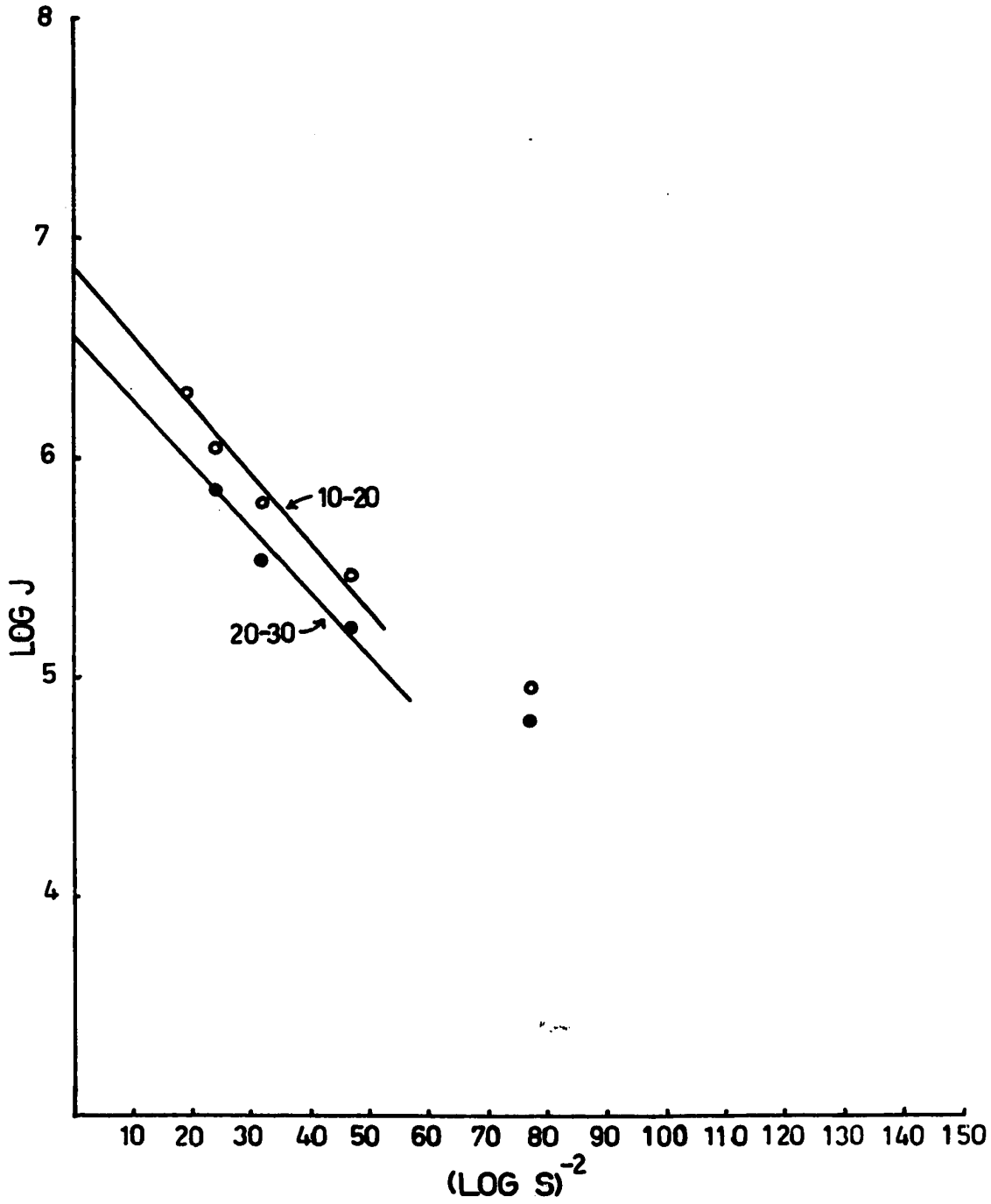
8
7
6
5
4
LOG J
10-20
20-30
10 20 30 40 50 60 70 80 90 100 110 120 130 140 150
(LOG S)$^{-2}$

Figure 13. Plot of Relative Frequency of Crystallization vs Supersaturation for lithium p-nitrobenzylsulfoacetate. Size range 10 - 20 μ. 506 droplets.

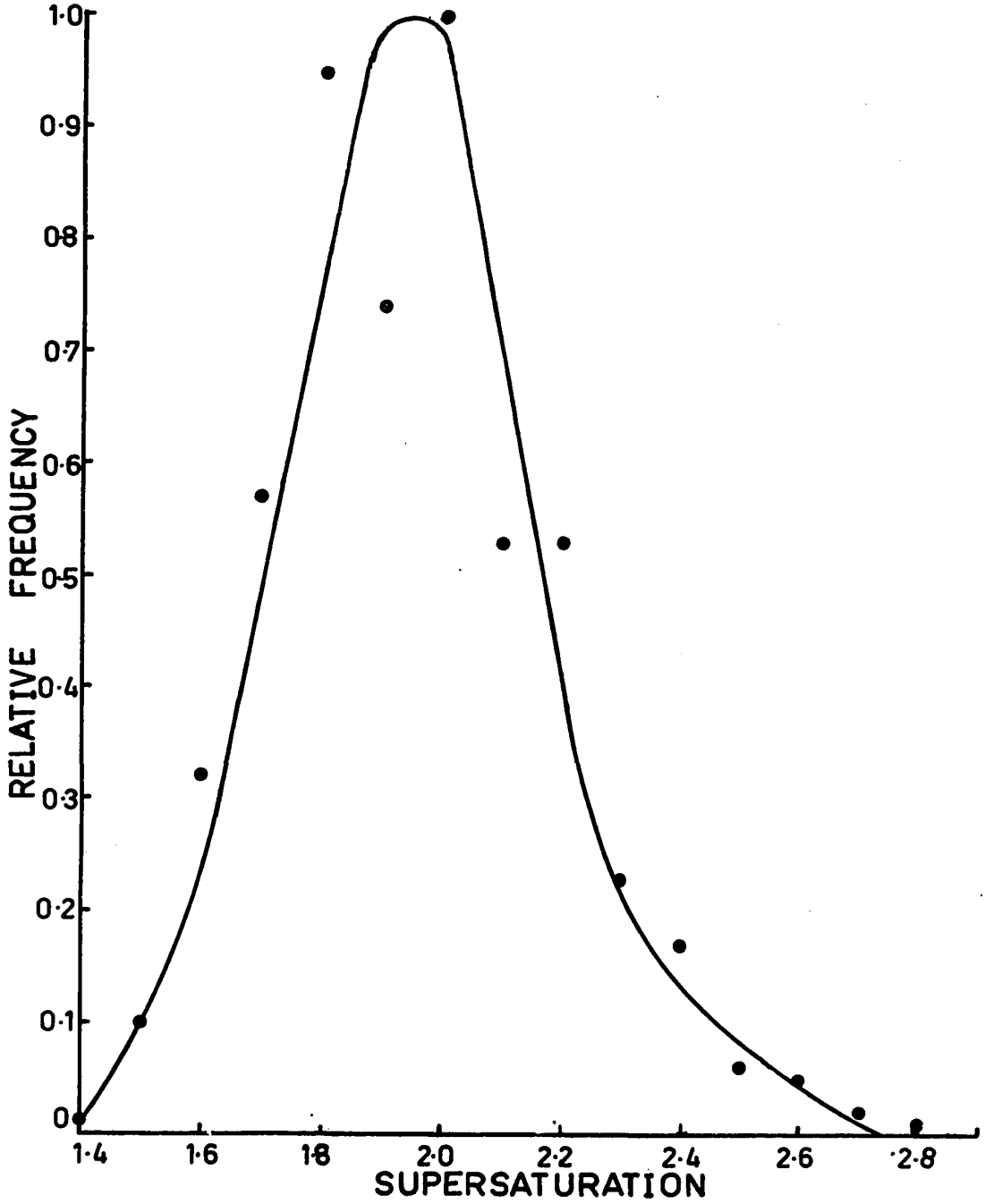
1·0
0·9
0·8
0·7
0·6
0·5
0·4
0·3
0·2
0·1
0
RELATIVE FREQUENCY
1·4
1·6
1·8
2·0
2·2
2·4
2·6
2·8
SUPERSATURATION

Figure 14. Plot of Probability of Crystallization vs Supersaturation for lithium p-nitrobenzylsulfoacetate. Size range 10 - 20 μ. 506 droplets.

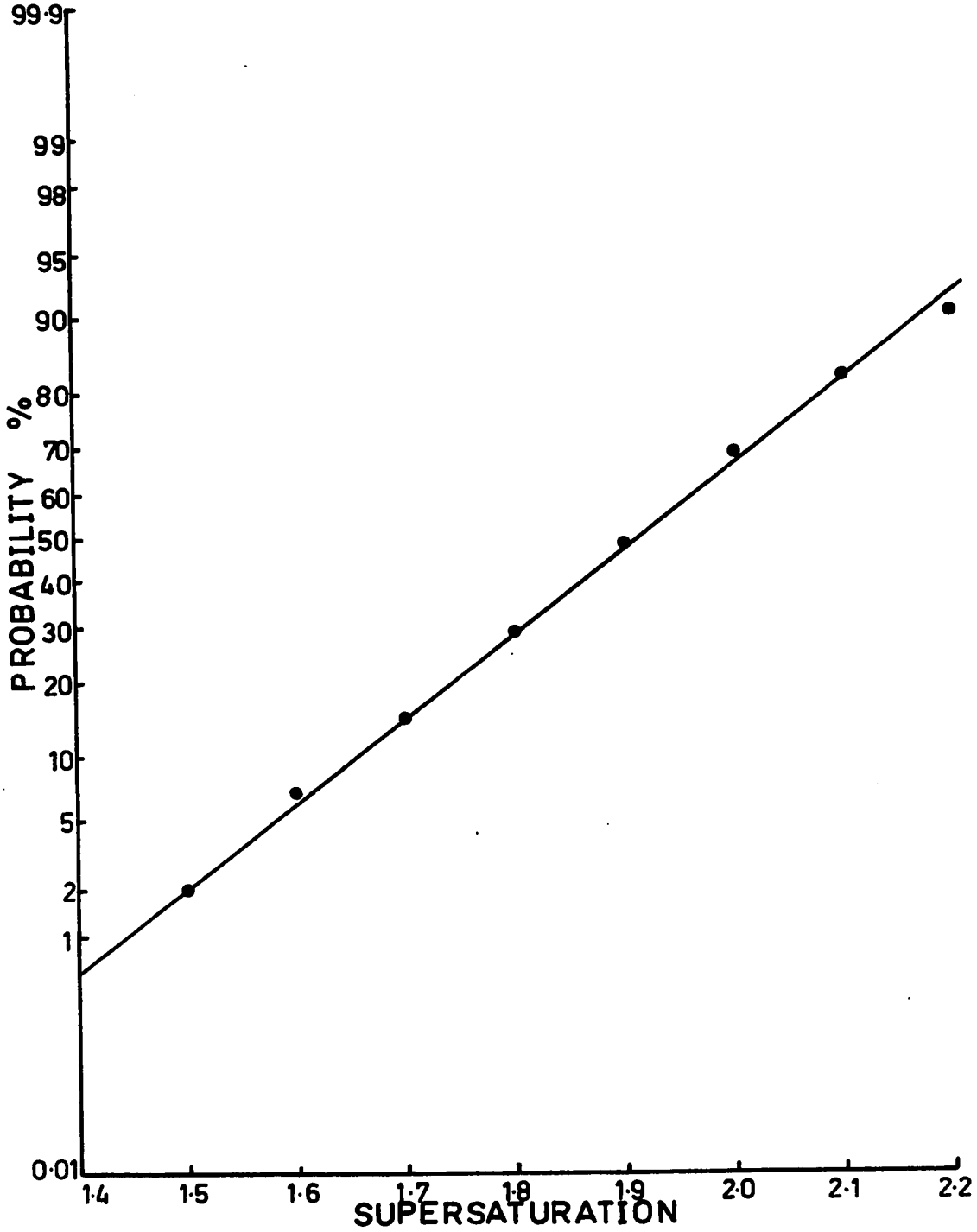
99·9
99
98
95
90
80
70
60
50
40
30
20
10
5
2
1
0·01
PROBABILITY %
1·4
1·5
1·6
1·7
1·8
1·9
2·0
2·1
2·2
SUPERSATURATION

Figure 15. Plots of $\underline{\log J}$ vs $\underline{(\log S)^{-2}}$ for lithium p-nitrobenzylsulfoacetate.

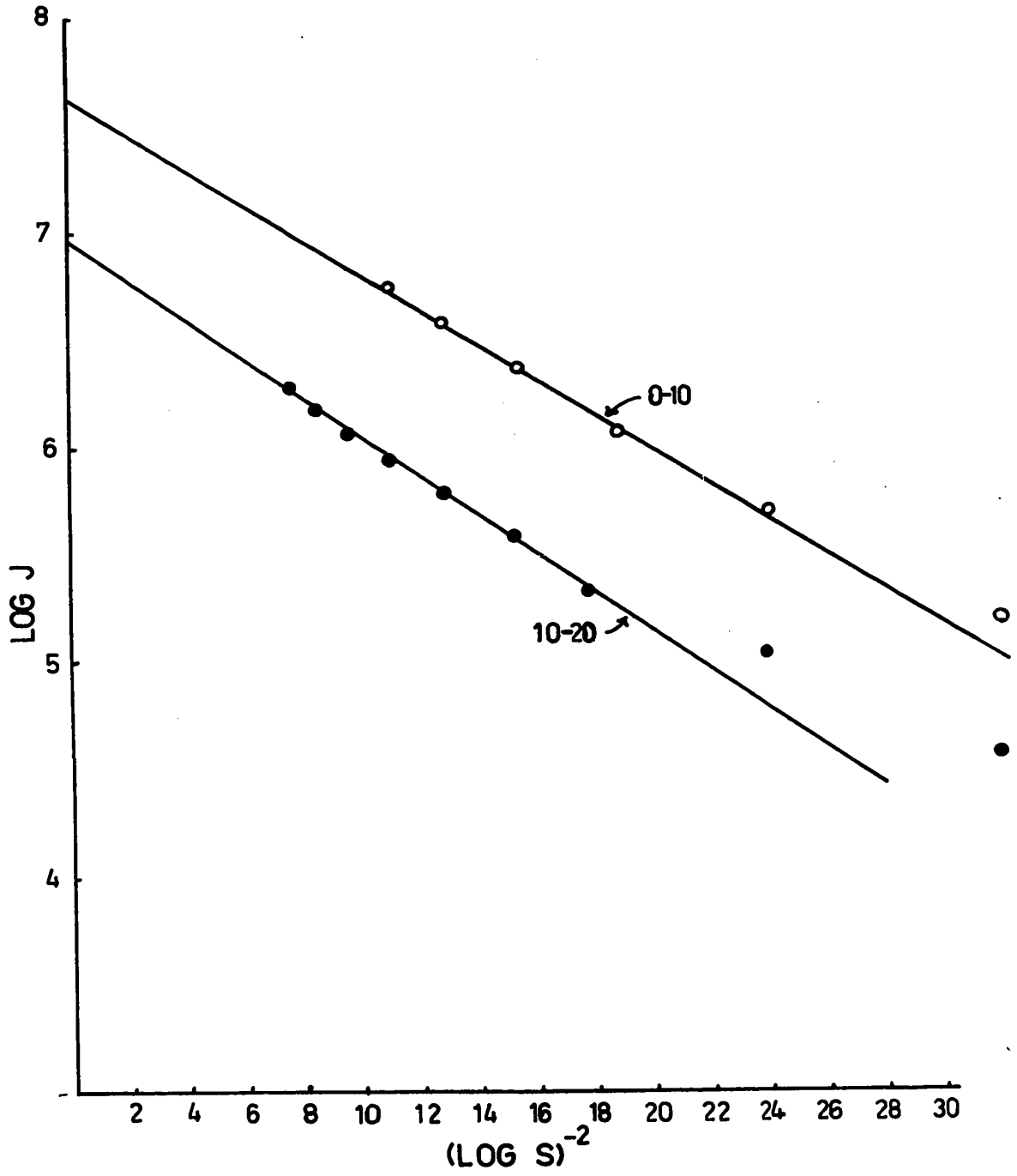
8
7
6
5
4
LOG J
0-10
10-20
2
4
6
8
10
12
14
16
18
20
22
24
26
28
30
(LOG S)$^{-2}$

Figure 16. Plot of Relative Frequency of Crystallization vs Supersaturation for lithium p-bromophenacylsulfoacetate. Size range 10 - 20 μ. 113 droplets.

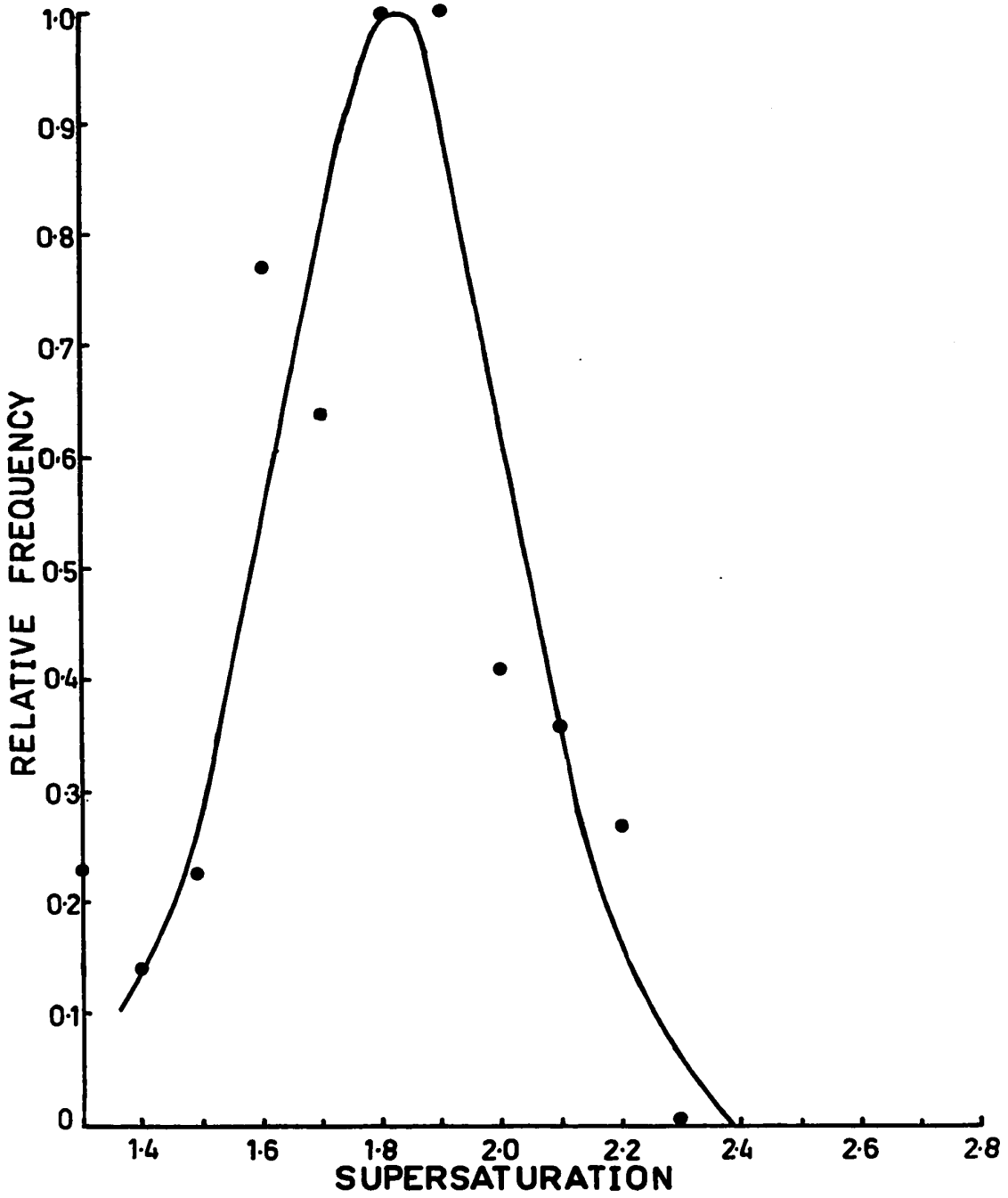
RELATIVE FREQUENCY
1·0
0·9
0·8
0·7
0·6
0·5
0·4
0·3
0·2
0·1
0
1·4
1·6
1·8
2·0
2·2
2·4
2·6
2·8
SUPERSATURATION

Figure 17. Plot of Probability of Crystallization vs Supersaturation for lithium p-bromophenacylsulfoacetate. Size range 10 - 20 μ. 113 droplets.

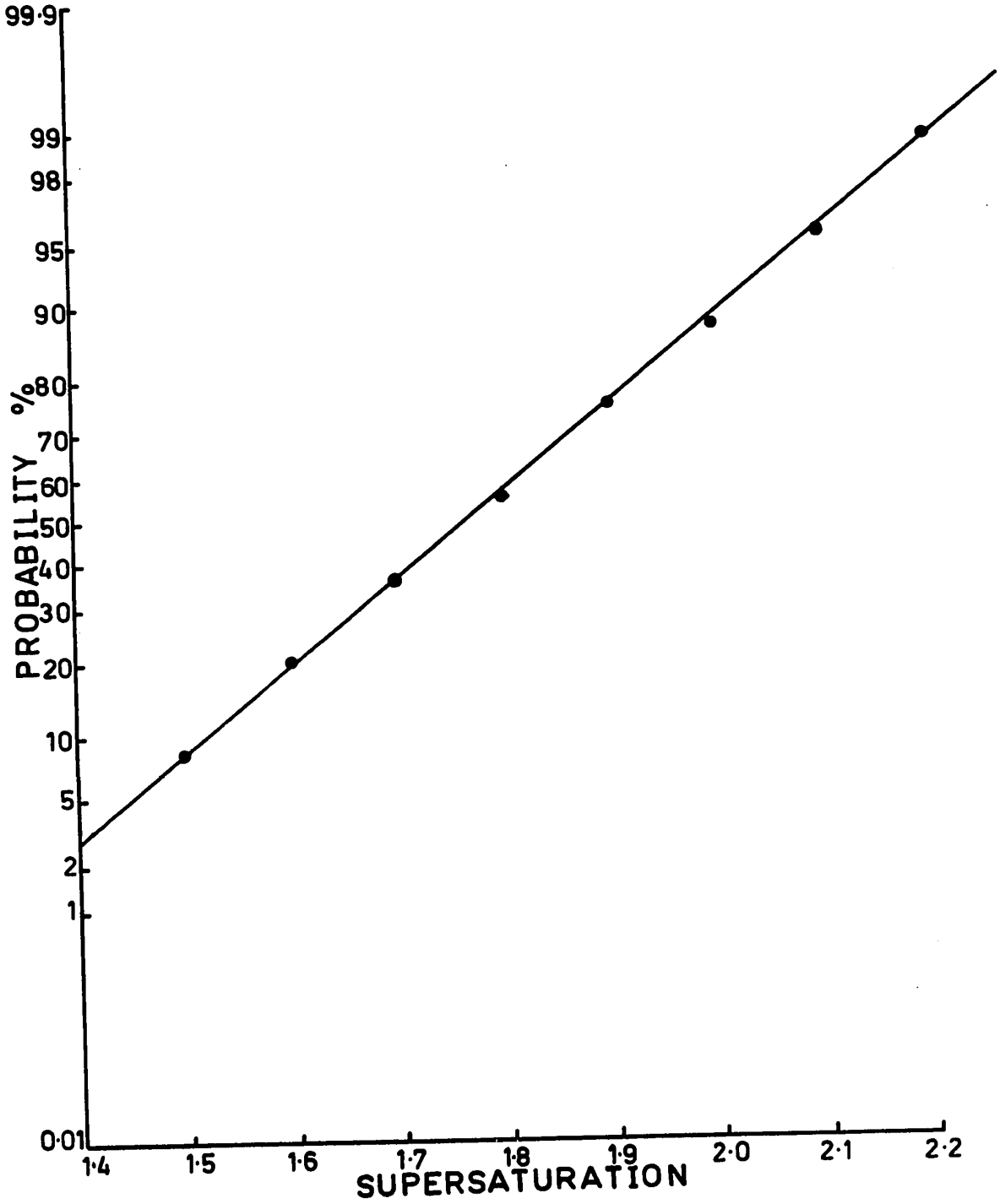
99·9
99
98
95
90
80
70
60
50
40
30
20
10
5
2
1
0·01
PROBABILITY %
1·4
1·5
1·6
1·7
1·8
1·9
2·0
2·1
2·2
SUPERSATURATION

Figure 18. Plots of $\underline{\log J}$ vs $\underline{(\log S)^{-2}}$ for lithium p-bromophenacylsulfoacetate.

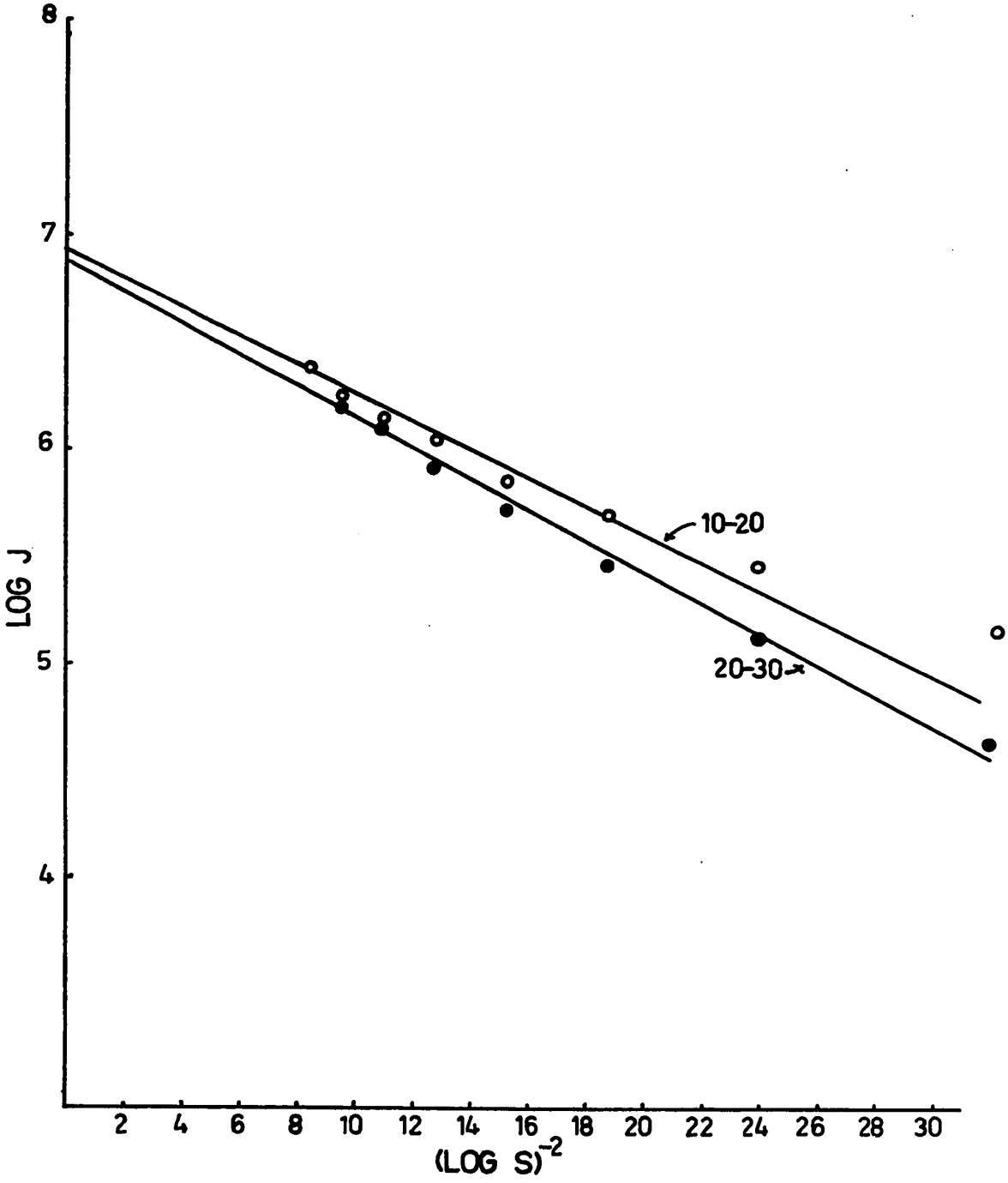
8
7
6
5
4
LOG J
10-20
20-30
2
4
6
8
10
12
14
16
18
20
22
24
26
28
30
(LOG S)$^{-2}$

bability paper. Linear relationships between log J and $(\log S)^{-2}$ were found also. One problem arose, however, for the case of lithium p-nitrophenacylsulfoacetate in the plot of log J vs $(\log S)^{-2}$. Because of the very low values of supersaturation over which this compound nucleated, the plot extended into the region near where $(\log S)^{-2} \rightarrow \infty$ (ie. near $S \rightarrow 1$), thus it was necessary to exclude from the least square fit those few low values of S which gave rise to this explosive increase.

Those nucleation parameters of interest, (n^*, r^*, ΔG^*) discussed in Section I.B.1. were calculated using equations (4), (5), and (6). The resulting values for each of them are compiled in Table 3 along with other useful derived data (log A, σ, S^*) for each size group of each compound studied.

As may have been anticipated, it can be seen that the value of the interfacial energy is the same for each volume range. The values for the size of the critical nucleus are also equal within experimental error. It would be necessary to study a much wider range of droplet sizes, in order to assess the effect of droplet volume on nucleation parameters.

Also from Table 3 it can be seen that there is close agreement among the values of the interfacial energy and the pre-exponential constant reported for each ester studied. Since these compounds are structurally very similar, it is not surprising to find such similarity. However, the large discrepency between these values and normally expected values requires further comment.

Generally, calculated values of log A are found to be between 25 and 30, while the macroscopic values of σ are of the order of 100 - 200 ergs-cm^{-2}. In order to understand the large differences between these values and those obtained in this work (see Table 3), it is necessary to

TABLE 3

NUCLEATION RESULTS

	1	2	3	4
v x 10^{22}(cm^3)	2.63	2.64	2.54	2.9
10 - 20μ				
slope†	0.159	0.0285	0.0846	0.0669
intercept†	7.21	6.78	6.89	6.92
σ(ergs/cm^2)	4.83	2.71	4.01	3.36
S*	1.41	1.16	1.29	1.25
n*	97	209	124	141
r*(Å)	19.2	24.7	19.6	21.4
ΔG*(kcal/mole)	9.48	8.86	9.10	9.10
20 - 30μ			(0-10μ)	
slope†	0.155	0.0269	0.0818	0.0696
intercept†	6.81	6.47	7.64	6.83
σ(ergs/cm^2)	4.79	2.66	3.97	3.41
S*	1.42	1.16	1.27	1.26
n*	90	201	148	135
r*(Å)	18.6	24.4	20.8	21.2
ΔG*(kcal/mole)	8.98	8.49	10.1	9.03

KEY
1 lithium p-bromobenzylsulfoacetate
2 lithium p-nitrophenacylsulfoacetate
3 lithium p-nitrobenzylsulfoacetate
4 lithium p-bromophenacylsulfoacetate

---

† from least squares fit of log J vs $(\log S)^{-2}$

reconsider the assumptions of classical nucleation theory. It will be recalled that the basic theory considers only the equilibrium size and shape of the aggregate required to form the critical nucleus. There is no consideration given to the effect of liquid structure on nucleation. The influence of the structure of a solution on the nucleation parameters appears in two ways. First, it may raise or lower the energy barrier, ΔG^*, depending on the amount of molecular rearrangement and desolvation, and, secondly, it may affect the pre-exponential kinetic constant.

Compared with crystal nulceation from isotropic solution a lowering of the energy barrier to nucleation should result for the transformation from a highly structured mesophase to a crystal of similar structure because only slight molecular re-arrangements are required. In this study the lowering of ΔG^* has been reflected in the lower than normal value of σ. Any significant amount of hydrogen bonding which would help to relieve excess surface energy would also contribute to the lowering of σ.

To our knowledge the only other work published on nucleation from liquid crystalline systems is the recent work of Pochan and Gibson (71, 72). They have studied the nucleation of thin films of several cholesteric liquid crystalline melts by measuring the time required for the appearance of a crystal in a heated sample plunged into a thermostated bath. Their values for the interfacial energy are of the same order of magnitude as those reported in this work and are presented for comparison in Table 4.

The pre-exponential factor is a kinetic term and thus depends on the frequency of collision of monomers with the critical-sized aggregate. This term is usually lower for solutions than for melts because

TABLE 4

INTERFACIAL ENERGY VALUES FOR PURE CHOLESTERYL DERIVATES REPORTED BY POCHAN AND GIBSON (72)

Cholesteryl Derivative	$\bar{\sigma} = (\sigma_u^2 \sigma_e)^{1/3}$ ergs/cm^2
Formate	2.82
Propionate	1.07
Pentanoate	1.17
Hexanoate	1.57
Nonanoate	2.25
Chloride	3.92

of the smaller number of monomers available. Furthermore it is affected by the increased viscosity of a supersaturated system since the rate of diffusion is lowered. In this study we have ignored the effect of the extensive micellar structure of the solutions prior to nucleation. Until these systems have been studied more fully it will be difficult to quantitatively account for their effect on the nucleation event. It is clear, however, that whether an embryo is considered to form by statistical fluctuations within a micelle or by molecular transport between them, micelles cause a serious restriction in the number of monomers available for collision.

III.C.4. ERRORS

Generally researchers in the field of nucleation are negligent in reporting errors. In view of the limitations in the applicability of nucleation theory outlined in Section I.B.3. this is not surprising. In fact it would be mis-leading to report, for example, the size of the critical nucleus as 100 $\pm$ 10 molecules, since this is attaching too much confidence to the quantitative reliability of the present theory. Usually if the order of magnitude is the same as that reported for similar compounds, the result is acceptable. Here, however, we will report the experimental errors involved in the various measurements leading to the solution to the nucleation rate equation.

The governing error in the droplet contraction technique is the measurement of the droplet diameter. The droplets were measured on a millimeter scale and the absolute error in the measurement of any droplet diameter was thus $\pm$ 0.2 mm. This means that the relative error in supersaturation for a 20μ droplet (measuring about 12-13 mm) is about 5%.

Other errors will be illustrated for the specific case of li-

thium p-bromobenzylsulfoacetate. The median was selected as the most suitable diameter to represent the size range of each group of droplets (the distribution was not symmetrical). Thus in the range 10 - 20μ, 70% of the droplets were 16 ± 2μ, while 68% of those in the range 20 - 30μ were 23 ± 2μ. For the most representative rate of change of supersaturation with time, the distribution was quite symmetrical so that the mean value was used. The mean with its standard deviation was 0.010 ± 0.003 $min.^{-1}$ for the range 10 - 20μ and 0.014 ± 0.003 $min.^{-1}$ for the range 20 - 30μ . The fit of the log J vs $(\log S)^{-2}$ data was performed by a linear least squares method with the following results and standard deviations:

for the group 10-20μ the slope was - 0.159±0.001 and intercept 7.209±0.007

for the group 20-30μ the slope was - 0.155±0.001 and intercept 6.806±0.005.

III.D. SUMMARY

During the course of this work four new esters of sulfoacetic acid were prepared and characterized. Their supersaturated solutions were found to exhibit lyotropic liquid crystalline behaviour and advantage was taken of this to make them interesting subjects for a nucleation study.

The droplet contraction technique, useful for studying the homogeneous nucleation of solids from aqueous solution, was employed to study the various phase changes which occurred as the solution concentration increased. These phase changes were readily observed using plane polarized light. Up to three different liquid crystalline mesophases for a single compound were observed and their existence was explained by analogy with the well-known aliphatic sulfonic acid soaps. There were indications that the mesophase to mesophase and the mesophase to solid phase transformations exhibited the metastability associated with a nucleation energy barrier.

The nucleation of the solid phase was interpreted in terms of the classical nucleation theory. As is normal for highly soluble substances the critical supersaturations were found to be very low and the numbers of molecules involved in the critical nuclei was high. Unlike other cases, however, the interfacial energy term was quite low. This is interpreted in terms of the pre-nucleation liquid structure. The values for the pre-exponential kinetic constant, although much lower than calculated values, were consistent with usual experimental evaluations.

The results of this work may lead to a more extensive study of the relationship between liquid structure and crystallization phenomena. With renewed interest in the chemistry of concentrated aqueous solutions,

the application of laser-beams is expected to gain prominence in the study of supersaturated solutions. In this respect the scattering of laser-beams by liquid crystalline solutions in which mesophase to mesophase transformations are occurring can be used to evaluate the entropy change of the process.

As mentioned in Section III.B.3. the liquid crystalline behaviour is exhibited only in supersaturated systems. Thus, no reference equilibrium concentration is available to measure the metastability of the transformations. Such a concentration may be obtainable from a supercooling experiment in which the reverse transition can be easily brought about by heating. Furthermore, a supercooling experiment to verify the results of this study would be of great interest, since there are few systems available for nucleation studies which lend themselves to independent verification.

The droplet contraction technique requires some experimental improvements. First, a method for preparing uniform-sized droplets in evenly populated dispersions would provide a more uniform rate of change of supersaturation, $(\frac{dS}{dt})$ and thus require the measurement of only a few representative droplets to provide dS/dt. This would reduce much of the tedious and time consuming work of measuring droplets. Also the provision of a statistically significant number of mono-sized droplets would remove the difficulties associated with the grouping of droplets into size ranges.

With the present availability of automated scanning densitometers it may be worthwhile to adapt such a device to scan a photographic record of the experiment for the measurement of droplet sizes and the determination of phase changes. This would increase accuracy, remove human

prejudice errors and reduce the amount of time required for data acquisition.

APPENDIX 1

CHARACTERIZING SPECTRA OF THE FOUR ESTERS

U.V.-Visible Spectral Data

	λ_{max}	ε_m
lithium p-bromobenzylsulfoacetate	222	11,500
lithium p-nitrobenzylsulfoacetate	273	9,000
lithium p-nitrophenacylsulfoacetate	267	14,700
lithium p-bromophenacylsulfoacetate	263	17,700

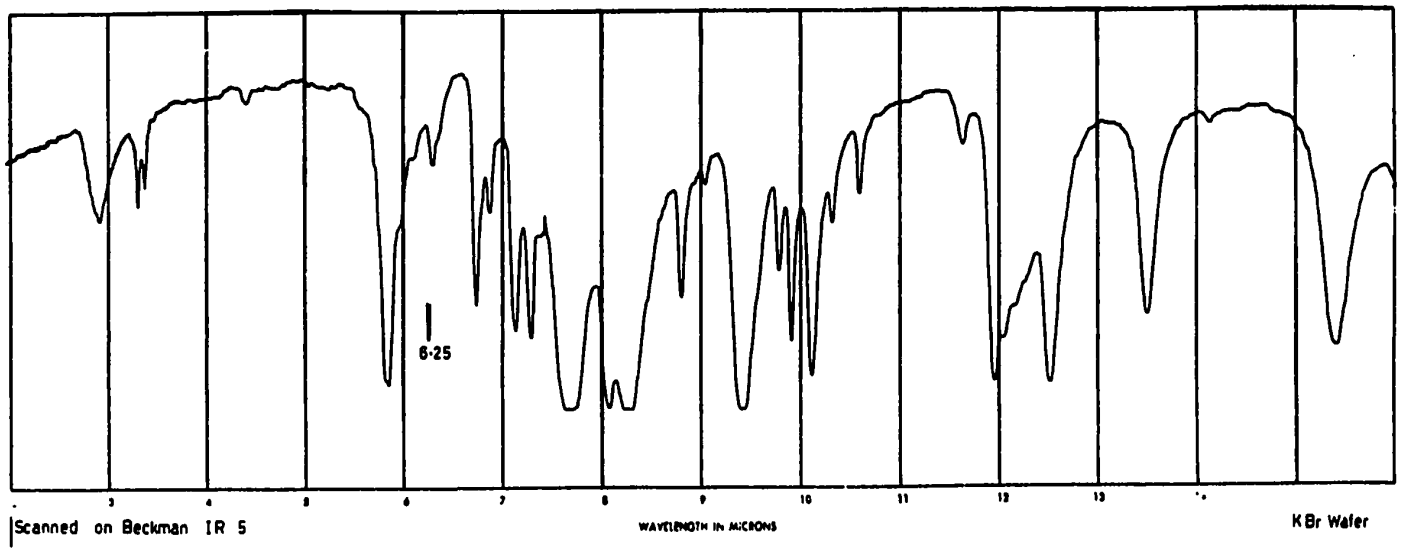

Infra red spectrum of lithium p-bromobenzylsulfoacetate

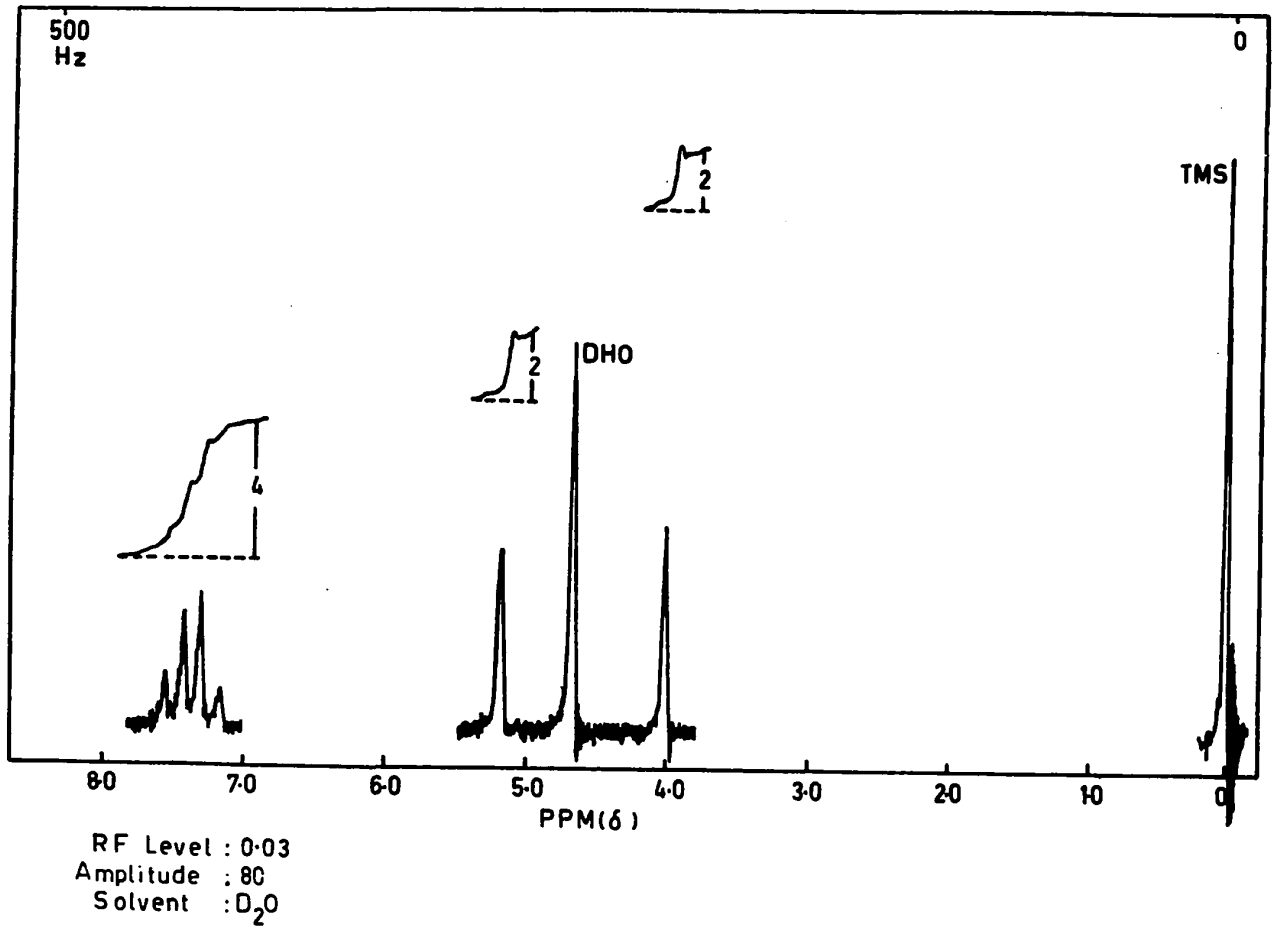

N.M.R. spectrum of lithium p-bromobenzylsulfoacetate

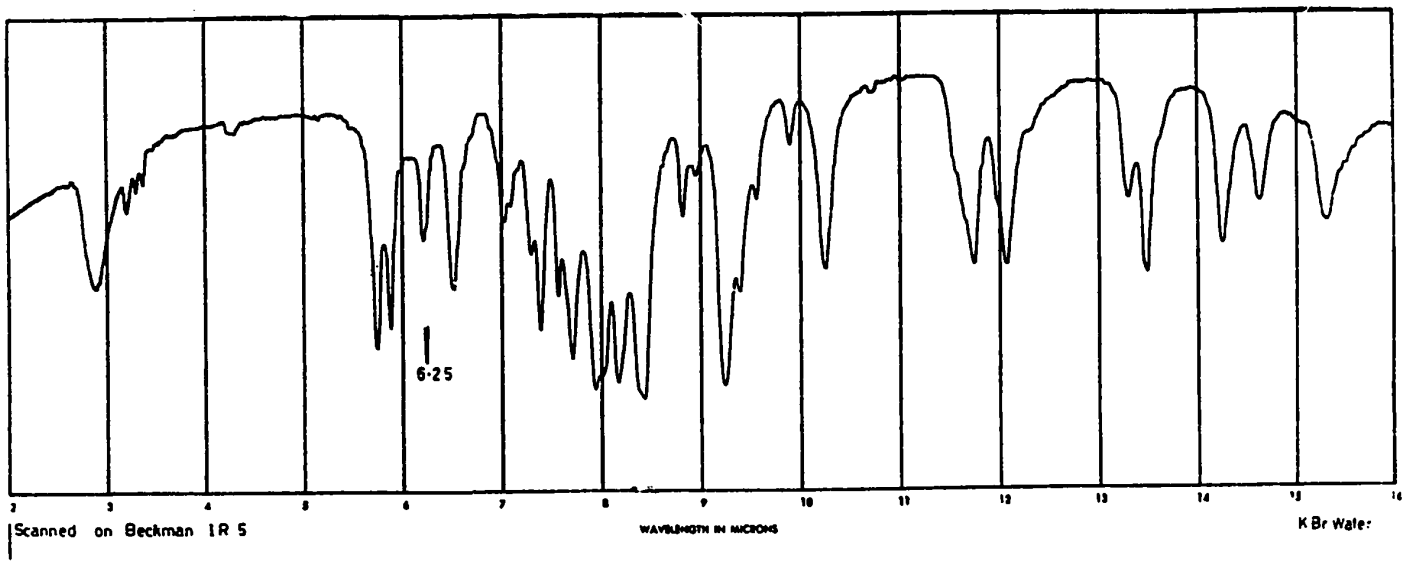

Infra red spectrum of p-nitrophenacylsulfoacetate

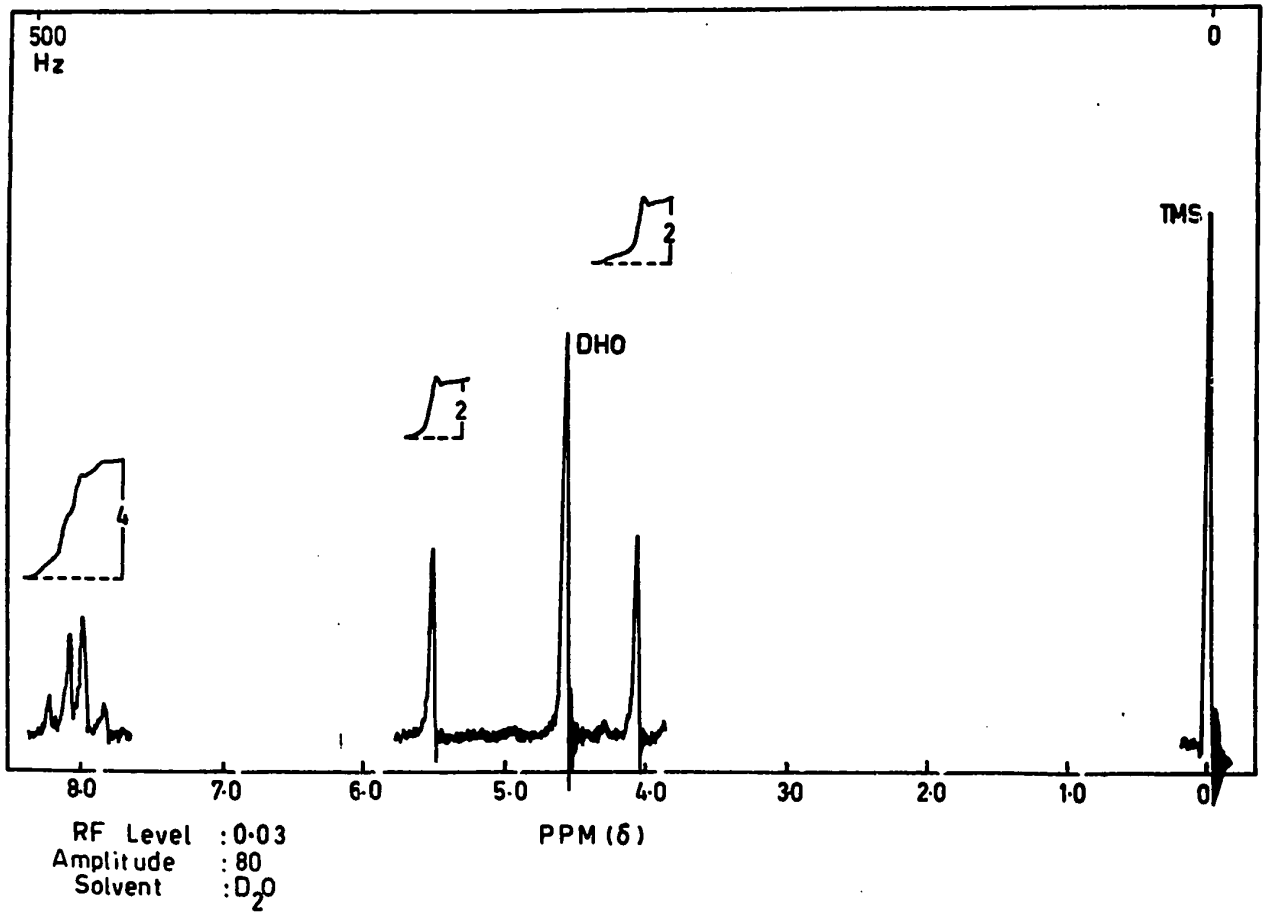

N.M.R. spectrum of lithium p-nitrophenacysulfoacetate

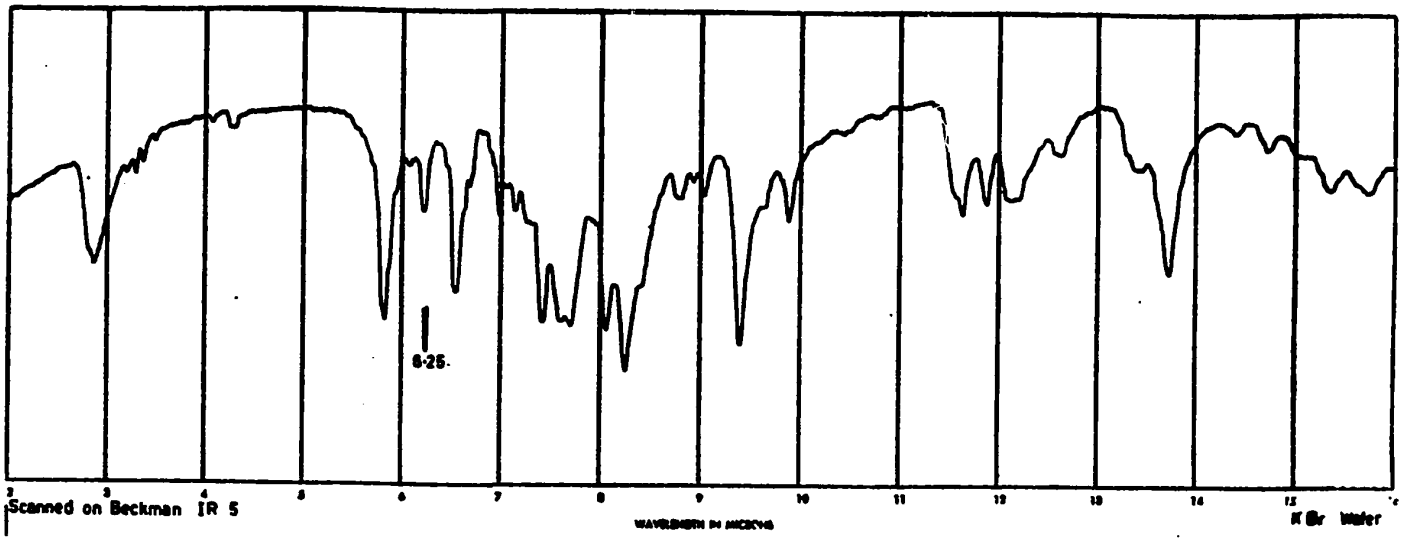

Infra red spectrum of lithium p-nitrobenzylsulfoacetate

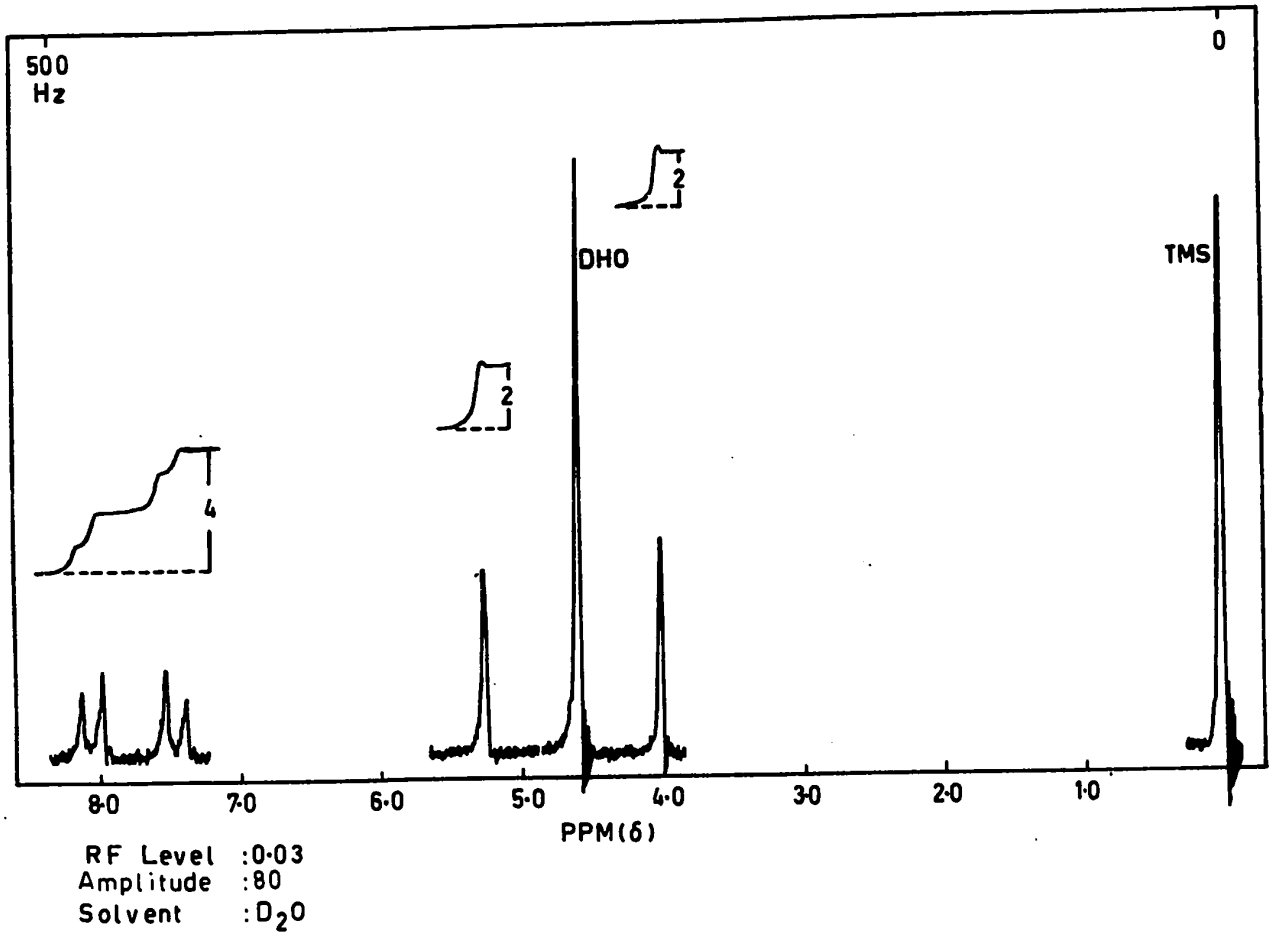

N.M.R. spectrum of lithium p-nitrobenzylsulfoacetate

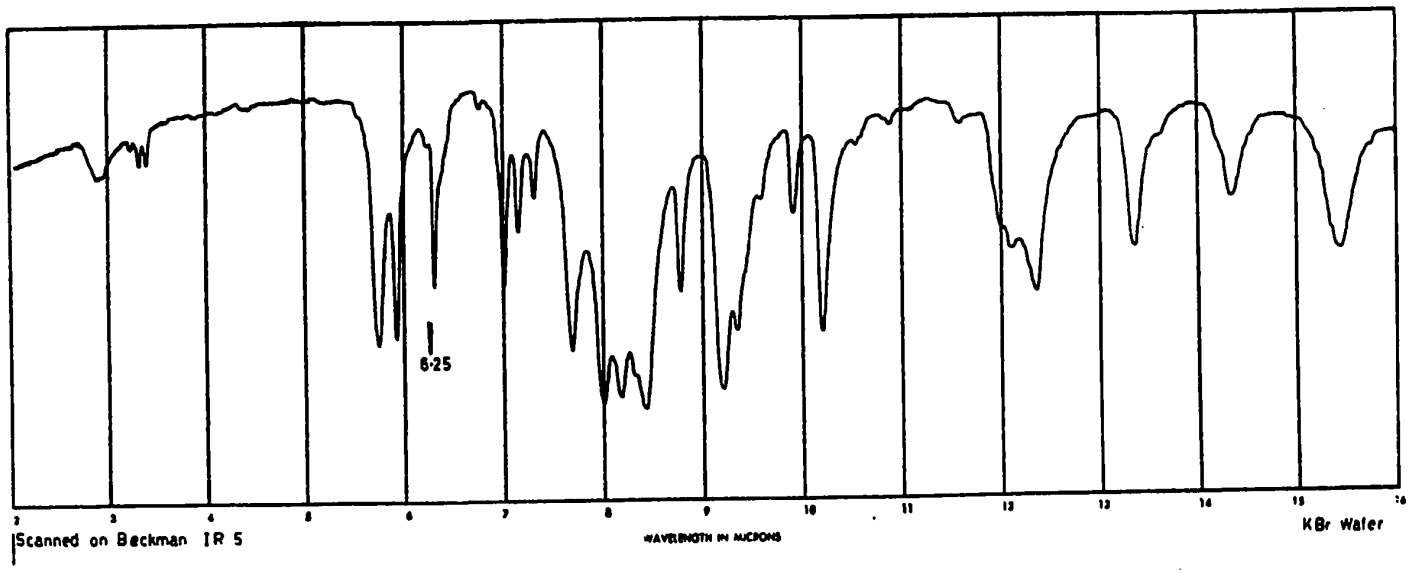

Infra red spectrum of lithium p-bromophenacylsulfoacetate

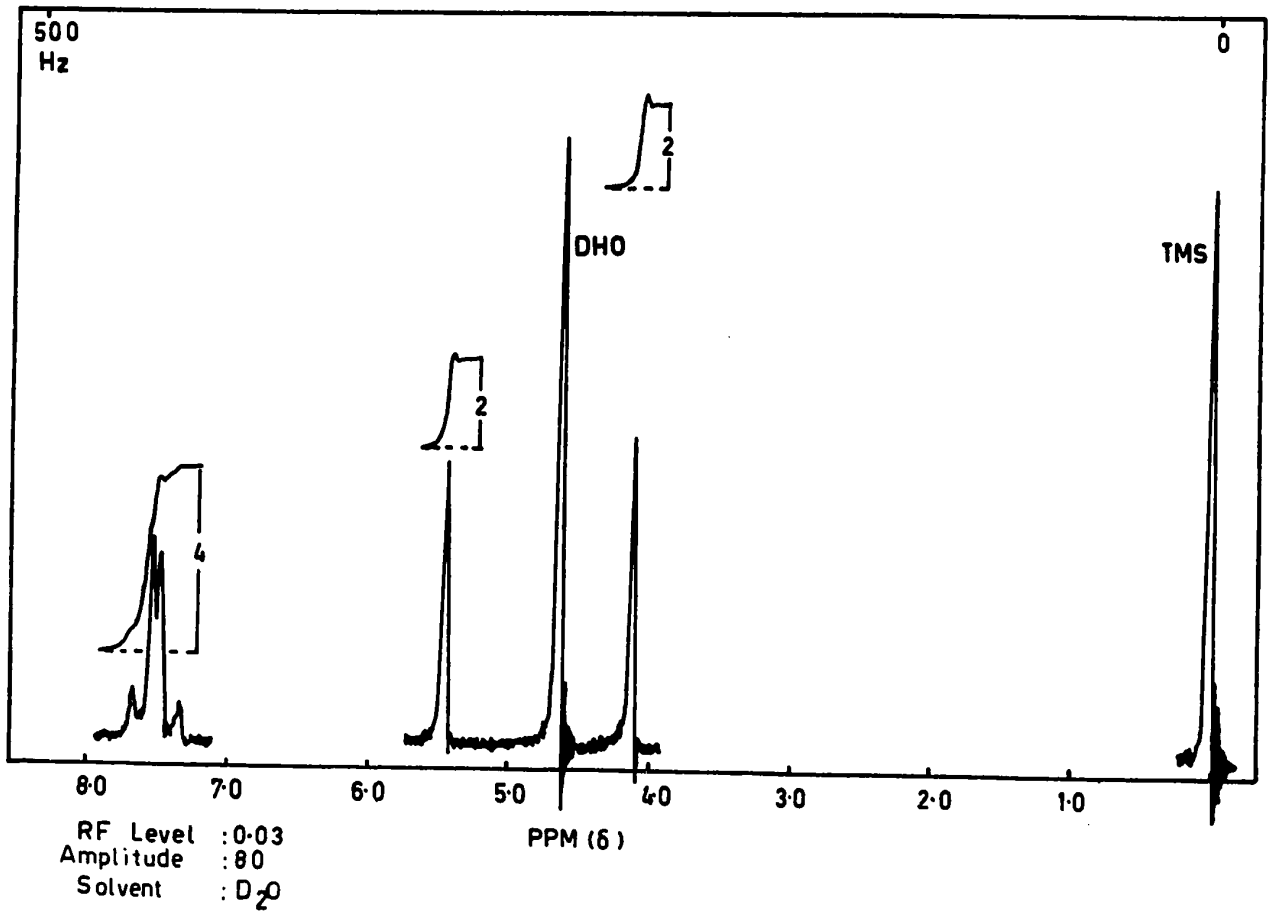

N.M.R. spectrum of lithium p-bromophenacylsulfoacetate

APPENDIX 2

CALCULATION OF SOLUTE CONCENTRATION IN DROPLETS DISPERSED IN SILICONE FLUID - AN IDEAL CASE

In the droplet contraction technique the concentration of the solute in a droplet dispersed in a silicone fluid increases by the selective extraction of water from the droplet. The process involves physical transfer (ie. no chemical reaction at the interface) from a spherical droplet into a stagnant medium. Below is the derivation of the relationship between the concentration and time for an ideal case.

Assumptions:

1. The concentration of the transfering component in the bulk phase remains constant during the time interval (ie. small amount of water transferred).
2. The concentration at the droplet/bulk interface corresponds to equilibrium conditions.
3. The droplet has uniform concentration.
4. The equilibrium concentration for the transferring component is independent of the concentration of the non-transferring component in the droplet (realistic for low concentrations and small concentration changes).

Notation:

- c_∞ - concentration of water in bulk solution
- c^* - equilibrium concentration of water in the silicone phase at the droplet surface
- c_s - solute concentration
- D - droplet diameter at any time
- D_o - initial droplet diameter

m - mass

V - volume

ρ - density

α - is a diffusion coefficient (cm^2-sec^{-1})

Assuming no volume change on mixing then the concentration of a species (S) in a solvent (w) is given by

$$c_s = \frac{m_s}{V_s + V_w}$$

so that $$\frac{dc_s}{dt} = -m_s (V_s + V_w)^{-2} \frac{dV_w}{dt} \qquad \text{(A-1)}$$

$\frac{dV_w}{dt}$ is related to the rate of mass transfer from the water droplet

$$\frac{dm_w}{dt} = -k_c \pi D^2 (c^* - c_\infty)$$

where k_c is a mass transfer coefficient given by $k_c = \frac{2\alpha}{D}$.

From the density relation $m_w = \rho_w V_w$

then $$\rho_w \frac{dV_w}{dt} = -k_c \pi D^2 (c^* - c_\infty).$$

Assuming that the loss in total volume equals the loss of water

$$\frac{dV_w}{dt} = \frac{dV_t}{dt} = \frac{-k_c \pi D^2}{\rho_w} (c^* - c_\infty).$$

Since $$V_t = \frac{\pi D^3}{6}, \text{ then } \frac{dV_t}{dt} = \frac{3\pi D^2}{6} \frac{dD}{dt} \qquad \text{(A-2)}$$

giving $$\frac{dD}{dt} = \frac{-2k_c (c^* - c_o)}{\rho_w} = \frac{-2}{\rho_w} \left(\frac{2\alpha}{D}\right) (c^* - c_\infty). \qquad \text{(A-3)}$$

Integrating this expression we have

$$\int_{D_o}^{D} DdD = \int_{o}^{t} \frac{4\alpha}{\rho_w} (c^* - c_\infty)\, dt$$

$$D_o^2 - D^2 = k_2 t \quad \text{where } k_2 = \frac{8\alpha}{\rho_w} (c^* - c_\infty) \text{ is a constant}$$

Thus $D^2 = D_o^2 - k_2 t$ is a straight line for D^2 vs t. (A-4)

Returning to equation (A-1) and using equations (A-2) and (A-3) we have

$$\frac{dc_s}{dt} = -m_s V_t^{-2} \frac{dV_t}{dt} = -m_s \left(\frac{6}{\pi}\right)^2 \frac{1}{D^6} \left[3D^2 \frac{\pi}{6} \frac{dD}{dt}\right]$$

$$= -m_s \left(\frac{6}{\pi}\right)^2 \frac{1}{D^6} \left[3D^2 \frac{\pi}{6} \frac{4\alpha}{\rho_w D} (c^* - c_\infty)\right]$$

$$= k_1 \frac{1}{D^5} \qquad \text{(A-5)}$$

here $k_1 = \frac{72}{\pi} \frac{m_s}{\rho_w} \alpha (c^* - c_\infty)$ is a constant.

Integrating expression (A-5) noting relation (A-4) gives

$$\int_{c_{s_o}}^{c_s} dc_s = \int_{o}^{t} k_1 (D_o^2 - k_2 t)^{-5/2} \left(\frac{-1}{k_2}\right) d (D_o^2 - k_2 t)$$

$$c_s - c_{s_o} = \frac{6m_s}{\pi} \left[\frac{1}{(D_o^2 - k_2 t)^{3/2}} - \frac{1}{D_o^3}\right] \qquad \text{(A-6)}$$

where $\frac{2k_1}{3k_2}$ reduces to $\frac{6m_s}{\pi}$. Equation (A-6) thus gives the concentration at any time. For our purposes we want the supersaturation - $S = \frac{c_s}{c_{s_o}}$.

From equation (A-6)

$$\frac{c_s}{c_{s_o}} - 1 = \frac{6m_s}{\pi c_{s_o}} \left[\frac{1}{D^3} - \frac{1}{D_o^3}\right]$$

But $$c_{s_o} = \frac{m_s}{V_t} = \frac{6m_s}{\pi D_o^3}$$

thus $$\frac{c_s}{c_{s_o}} = 1 + \frac{6m_s}{\pi}\left(\frac{\pi D_o^3}{6m_s}\right)\left[\frac{1}{D^3} - \frac{1}{D_o^3}\right]$$

$$= 1 + \left(\frac{D_o}{D}\right)^3 - 1$$

Therefore, $$S = \frac{c_s}{c_{s_o}} = \left(\frac{D_o}{D}\right)^3$$ for an ideal case.

APPENDIX 3

COMPUTER PROGRAMS

PROGRAM 1

This program was used to calculate the supersaturation at each time interval. In the input deck each card contained the raw data for a separate droplet - the diameter (in arbitrary units) for each time interval, the final diameter, the time for each phase transition and the field of view from which the data was taken. The cards were arranged in order according to increasing final diameter.

Program 1 converts the diameters to microns and records the number of droplets in any size group specified by LIMIT1 and LIMIT2. The supersaturation for each time interval is calculated. The program provides a punched output for these supersaturations and a tabulation of the supersaturation at crystallization, the time of each phase transition and the field of view.

PROGRAM 2

This program was used only to sort the droplets into size groups. The data deck was arranged in order of increasing final diameter.

Program 2 converts the final diameter to microns with the factor SCALE. By suitable choice of LIMIT1 and LIMIT2, the number of droplets in any size range can be obtained.

PROGRAM 3

This program was used to calculate the number of droplets crystallized, the relative frequency of crystallization

and the probability of crystallization as a function of supersaturation. With minor changes it was used to determine the most suitable diameter, and the most suitable rate of change of supersaturation (see below).

Program 3 determines for each size group the number of droplets crystallized at each final supersaturation using the data deck provided by Program 1. From this the relative frequency and probability of crystallization are calculated. The number of droplets in each size range determined from Program 2, is read at the start of this program. The program provides a printed output as well as a graphic display of the relative frequency and probability of crystallization results.

To use the program for other cases requires only a change in the reference scale, SAT (I) and in the comparison terms, statements 000150 and 000153, to make them correspond to the scale of the input data.

PROGRAM 4 This program was used to fit the four values of supersaturation prior to crystallization to a straight line.

Program 4 reads the supersaturation values provided from Program 1 and determines the time intervals corresponding to the last four values of supersaturation. These pairs of supersaturation and time are then used in a standard linear least squares program. A punched output is provided for use with Program 3 to determine the most representative rate of change of supersaturation.

PROGRAM 5 This program was used to calculate the nucleation rate. The values for the best diameter and the best rate of change of super-

saturation were determined using a modified form of Program 3. The values of S, P, and $\frac{dP}{dS}$ were determined from the plots of probability as a function supersaturation.

Program 5 calculated J, the nucleation rate, log J, log S, and $(\log S)^{-2}$.

```
      PROGRAM TST (INPUT,OUTPUT,PUNCH,TAPE5=INPUT,TAPE6=OUTPUT,TAPE7=PUN
     1CH)
C     E17-LI.   ***P-BROMOBENZYL SULFOACETATE LITHIUM SALT***
C
C     CALCULATE THE SUPERSATURATION FROM THE DIAMETERS AT EACH TIME
C     THE DATA IS ENTERED PRE-SORTED ACCORDING TO INCREASING  D FINAL
C
000003      DIMENSION FORM(19), S(20), D(20), TITLE(16)
000003      REAL LEFT,RIGHT,ASPEC,FSPEC,XSPEC,BLANK,LIMIT1,LIMIT2
000003      READ(5,1000)TITLE
000011      WRITE(6,1001)TITLE
000017 1000 FORMAT(8A10)
000017 1001 FORMAT(1H1, 8A10//1X, 8A10)
000017      READ(5,10) LEFT,RIGHT,ASPEC,FSPEC,XSPEC,BLANK
C     NC GIVES THE NUMBER OF DROPLETS IN A SIZE GROUP
C     NN IS A RUNNING COUNT OF THE DROPLETS
C     NT IS THE NUMBER OF COLUMNS RESERVED FOR PUNCHING THE DIAMETER,D INCLUDING
C     BLANKS AND D-FINAL COLUMN
C     SCALE IS THE CONVERSION FACTOR TO GIVE D IN MICRONS
C     LIMIT DEFINES THE SIZE RANGE
C
000037      NN=0
000040      NC=0
000040      SCALE=1.818
000042      LIMIT1=5.0
000043      LIMIT2=15.0
000045      NT=16
000046      FORM(1)=LEFT
000050      FORM(NT+2)=RIGHT
000052   10 FORMAT(6A6)
C     TF IS THE CRYSTALLIZATION TIME
C     TL1,TL2, ARE LIQUID CRYSTAL TRANSITION TIMES
C      F IS THE FIELD OF VIEW
C
000052    1 READ (5,6)  (D(M),M=1,NT),TF,  TL1, TL2, F
000074      NN=NN+1
000076      IF (D(1) .EQ. 0.0 ) GO TO 5
000077      DO 11 M=1,NT
000100      D(M)=D(M)*SCALE
000102   11 CONTINUE
000104   12 N=NT
000106  104 CONTINUE
000106      IF (LIMIT2 .GT. 50.0) GO TO 5
000112      IF (D(N) .GT. LIMIT2 .AND. NC .EQ. 0) GO TO 103
```

Program 1

```
000122          GO TO 101
000122      103 LIMIT1=LIMIT2
000123          LIMIT2=LIMIT2+10.0
000125          GO TO 104
000126      101 CONTINUE
000126          IF(D(N) .GT. LIMIT1 .AND. D(N) .LE. LIMIT2) GO TO 100
000140          WRITE(6,102) LIMIT1,LIMIT2,NC
000151          LIMIT1=LIMIT2
000152          LIMIT2=LIMIT2+10.0
000154          NC=0
000155          GO TO 104
000155      100 NC=NC+1
000157          DO 2 M=1,NT
000160        2 S(M)=0.0
000163          DO 3 M=1,NT
C
C         CALCLLATE THE SUPERSATURATION, S
C
C
000165          IF (C(M) .EQ. 0.0) GO TO 3
000166          S(M)= (C(1)/C(M))**3
000172        3 CONTINUE
000175          DO 40 M=1,NT
000176          IF (S(M) .EQ. 0.0) GO TO 20
000177          FORM(M+1)=FSPEC
000201          GO TO40
000201       20 FORM(M+1)=ASPEC
000203          S(M)=BLANK
000205       40 CONTINUE
000210          WRITE(6,FORM) (S(M),M=1,NT),TF,TL1, TL2, F
000232          WRITE(7,FORM) (S(M),M=1,NT),TF,TL1, TL2, F
000254       30 CONTINUE
000254          GO TO 1
000255        5 NTOTAL=NN-1
000257          WRITE(6,102) LIMIT1,LIMIT2,NC
000271      102 FORMAT(32H NUMBER OF DROPLETS IN THE RANGE  ,1F4.0, 3H TO ,
                1 1F4.0, 8H MICRONS  , I15)
000271          WRITE(6,7) NTOTAL
000277        6 FORMAT(16F4.1, 4F4.0)
000277        7 FORMAT( 26H TOTAL NUMBER OF DROPLETS  , I15)
000277          STOP
000301          END
```

```
                PROGRAM TST (INPUT,OUTPUT,TAPE5=INPUT,TAPE6=OUTPUT)
        C       SEPARATING DROPLETS  INTO SIZE RANGES ACCORDING TO FINAL DIAMETERS
000003          REAL LIMIT1, LIMIT2
000003          LIMIT1=0.0
000004          LIMIT2=5.0
000005          M=0
000007        3 READ(5,4) D
000015          SCALE=2.0
000017        2 CONTINUE
000017          IF (D .EQ. 0.0) GO TO 5
000020          IF (D .GT. LIMIT1 .AND. D .LE. LIMIT2) GO TO 1
000031          IF (D .LE. LIMIT1) GO TO 7
000033        5 WRITE(6,6) LIMIT1, LIMIT2, M
000045          IF (D .EQ. 0.0)  STOP
000050          LIMIT1=LIMIT2
000051          LIMIT2=LIMIT2 +5.0
000053          M=0
000054          GO TO 2
000054        1 M=M+1
000056          GO TO 3
000056        4 FORMAT(64X,1F4.1)
000056        6 FORMAT(///33H NUMBER OF DROPLETS IN SIZE RANGE ,1F4.0,3H TO ,1F4.0
               1 ,3H IS , I14///)
000056        7 WRITE(6,8) LIMIT1, D, M
000070        8 FORMAT(///15H D IS LESS THAN    , 2F4.0, 1I4)
000070          STOP
000072          END

UNUSED COMPILER SPACE
010300
```

Program 2

```
                      PROGRAM TST (INPUT,OUTPUT,TAPE5=INPUT,TAPE6=OUTPUT)
                C
                CC    E17-LI+   ***P-BROMOBENZYL SULFOACETATE LITHIUM SALT***
                CCC
                C     CALCULATE NUMBER, RELATIVE FREQUENCY, AND PROBABILITY OF CRYS N VS. S
 000003                DIMENSION S(500), SAT(51), NCS(51), RFCS(51), PROB(51), GRAPH(101)
                     1, NJ(10),TITLE(16), Y(10), TIME(20)
 000003                REAL LIMIT1, LIMIT2
                C     LIMIT IS THE RANGE OF DIAMETERS, NM IS THE NUMBER OF DROPS
 000003                READ(5,1000) TITLE
 000011          1000  FORMAT(8A10)
 000011                WRITE(6,1001) TITLE
 000017          1001  FORMAT( 1H1 ,8A10///1X, 8A10//)
 000017                READ(5,1) DOT, X, BLANK
 000031             1  FORMAT(3A1)
                C
                CC    L IS THE NUMBER OF THE SIZE GROUP
                CCC   NJ IS THE NUMBER OF DROPLETS PER SIZE GROUP
                CCCC  LG IS THE NUMBER OF SIZE RANGES
                CCCCC NT IS THE NUMBER OF TIME INTERVALS
                C
 000031                L=0
 000032                LG=3
 000033                NT=14
 000034                LIMIT2=10.0
 000036                READ(5,4) (NJ(I), I=1,LG)
 000050                READ(5,904) (TIME(I), I=1,NT)
 000063           904  FORMAT(20F4.0)
 000063             4  FORMAT(5I5)
 000063             6  L=L+1
 000065                IF (L .GT. LG) STOP
 000071                NM=NJ(L)
 000073                LIMIT1=LIMIT2
 000074                LIMIT2=LIMIT2+10.0
 000076                IF (NJ(L) .EQ. 0)  GO TO 6
                C
                CCC   S IS THE SUPERSATURATION
                C
 000077                DO 2 N=1,NM
 000101                READ(5,3) S(N)
 000106                IF(S(N)  .EQ. 0.0) GO TO 5
 000110                GO TO 2
 000110             5  MM=N-1
 000112                WRITE(6,10) MM
 000120            10  FORMAT(40H ***NOT ENOUGH DATA FOR SPECIFIED NM, N=   , 1I3,3H***  )
 000120                GO TO 8
 000121             2  CONTINUE
 000124                GO TO 11
```

Program 3

```
000124        8 CONTINUE
000124          NM=MM
000126       11 CONTINUE
000126        3 FORMAT(60X, 1F4.1)
C
CC      WE WANT TO KNOW THE NUMBER(NCS) CRYSTALLIZED AS A FUNCTION OF SUPERSAT N
CC      DEFINE A SCALE OF SUPERSATURATION SAT(I)
C
000126          DO 200 I=1,51
000130      200 SAT(I)=1.0+FLOAT(I-1)/10.0
000137          DO 203 I=1,51
000140      203 NCS(I)=0.0
000143          MM=1
000144          DO 201 I=1,51
000146          DO 201 N=MM,NM
C
CC      WE WANT TO COMPARE S AT THE FIRST DECIMAL PLACE. THE 0.001 PREVENTS A
CC      POINT FROM BEING COUNTED TWICE(EX. 1.05 WOULD THEN COUNT AS 1.0 AND 1.1).
C
000150          SS=S(N     )+0.001-SAT(I)
000153          IF (ABS(SS) .LE. 0.05) GO TO 202
000157          GO TO 201
000160      202 NCS(I)=NCS(I)+1
000163      201 CONTINUE
C
CC      SELECT NCSMAX, THE LARGEST VALUE OF NCS
C
000170          NCSMAX=0
000171          DO 300 I=1,51
000172          IF ( NCS(I)    .GT. NCSMAX)     GO TO 301
000176          GO TO 300
000176      301 NCSMAX=NCS(I)
000200      300 CONTINUE
C
CC      DETERMINE THE RELATIVE FREQUENCY OF CRYSTALLIZATION(RFCS) AS A FUNCTION
CC      OF SUPERSATURATION
C
000202          SUMP=0.0
000203          DO 302 I=1,51
000205          RFCS(I)=FLOAT(NCS(I))/FLOAT(NCSMAX)
C
CC      DETERMINE THE PROBABILITY(PROB) OF CRYSTALLIZATION AS A FUNCTION
CC      OF SUPERSATURATION
C
```

```
000210          SUMP=SUMP+FLOAT(NCS(I))
000213          PROB(I)=SUMP/FLOAT(NM)
000216          WRITE(6,7) SAT(I),NCS(I),RFCS(I),PROB(I)
000232        7 FORMAT(1F10.1, 1I5, 2F7.2)
000232      302 CONTINUE
            C
            C     PLOT RFCS AS A FUNCTION OF SUPERSATURATION
            C
000234          WRITE(6,71)
000240          WRITE(6,78) LIMIT1,LIMIT2
000250       78 FORMAT(98H RELATIVE FREQUENCY AND PROBABILITY OF CRYSTALLIZATION A
                1S A FUNCTION OF SUPERSATURATION FOR GROUP  , 1F3.0, 3H TO , 1F3.0,
                29H MICRONS.  )
000250          WRITE(6,79) NM
000256       79 FORMAT(2X, 19H NUMBER OF DROPLETS   , 1I4)
            C
            C     BLANK THE ARRAY
            C
000256          DO 801 I=1,101
000260      801 GRAPH(I)=BLANK
            C
            C     PUT A DOT IN GRAPH(1) TO REPRESENT THE Y-AXIS(RFCS), GOING FROM 0 TO 1
000264          GRAPH(1)=DOT
000265          GRAPH(56)=DOT
            C
            C     COMPUTE THE LOCATION OF THE PLOTTING SYMBOL
000266          DO 802 K=1,51
000267          IF (K .EQ. 51) GO TO 804
000271          DO 803 N=1,41
000272      805 R=RFCS(N  )*50.0-0.5
000275          J=51.0-R
000300          P=PROB(N  )*50.0-0.5
000304          I=51.0-P
000306          LL=56+N
000310          IF (I .EQ. K) GO TO 809
000313          GO TO 810
000313      809 GRAPH(LL)=X
000315      810 CONTINUE
000315          IF (J.EQ.K) GO TO 808
000317          GO TO 803
000320      808 GRAPH(N)=X
000322      803 CONTINUE
000324          GO TO 811
            C
            C     PUT A ROW OF DOTS TO REPRESENT THE X-AXIS(S), GOING FROM 1.0 TO 4.9
000325      804 CONTINUE
000325          DO 806 J=1,41
000327          I=56+J
```

```
000330          GRAPH(I)=DOT
000333      806 GRAPH(J)=DOT
000336      811 CONTINUE
000336          J2=101
000337          WRITE(6,70) (GRAPH(JK),JK=1,J2)
000352      813 CONTINUE
000352          DO 807 J=1,101
000354      807 GRAPH(J)=BLANK
000360          GRAPH(1)=DOT
000361          GRAPH(56)=DOT
000361      802 CONTINUE
000364          WRITE(6,73)
000367      600 CONTINUE
000367          GO TO 6
000370       70 FORMAT(1H ,101A1)
000370       73 FORMAT(1HR)
000370       71 FORMAT(1HQ)
000370          END

UNUSED COMPILER SPACE
006700
```

```
                PROGRAM TST (INPUT,OUTPUT,PUNCH,TAPE5=INPUT,TAPE6=OUTPUT,TAPE7=PUN
               1CH)
      C         LEAST SQUARES FIT OF S VS TIME
000003          DIMENSION TITLE(10),S(20), X(20), Y(20),TIME(20)
000003          READ(5,100) TITLE
000011          WRITE(6,101) TITLE
000017          N=4
000020          NT=16
      C         NCOUNT IS A COUNT OF THE NUMBER OF DROPLETS
000021          NCOUNT=1
      C         X IS TIME
      C         Y IS SUPERSATURATION
000022          READ(5,102) (TIME(I), I=1,NT)
000035        2 READ(5,103) (S(I),I=1,NT)
000050          IF (S(1) .EQ. 0.0)  STOP
000053          I=5
000054          DO 4 M=1,NT
000056          J=NT+1-M
000060          IF(S(J) .EQ. 0.0) GO TO 4
000062          I=I-1
000063          IF(I .EQ. 0) GOTO 3
000064          X(I)=TIME(J)
000065          Y(I)=S(J)
000067        4 CONTINUE
000072        3 CONTINUE
      C-----LEAST SQUARES PROGRAM.
000072          A = N
000073          SIGX = 0.0
000074          SGDXY = 0.0
000075          SGDX2 = 0.0
000076          SIGY = 0.0
000077          SIGY2 = 0.0
000100          SIGXY = 0.0
000102          DO 6 I = 1,N
000103        6 SIGX = SIGX + X(I)
000107          XBAR = SIGX/A
000111          DO 7 L = 1,N
000112          DELX = X(L) - XBAR
000114          SGDXY = SGDXY + Y(L)*DELX
000117          SGDX2 = SGDX2 + DELX**2
000121          SIGY2 = SIGY2 + Y(L)**2
000123          SIGY = SIGY + Y(L)
000125          SIGXY = SIGXY + X(L)*Y(L)
000130        7 CONTINUE
000133          SLOPE = SGDXY/SGDX2
000134          SYDX2 = (SIGY2 - ((SIGY**2)/A) - SLOPE*SIGXY + (SLOPE*SIGX*SIGY/A)
               1)/(A - 2.0)
000147          SAO=SYDX2/A
```

```
000151           SBQ=SYDX2/SGDX2
000153           IF (ABS(SBQ) .LE. 0.00000001) GO TO 10
000157           GO TO 11
000160        10 SBQ=0.0
000161        11 CONTINUE
000161           IF (ABS(SAQ) .LE. 0.00000001) GO TO 12
000165           GO TO 13
000165        12 SAQ=0.0
000166        13 CONTINUE
000166           SB=SQRT(SBQ)
000170           YBAR = SIGY/A
000172           CEPT = YBAR - SLOPE*XBAR
000175           SA=SQRT(SAQ)
000200           WRITE(6,104) (S(I), I=1,NT), SLOPE, CEPT, SB, SA
000221           WRITE(7,106) NCOUNT, SLOPE, CEPT, SB, SA
000237       106 FORMAT(1I4, 4F10.5)
000237           NCOUNT=NCOUNT+1
000241           GO TO 2
000241       100 FORMAT(10A8)
000241       101 FORMAT(1H0,10A8//)
000241       102 FORMAT(20F4.0)
000241       103 FORMAT(20F4.1)
000241       104 FORMAT(1X, 16F4.1, 10X, 4F10.5)
000241       105 CONTINUE
000241           STOP
000243           END

UNUSED COMPILER SPACE
007500
```

```
                PROGRAM TST (INPUT,OUTPUT,TAPE5=INPUT,TAPE6=OUTPUT)
          C
          CC    CALCULATE THE RATE OF NUCLEATION
          C
000003            DIMENSION TITLE(16), HEAD(8)
000007            REAL J, LJ, LS
000003            READ(5,1000) HEAD
000011            DO 6 N=1,4
000013            READ(5,1000) TITLE
000029            WRITE(6,1001)TITLE
          C
          CC    D IS THE SIZE GROUP DIAMETER IN MICRONS
          CC    SLOPE IS THE RATE OF CHANGE OF S
          CC    DELS IS THE SUPERSATURATION INTERVAL
          CC    S IS THE SUPERSATURATION
          CC    P IS THE PROBABILITY AS A FRACTION
          CC    DELP IS THE PROBABILITY CHANGE OVER DELS
          CC    J IS THE RATE OF NUCLEATION
          C
000026        5 READ(5,1) D, SLOPE, DELS
000040            IF (D.EQ. 0.0) GO TO 6
000041            WRITE(6,1002) HEAD
000047            V=(4.0*3.1416/3.0)*(D*0.0001/2.0)**3
000054        4 READ(5,1) S,P, DELP
000066            IF (S .EQ. 0.0) GO TO 5
000067            J=(SLOPE*DELP)/(V*(1.0-P)*DELS*60.0)
000075            SSQ=1.0/(ALOG10(S))**2
000101            LJ=ALOG10(J)
000103            LS=ALOG10(S)
000106            WRITE(6,3) S,LS, SSQ, J, LJ
000123            GO TO 4
000124        6 CONTINUE
000126            1 FORMAT(10F5.1)
000126            3 FORMAT(1X, 1F7.1, 3(1E14.3, 1F8.3))
000126     1001 FORMAT(1H1,8A10/8A10)
000126     1000 FORMAT(    8A10)
000126     1002 FORMAT(//1X, 8A10//)
000126            STOP
000130            END

UNUSED COMPILER SPACE
010100
```

APPENDIX 4

RELATIVE FREQUENCY AND PROBABILITY OF CRYSTALLIZATION

The data for the size groups 0 - 10, 20 - 30, 30 - 40 microns are given in the form of relative frequency and probability of crystallization as a function of supersaturation. These plots were the basis of the results given in Section III.C.3.

KEY

Figures A-1, A-2	lithium p-bromobenzylsulfoacetate	20-30μ -	200 droplets
A-3	lithium p-bromobenzylsulfoacetate	30-40μ -	60 droplets
Figures A-4, A-5	lithium p-nitrophenacylsulfoacetate	20-30μ -	224 droplets
A-6	lithium p-nitrophenacylsulfoacetate	30-40μ -	54 droplets
Figures A-7, A-8	lithium p-nitrobenzylsulfoacetate	0-10μ -	85 droplets
Figures A-9, A-10	lithium p-bromophenacylsulfoacetate	20-30μ -	113 droplets

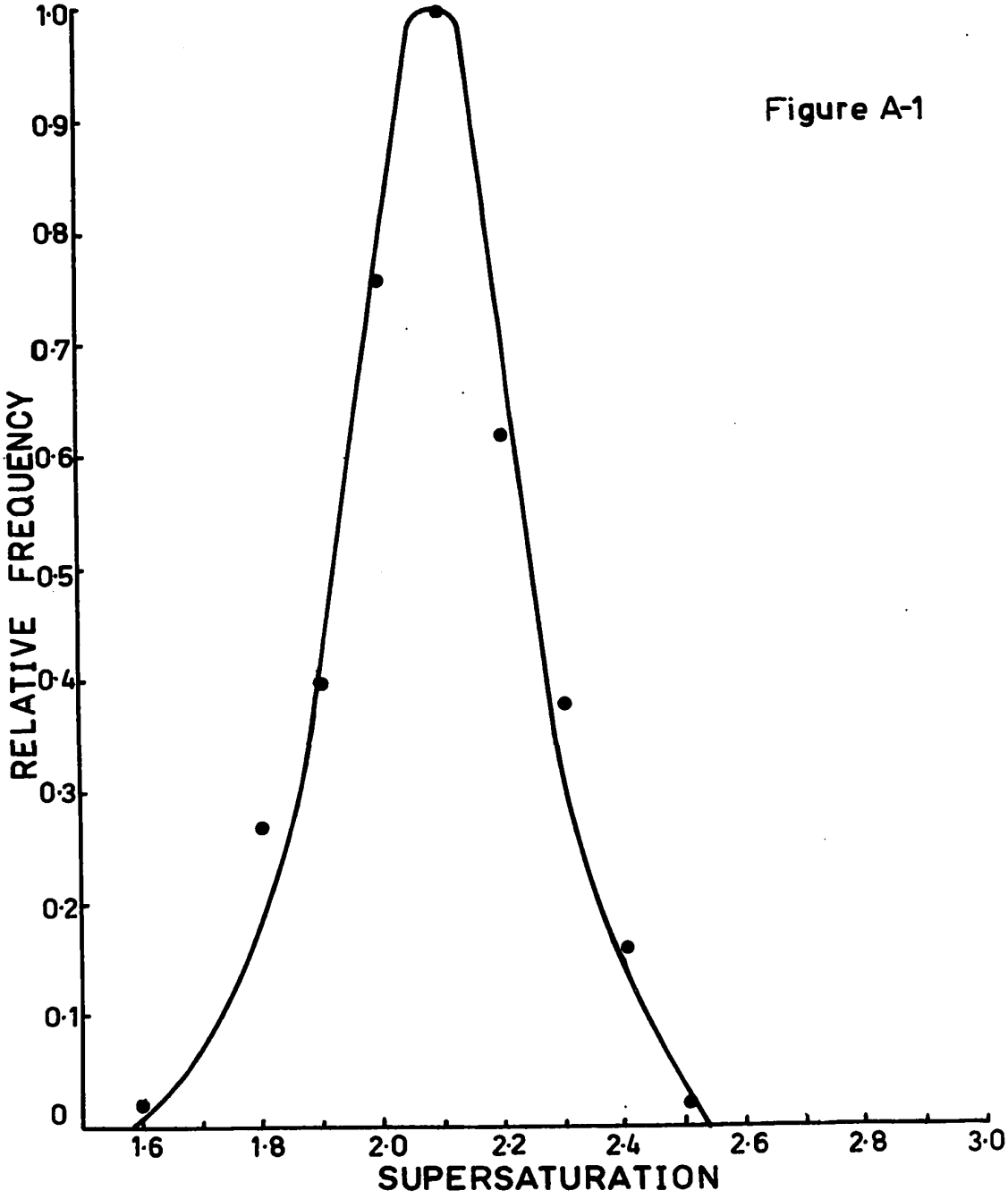
1·0
0·9
0·8
0·7
0·6
0·5
0·4
0·3
0·2
0·1
0
RELATIVE FREQUENCY
1·6
1·8
2·0
2·2
2·4
2·6
2·8
3·0
SUPERSATURATION

Figure A-1

Figure A-2

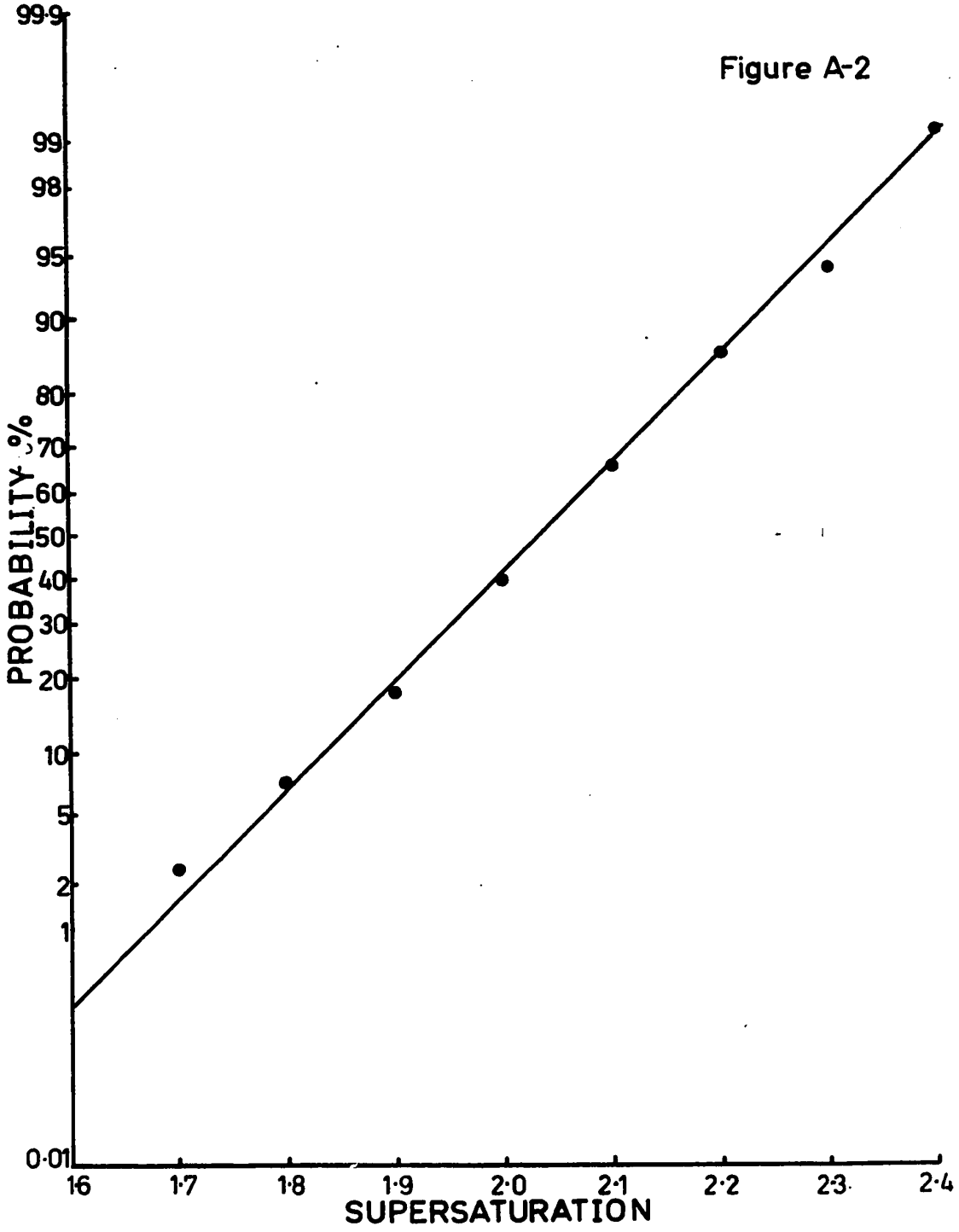
99·9
99
98
95
90
80
70
60
50
40
30
20
10
5
2
1
0·01
PROBABILITY %
1·6
1·7
1·8
1·9
2·0
2·1
2·2
2·3
2·4
SUPERSATURATION

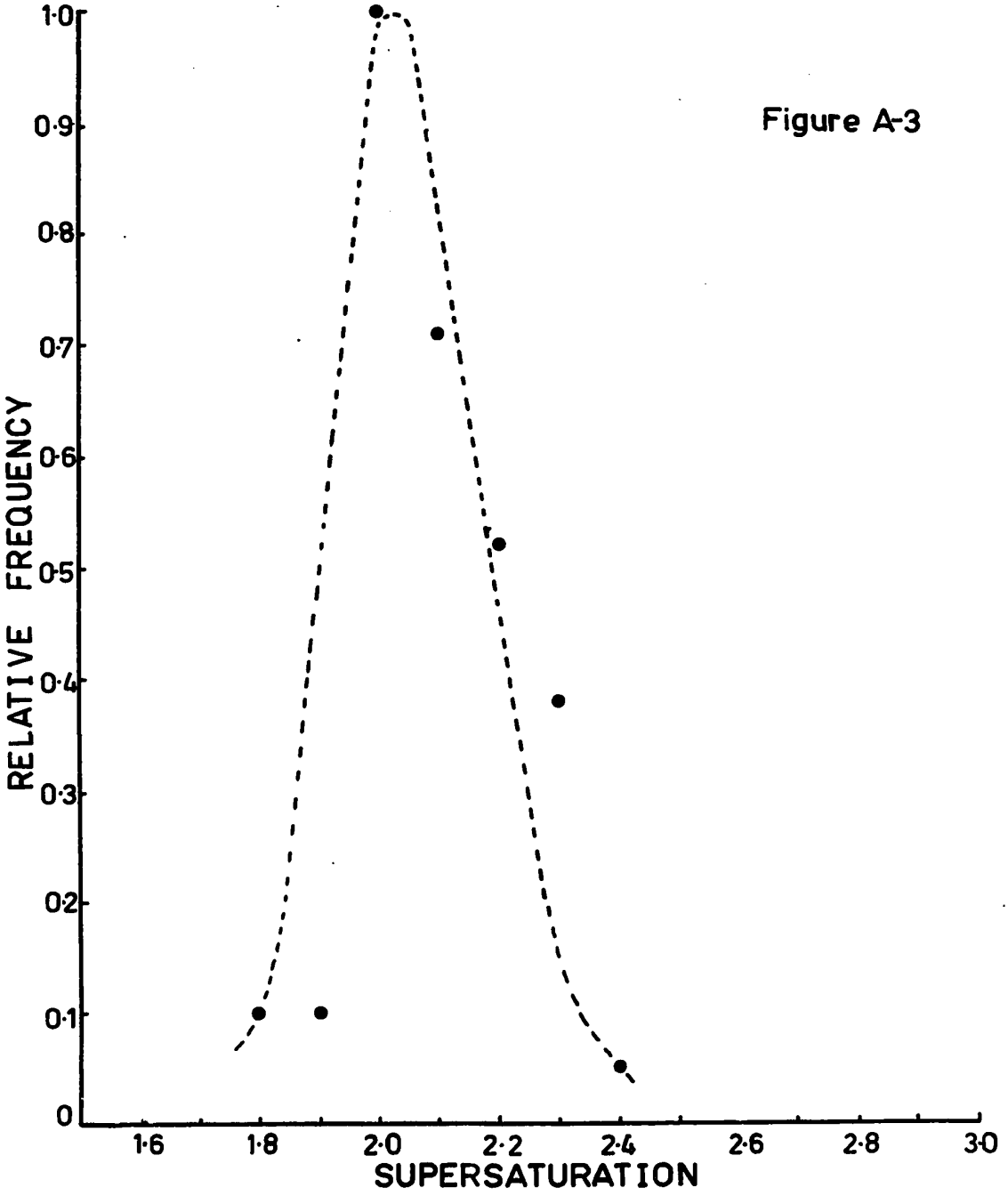
1·0
0·9
0·8
0·7
0·6
0·5
0·4
0·3
0·2
0·1
0
RELATIVE FREQUENCY
1·6
1·8
2·0
2·2
2·4
2·6
2·8
3·0
SUPERSATURATION

Figure A-3

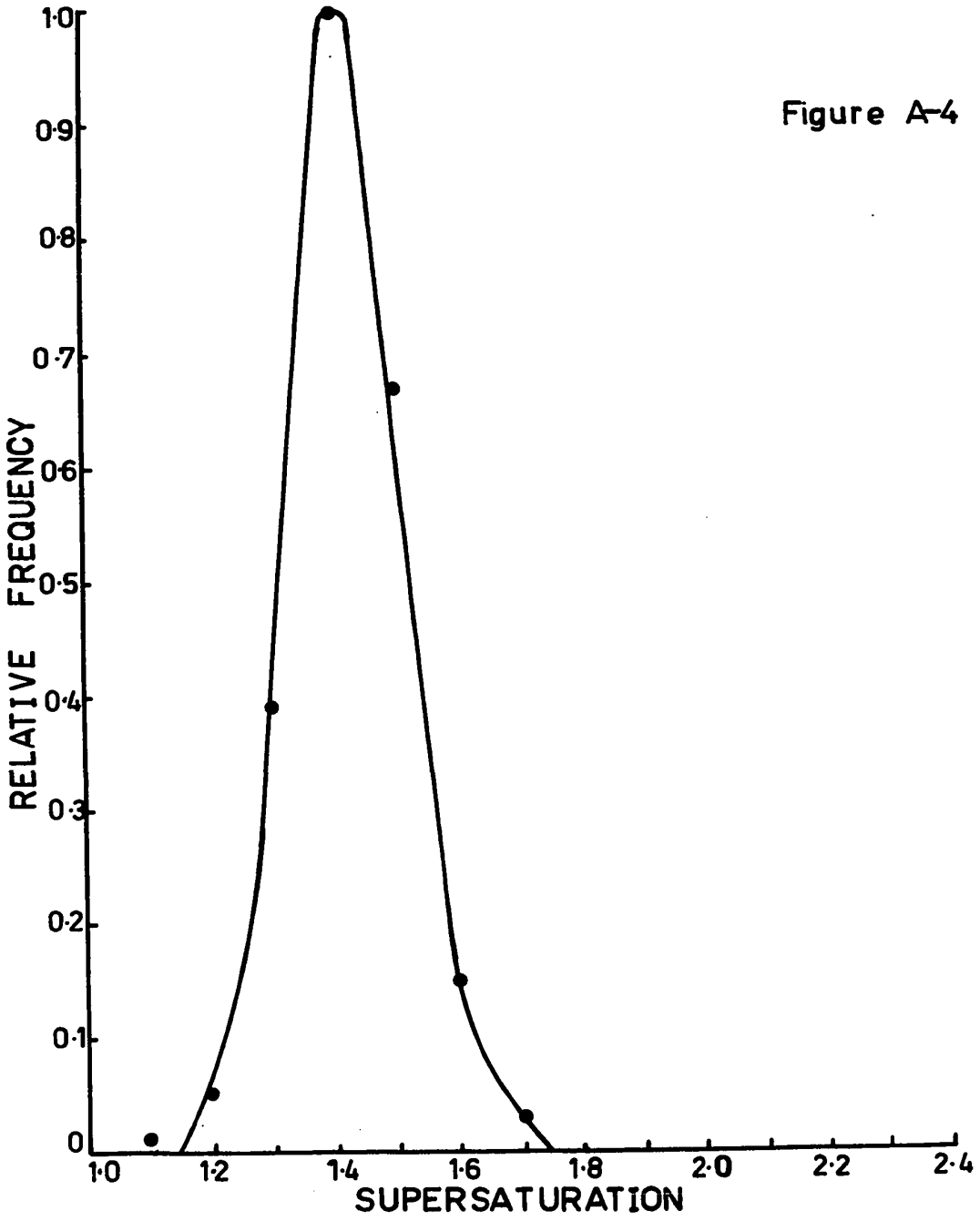
1·0
0·9
0·8
0·7
0·6
0·5
0·4
0·3
0·2
0·1
0
RELATIVE FREQUENCY
1·0
1·2
1·4
1·6
1·8
2·0
2·2
2·4
SUPERSATURATION

Figure A-4

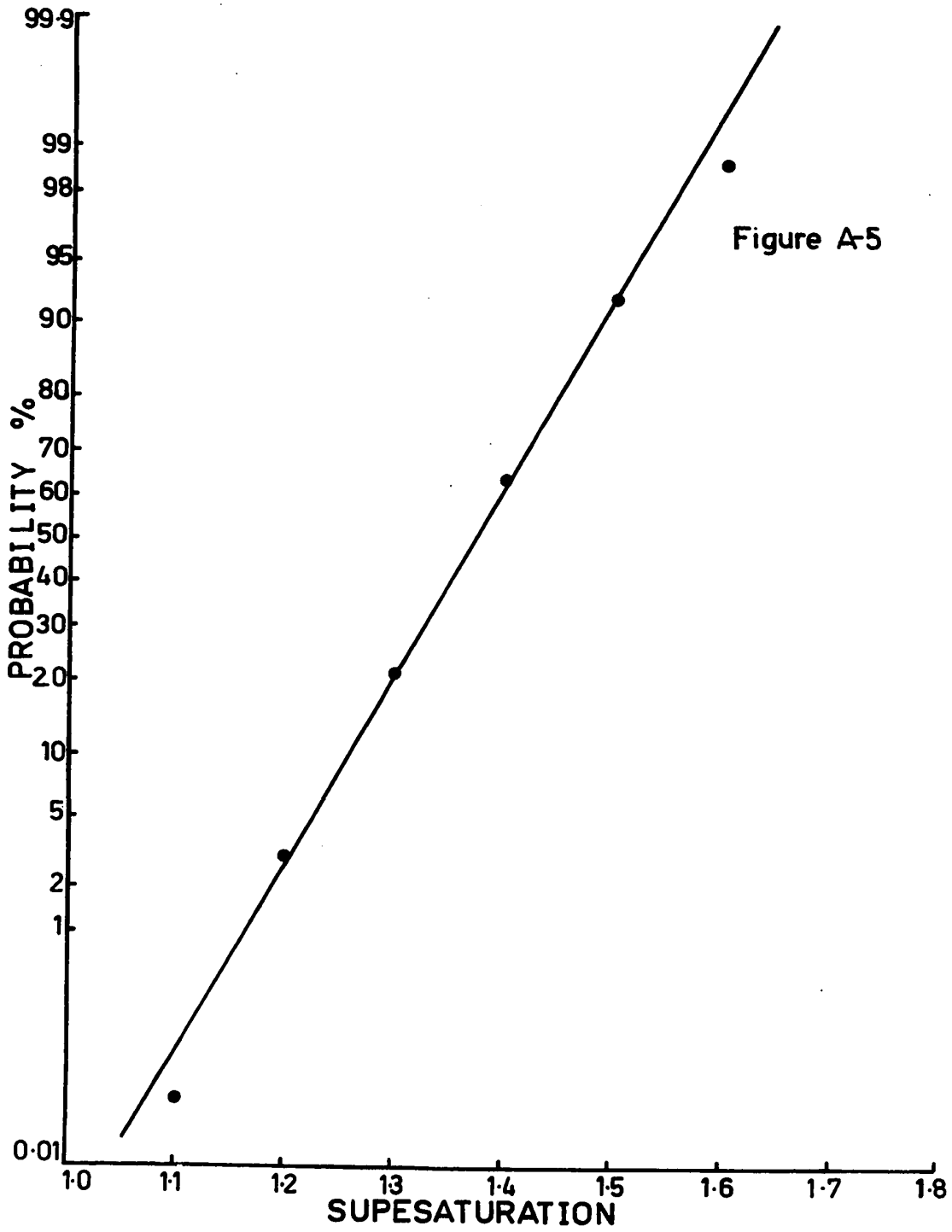
99·9
99
98
95
90
80
70
60
50
40
30
20
10
5
2
1
0·01
PROBABILITY %
1·0
1·1
1·2
1·3
1·4
1·5
1·6
1·7
1·8
SUPESATURATION

Figure A-5

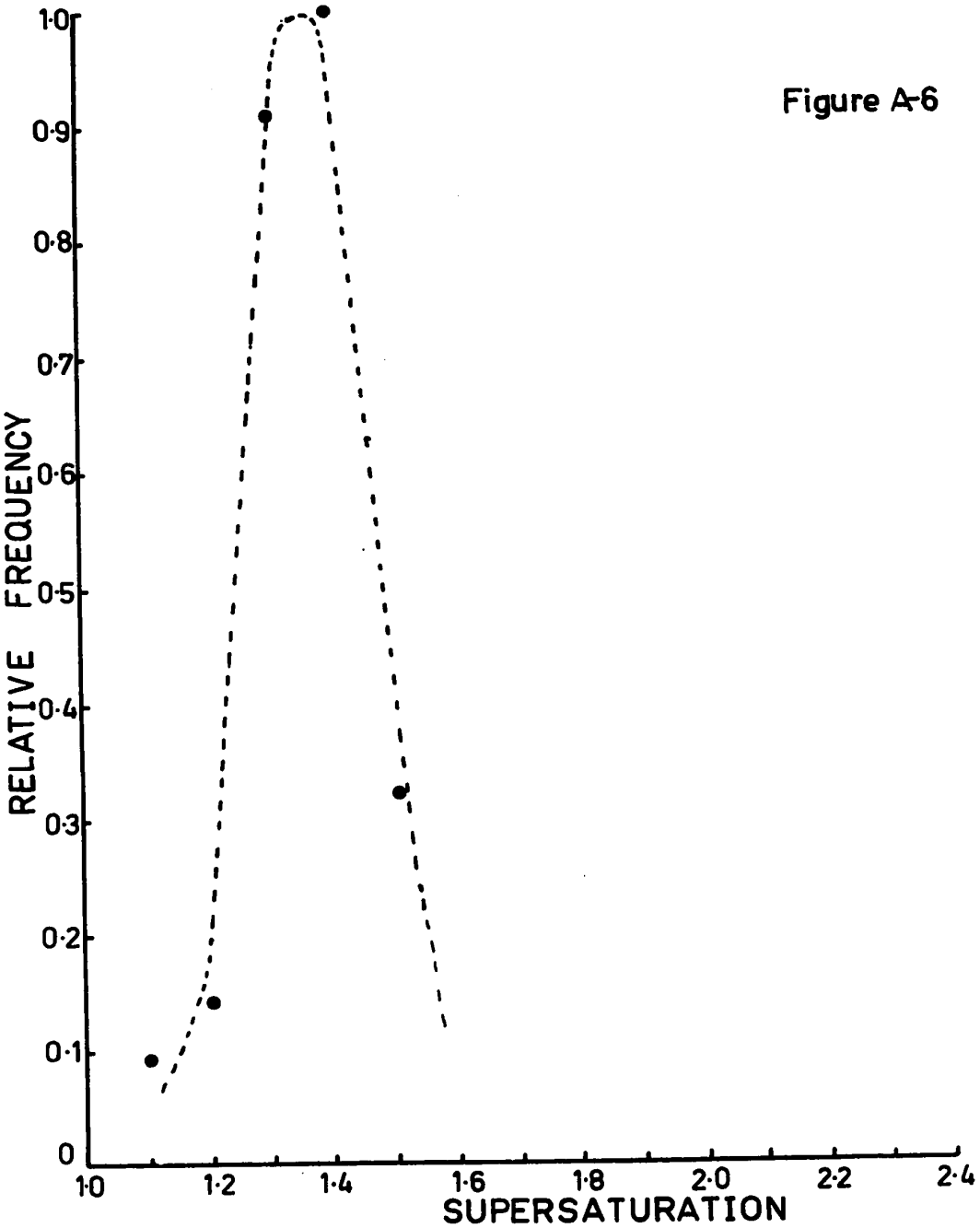
RELATIVE FREQUENCY
1·0
0·9
0·8
0·7
0·6
0·5
0·4
0·3
0·2
0·1
0
1·0
1·2
1·4
1·6
1·8
2·0
2·2
2·4
SUPERSATURATION

Figure A-6

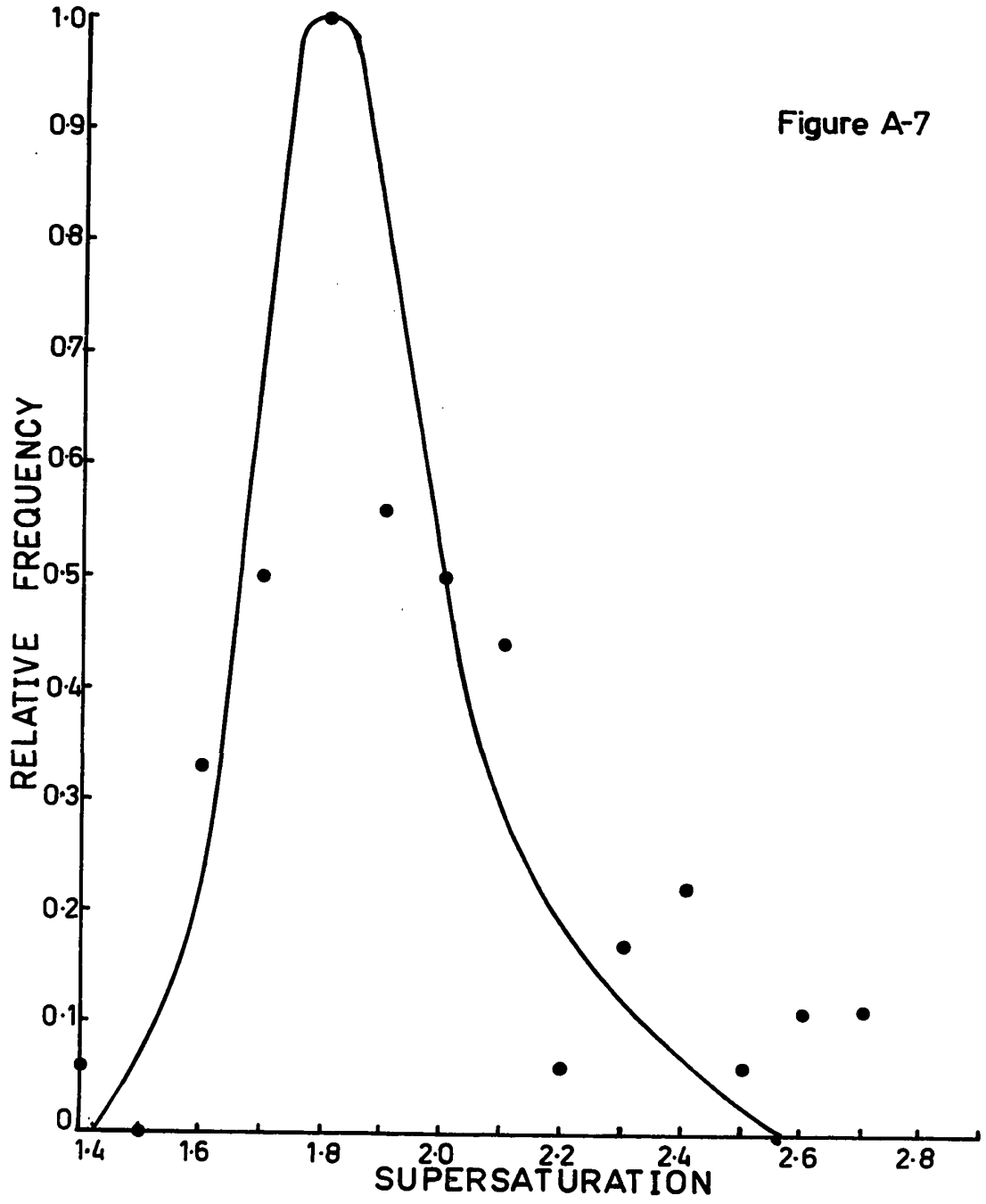
1·0
0·9
0·8
0·7
0·6
0·5
0·4
0·3
0·2
0·1
0
RELATIVE FREQUENCY
1·4
1·6
1·8
2·0
2·2
2·4
2·6
2·8
SUPERSATURATION

Figure A-7

Figure A-8

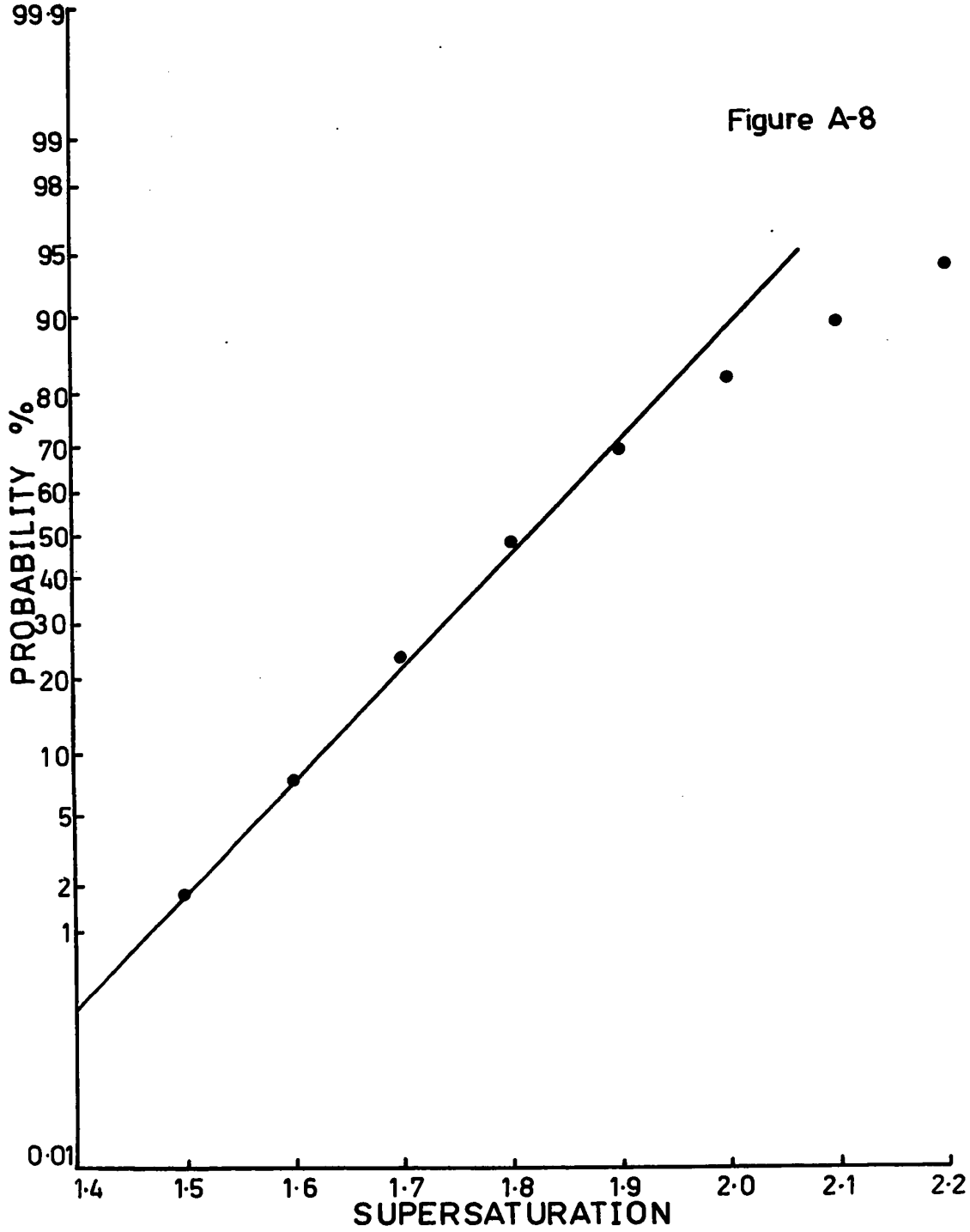
99·9
99
98
95
90
80
70
60
50
40
30
20
10
5
2
1
0·01
PROBABILITY %
1·4
1·5
1·6
1·7
1·8
1·9
2·0
2·1
2·2
SUPERSATURATION

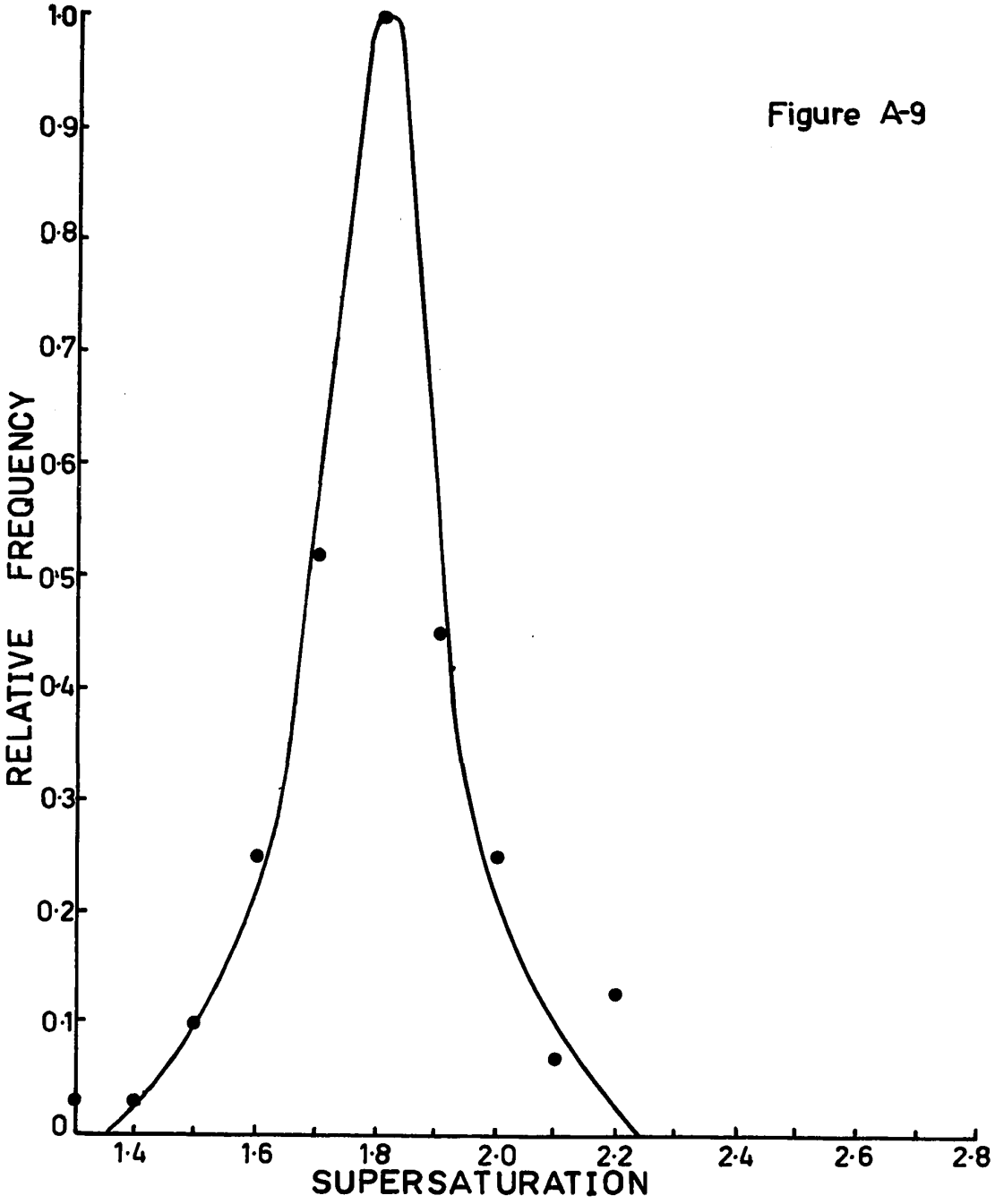
1·0
0·9
0·8
0·7
0·6
0·5
0·4
0·3
0·2
0·1
0
RELATIVE FREQUENCY
1·4
1·6
1·8
2·0
2·2
2·4
2·6
2·8
SUPERSATURATION

Figure A-9

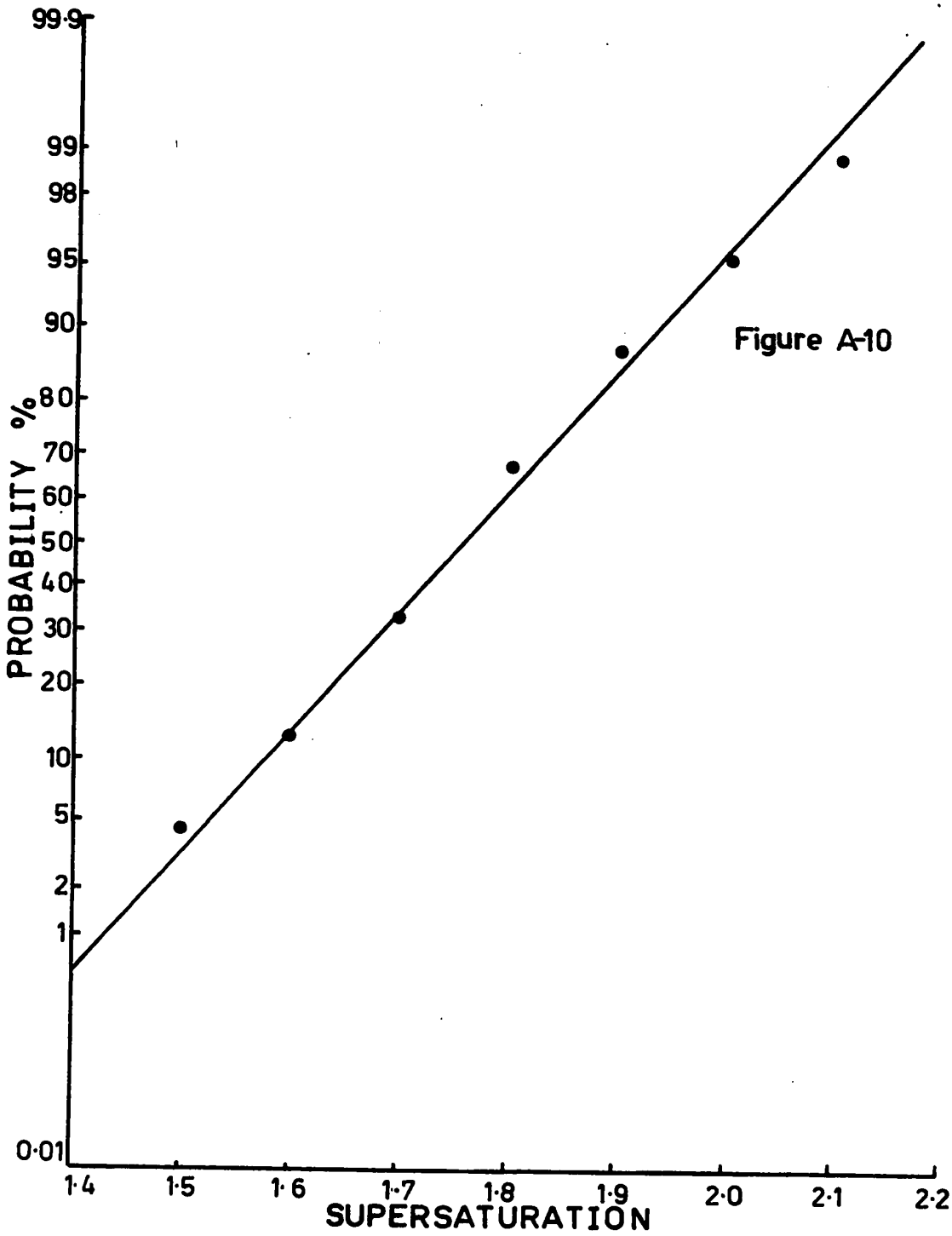
99·9
99
98
95
90
80
70
60
50
40
30
20
10
5
2
1
0·01
PROBABILITY %
1·4
1·5
1·6
1·7
1·8
1·9
2·0
2·1
2·2
SUPERSATURATION

Figure A-10

APPENDIX 5

PFHS ATTEMPTS TO STUDY THE NUCLEATION OF INSOLUBLE ALCOHOLS

As mentioned in the body of this thesis, one of the original aims of this project was the study of the nucleation of insoluble organic compounds from aqueous solution using PFHS. Thus, it was necessary to select and prepare compounds which could be used to generate an insoluble product from soluble precursors. The method of their preparation has been given in detail in Section II. We were unable to couple the PFHS reaction with the droplet technique. Here we wish to record our attempts to solve this problem and the difficulties involved.

EXPERIMENTAL

In order to achieve the highest possible concentration of insoluble material to reach the supersaturation level necessary for the homogeneous nucleation of insoluble materials required the use of saturated ester solutions. In preliminary experiments 0.5 ml of ester solution were stirred vigorously with a micro-stirring bar in a 1-ml beaker and the concentrated base was added using a micrometer buret. The time interval was measured from the moment of addition of the base until the first visual observation of the precipitate.

Droplet experiments were carried out using similar procedure to that given in Section II but replacing the silicone fluids with light and heavy mineral oils. A sample of the reacting solution was taken as soon as possible after mixing. Usually 15-20 sec were required before crystallization occurred in the beaker. This was sufficient time to produce the droplets; a further 3-5 minutes was necessary to prepare the dispersion

for recording.

RESULTS AND DISCUSSION

The first attempts to use the PFHS-droplet method in this study involved sodium p-nitrobenzylsulfoacetate. The hydrolysis of this ester using NaOH could be readily controlled; however, the resulting supersaturation (of the order 10-20) was insufficient to cause crystallization in the droplets. The solubility of the ester was increased by an order of magnitude by using its lithium salt. In this case the equivalent amount of LiOH required to give complete reaction caused instantaneous precipitation of the alcohol. Cooling the solution slowed the reaction somewhat but also decreased the solubility of the ester. Ammonium hydroxide and organic amines were tried as the basic reagent (see Table A1), but, these presented other problems. In particular the amines increased the solubility of the alcohol and in effect decreased the attainable supersaturation.

The hydrolysis of lithium p-nitrobenzylsulfoacetate could be controlled in the beaker using NH_4OH or several primary amines as noted in Table A-1. The alcohol, however, did not crystallize from the droplets; instead numerous bubbles were discharged from each droplet. The droplets could be induced to crystallize if touched with a fine wire but would not crystallize spontaneously even on standing overnight. It was at first believed that the bubbles were gaseous, but no reasonable explanation for the liberation of a gas from a basic solution could be found. In view of the comments (see below) for the analogous lithium-p-bromobenzylsulfoacetate, it is clear that the alcohol must be separating as an oil.

For the hydrolysis of lithium p-bromobenzylsulfoacetate the only reagent attempted was LiOH. An equivalent amount of LiOH solution added to the saturated ester solution in the bulk caused the alcohol to

TABLE A-1

Some reagents used in the hydrolysis of the lithium esters

base/ Li - sulfoacetate ester	Time interval for crystallization		
	p-nitrobenzyl	p-bromophenacyl	p-nitrophenacyl
3N LiOH	3 sec.	inst.	gummy residue
conc NH_4OH	3 min.	2 sec.	gummy residue
3N tetramethylammonium hydroxide	2 phases separate	inst.	gummy residue
6N ethylene diamine	3 min.	4 sec.	
6N hydrazine	35 sec.	5 sec.	16 sec.
pyridine	N.R.	N.R.	N.R.
hydroxylamine (with LiOH)	inst. to 3 min.	inst. to 15 sec.	inst. to 2 min.
dimethylamine (25%)	N.R.	3 sec.	
diethylamine	N.R.	2 sec.	
lycine (conc. not recorded)	N.R.	N.R.	
ethylamine		3 sec.	
ethylene diamine		N.R.	N.R.
triethanolamine		45 sec.	
diethylenetriamine	6 min.	6 sec.	
triethylenetetramine	15 min.	11 sec.	
methyldiethanolamine	N.R.	30 sec.	
triethylamine	N.R.	3 sec.	
trimethylamine	N.R.	5 sec.	
piperidine	2 liquid phases after 10 min.	2 sec.	gummy polymer

separate as an oil after 10-15 sec. This subsequently solidified.

The hydrolysis of lithium p-nitrophenacylsulfoacetate solutions could not be controlled with the reagents that were attempted. Usually a gummy polymeric tar was deposited immediately upon addition of base.

For the case of lithium p-bromophenacylsulfoacetate crystallization within the droplets could be observed by use of a specially developed technique. Reaction of a saturated solution of this ester with 1N NH_4OH gave a precipitate in 12-15 sec. By preparing the dispersion in kerosene (in which the droplets would settle without centrifugation) a preparation could be made ready for photographing within 25 sec. Under these conditions some droplets were seen to crystallize spontaneously. However, the conditions could not be adjusted to give a dispersion mostly free of crystals at the start and completely crystallized at the end. Also, those droplets crystallizing were usually greater than 40 microns, suggesting heterogeneous nucleation. Furthermore, all of the crystallization activity was complete within 2 minutes of mixing of the reagents, making the nucleation parameters too dependent on the rate of chemical reaction to be of practical use.

As indicated in Table A-1 a few organic bases were found which gave a reasonable reaction time with lithium p-bromophenacylsulfoacetate. Attempts to use the conventional technique described above for lithium p-nitrobenzylsulfoacetate resulted in either no crystallization or in fine crystals which grew into the mineral oil and catalysed the nucleation of neighbouring droplets.

This part of the project was investigated quiet thoroughly because of its importance in assessing the classical nucleation theory. Many of the discrepencies between the experimental findings and the theoretical

predictions in the literature have been explained in terms of the high degree of solvation in ionic systems and the electrolytic nature of inorganic systems. This project if it had been successful may have gained greater insight into these discrepencies since these problems are not involved in the case of hydrophobic organic compounds.

APPENDIX 6

TABLES OF RAW DATA

TABLE A-2

Number crystallized, relative frequency and probability of crystallization

Lithium p-bromobenzylsulfoacetate

size group	10 - 20 μ			20 - 30 μ			30 - 40 μ		
S	N	RF	P	N	RF	P	N	RF	P
1.0									
1.1									
1.2									
1.3									
1.4									
1.5									
1.6	2	.02	.00	1	.02	.01			
1.7	8	.06	.02	0	.00	.01			
1.8	40	.30	.10	15	.27	.08	2	.10	.03
1.9	39	.30	.19	22	.40	.19	2	.10	.07
2.0	91	.69	.38	42	.76	.40	21	1.00	.42
2.1	132	1.00	.65	55	1.00	.68	15	.71	.67
2.2	70	.53	.80	34	.62	.84	11	.52	.85
2.3	61	.46	.93	21	.38	.95	8	.38	.98
2.4	22	.17	.97	9	.16	1.00	1	.05	1.00
2.5	10	.08	1.00	1	.02	1.00	0	.00	1.00
2.6	2	.02	1.00	0	.00	1.00	0	.00	1.00
2.7	0	.00	1.00	0	.00	1.00	0	.00	1.00
Total	477			200			60		

Lithium p-nitrophenacylsulfoacetate

size group	10 - 20 μ			20 - 30 μ			30 - 40 μ		
S	N	RF	P	N	RF	P	N	RF	P
1.0									
1.1	2	.01	.01	1	.01	.00	2	.09	.04
1.2	2	.01	.01	5	.05	.03	3	.14	.09
1.3	25	.18	.08	38	.39	.20	20	.91	.46
1.4	100	.73	.36	97	1.00	.63	22	1.00	.87
1.5	137	1.00	.75	65	.67	.92	7	.32	1.00
1.6	64	.47	.93	15	.15	.99	0	.00	1.00
1.7	21	.15	.99	3	.03	1.00	0	.00	1.00
1.8	5	.04	1.00	0	.00	1.00	0	.00	1.00
1.9	0	.00	1.00	0	.00	1.00	0	.00	1.00
Total	356			224			54		

TABLE A-2
(continued)

Lithium p-nitrobenzylsulfoacetate

size group	0 - 10 μ			10 - 20 μ			20 - 30 μ		
S	N	RF	P	N	RF	P	N	RF	P
1.0									
1.1									
1.2									
1.3									
1.4	1	.06	.01	1	.01	.00			
1.5	0	.00	.01	10	.10	.02			
1.6	6	.33	.07	32	.32	.08			
1.7	11	.61	.19	56	.57	.20	2	.29	.07
1.8	18	1.00	.37	94	.95	.38	2	.29	.13
1.9	13	.72	.51	73	.74	.53	7	1.00	.37
2.0	9	.50	.60	99	1.00	.72	6	.86	.57
2.1	10	.56	.70	43	.43	.81	7	1.00	.80
2.2	9	.50	.79	43	.43	.89	5	.71	.97
2.3	1	.06	.80	23	.23	.94	1	.14	1.00
2.4	4	.22	.85	17	.17	.97	0	.00	1.00
2.5	4	.22	.89	6	.06	.98	0	.00	1.00
2.6	2	.11	.91	5	.05	.99	0	.00	1.00
2.7	2	.11	.93	2	.02	1.00	0	.00	1.00
2.8	2	.11	.95	1	.01	1.00	0	.00	1.00
2.9	2	.11	.97	0	.00	1.00	0	.00	1.00
3.0	0	.00	.17	0	.00	1.00	0	.00	1.00
3.1	1	.06	.98	1	.01	1.00	0	.00	1.00
3.2	0	.00	.98	0	.00	1.00	0	.00	1.00
Total	97			506			30		

Lithium p-bromophenacylsulfoacetate

size group	10 - 20 μ			20 - 30 μ		
S	N	RF	P	N	RF	P
1.0						
1.2						
1.3	5	.23	.04	1	.03	.01
1.4	3	.14	.07	1	.03	.02
1.5	5	.23	.12	4	.10	.05
1.6	17	.77	.27	10	.25	.14
1.7	14	.64	.39	21	.52	.33
1.8	22	1.00	.58	40	1.00	.68
1.9	22	1.00	.78	18	.45	.84
2.0	9	.41	.86	10	.25	.93
2.1	8	.36	.93	3	.07	.96
2.2	7	.32	.99	5	.13	1.00
2.3	0	.00	.99	0	.00	1.00
2.4	1	.05	1.00	0	.00	1.00
2.5	0	.00	1.00	0	.00	1.00
Total	113			113		

TABLE A-3

Most Representative Droplet Diameter

Li-sulfoacetate ester	0 - 10μ	10 - 20μ	20 - 30μ
p-bromobenzyl		16	23
p-nitrophenacyl		16	23
p-nitrobenzyl	9.5	14	
p-bromophenacyl		17	23

TABLE A-4

Most Representative Rate of Change of Supersaturation

Li-sulfoacetate ester	0 - 10μ	10 - 20μ	20 30μ
p-bromobenzyl		.010	.014
p-nitrophenacyl		.008	.008
p-nitrobenzyl	.014	.018	
p-bromophenacyl		.024	.028

TABLE A-5

Results for the rate of nucleation

E17-LI+ SALT
RESULTS FOR THE RATE OF NUCLEATION

size range	S	LOG S	1/SQ LOG S	J	LOG J
10 - 20μ	1.8	2.553E-01	15.346	5.738E+04	4.759
	1.9	2.788E-01	12.869	1.426E+05	5.154
	2.0	3.010E-01	11.035	2.853E+05	5.455
	2.1	3.222E-01	9.632	4.782E+05	5.680
	2.2	3.424E-01	8.529	6.960E+05	5.843
	2.3	3.617E-01	7.643	1.003E+06	6.001
	2.4	3.802E-01	6.918	1.295E+06	6.112
	2.5	3.979E-01	6.315	1.554E+06	6.192
20 - 30μ	S	LOG S	1/SQ LOG S	J	LOG J
	1.7	2.304E-01	18.830	7.896E+03	3.897
	1.8	2.553E-01	15.346	2.655E+04	4.424
	1.9	2.788E-01	12.869	6.443E+04	4.809
	2.0	3.010E-01	11.035	1.245E+05	5.095
	2.1	3.222E-01	9.632	2.006E+05	5.302
	2.2	3.424E-01	8.529	2.961E+05	5.471
	2.3	3.617E-01	7.643	4.141E+05	5.617
	2.4	3.802E-01	6.918	5.756E+05	5.760

E14-LI+ SALT
RESULTS FOR THE RATE OF NUCLEATION

	S	LOG S	1/SQ LOG S	J	LOG J
10 - 20μ	1.2	7.918E-02	159.498	1.371E+04	4.137
	1.3	1.139E-01	77.023	8.988E+04	4.954
	1.4	1.461E-01	46.831	2.926E+05	5.466
	1.5	1.761E-01	32.250	6.314E+05	5.800
	1.6	2.041E-01	24.001	1.135E+06	6.055
	1.7	2.304E-01	18.830	1.958E+06	6.292
20 - 30μ	S	LOG S	1/SQ LOG S	J	LOG J
	1.1	4.139E-02	583.650	9.428E+02	2.974
	1.2	7.918E-02	159.498	1.293E+04	4.112
	1.3	1.139E-01	77.023	6.239E+04	4.795
	1.4	1.461E-01	46.831	1.685E+05	5.227
	1.5	1.761E-01	32.250	3.425E+05	5.535
	1.6	2.041E-01	24.001	7.221E+05	5.859

TABLE A-5
(continued)

E9-LI+ SALT
RESULTS FOR THE RATE OF NUCLEATION

size range	S	LOG S	1/SQ LOG S	J	LOG J
0 - 10μ	1.5	1.761E-01	32.250	1.522E+05	5.182
	1.6	2.041E-01	24.001	4.899E+05	5.690
	1.7	2.304E-01	18.830	1.187E+06	6.074
	1.8	2.553E-01	15.346	2.369E+06	6.374
	1.9	2.788E-01	12.869	3.810E+06	6.581
	2.0	3.010E-01	11.035	5.675E+06	6.754
10 - 20μ	S	LOG S	1/SQ LOG S	J	LOG J
	1.5	1.761E-01	32.250	3.646E+04	4.562
	1.6	2.041E-01	24.001	1.071E+05	5.030
	1.7	2.304E-01	18.830	2.068E+05	5.316
	1.8	2.553E-01	15.346	3.861E+05	5.587
	1.9	2.788E-01	12.869	6.187E+05	5.791
	2.0	3.010E-01	11.035	8.726E+05	5.941
	2.1	3.222E-01	9.632	1.160E+06	6.064
	2.2	3.424E-01	8.529	1.519E+06	6.181
	2.3	3.617E-01	7.643	1.914E+06	6.282

E13-LI+ SALT
RESULTS FOR THE RATE OF NUCLEATION

	S	LOG S	1/SQ LOG S	J	LOG J
10 - 20μ	1.5	1.761E-01	32.250	1.450E+05	5.161
	1.6	2.041E-01	24.001	2.874E+05	5.458
	1.7	2.304E-01	18.830	4.771E+05	5.679
	1.8	2.553E-01	15.346	7.447E+05	5.872
	1.9	2.788E-01	12.869	1.091E+06	6.038
	2.0	3.010E-01	11.035	1.433E+06	6.156
	2.1	3.222E-01	9.632	1.774E+06	6.249
	2.2	3.424E-01	8.529	2.430E+06	6.386
20 - 30μ	S	LOG S	1/SQ LOG S	J	LOG J
	1.5	1.761E-01	32.250	4.242E+04	4.628
	1.6	2.041E-01	24.001	1.308E+05	5.117
	1.7	2.304E-01	18.830	2.908E+05	5.464
	1.8	2.553E-01	15.346	5.274E+05	5.722
	1.9	2.788E-01	12.869	8.253E+05	5.917
	2.0	3.010E-01	11.035	1.234E+06	6.091
	2.1	3.222E-01	9.632	1.570E+06	6.196

KEY: E17 - p-bromobenzylsulfoacetate
E14 - p-nitrophenacylsulfoacetate
E 9 - p-nitrobenzylsulfoacetate
E13 - p-bromophenacylsulfoacetate

TABLE A-6

Least Squares Fit of log J vs $(\log S)^{-2}$

Li-sulfoacetate ester/	size group	0 - 10μ	10 - 20μ	20 - 30μ
p-bromobenzyl	slope		-1.59×10^{-1}	-1.55×10^{-1}
	intercept		7.21	6.81
p-nitrophenacyl	slope		-2.85×10^{-2}	-2.68×10^{-2}
	intercept		6.77	6.47
p-nitrobenzyl	slope	-8.8×10^{-2}	-8.46×10^{-2}	
	intercept	7.64	6.89	
p-bromophenacyl	slope		-6.69×10^{-2}	-6.96×10^{-2}
	intercept		6.91	6.82

LITERATURE CITED

1. Lowitz, J. T., (1795) ref. 4 of Dunning, loc. cit. ref. 19.
2. Fahrenheit, D. B., (1724) ref. 1 of Dunning, loc. cit. ref. 19.
3. Ostwald, W., (1897), (1900) ref. 18 of Dunning, loc. cit. ref. 19.
4. Von Weimarn, P. P., (1926) ref. 3 of Melia, loc. cit. ref. 20.
5. Dufour, L., (1863) ref. 29 of Dunning, loc. cit. ref. 19.
6. Turnbull, D., J. Appl. Phys. 20 (1949) 817.
7. Turnbull, D., J. Chem. Phys. 20 (1952) 411.
8. White, M. L., Frost, A. A., J. of Colloid Sci. 14 (1959) 247.
9. Velazquez, J. A., Hileman, O. E. Jr., Talanta 17 (1970) 623.
10. Reinitzer, F., (1888) ref. 1. of Gray, loc. cit. ref. 48.
11. Lehmann, O., (1889) ref. 2, 3 of Gray, loc. cit. ref. 48.
12. Tamman, G., (1901); Nernst, W. (1906); Quinke, F., (1894), ref. 8 Gray, loc. cit. ref. 48.
13. Volmer, M., (1945) ref. 7 of Melia, loc. cit. ref. 20.
14. Frenkel, J., (1946) ref. 9 of Melia, loc. cit. ref. 20.
15. Turnbull, D., "Solid State Physics", Academic Press, New York, 1956.
16. Nielsen, A. E. "Kinetics of Precipitation" MacMillan, New York, 1964.
17. Walton, A. G. "The Formation and Properties of Precipitates" Interscience Publishers, New York, 1967.
18. Strickland - Constable, R. F. "Crystallization", Academic Press, London, 1968.
19. Zettlemoyer, A. C. ed. "Nucleation", Marcel Dekker, New York, 1969.
20. Melia, T. P., J. Appl. Chem. 15 (1965) 345.
21. La Mer, V. K., Ind. Eng. Chem. 44 (1952) 1270.
22. Bradley, R. S., Quart. Revs. 5 (1951).315.
23. Holloman, J. H., Turnbull, D., Prog. Met. Phys. 4 (1953) 368.

24. Farkas, L., (1927) ref. 67 of Dunning, loc. cit. ref. 19.

25. Volmer, M., Weber, A.,(1926) ref. 64 of Dunning, loc. cit. ref. 19.

26. Becker, R., Doring, W., (1935) ref. 73 of Dunning, loc. cit. ref. 19.

27. Zeldovich, J. B., (1943) ref. 70 of Dunning, loc. cit., ref. 19.

28. White, G. M., J. Chem. Phys. 50 (1969) 4672.

29. Turnbull, D., Fisher, J. C., J. Chem Phys. 17 (1949), 71.

30. Irish, D. E. "Raman Spectral Studies of Electrolytes" Seminar, Dalhousie University, 1972.

31. Nielson, A. E., Acta. Chem. Scand. 15 (1961) 441.

32. Bempah, O. A. Ph. D. Thesis, McMaster University, 1972.

33. Walton, A. G., loc. cit. ref. 19, pp. 256 - 257.

34. Binsbergen, F. L., Kolloid-Zeitschrift, Zeitschrift fur Polymere 237 (1970) 289.

35. Binsbergen, F. L., J. Cryst. Growth. 13/14 (1972) 44.

36. Lothe, J., Pound, G. M., loc. cit. ref. 19, pp. 109 - 149.

37. Melia, T. P., Moffitt, W. P., Nature 201 (1964) 1024.

38. Daee, M., Lund, L. H., Plummer. P. L. M., Kassner, J. L., Hale, B. N., J. Colloid and Interface Sci. 39 (1972) 65.

39. Nielson, A. E., Acta. Chem. Scand. 15 (1961) 441.

40. Vonnegut, B., J. Colloid Sci. 3 (1948) 563.

41. Nielson, A. E., Sarig, S., J. Cryst. Growth 8 (1971) 1.

42. Hanna, J. D., Hileman, O. E. Jr., Talanta 19 (1972) 894.

43. Hanna, J. D., Hileman, O. E. Jr., Can. J. Chem. 50 (1972) 2859.

44. Turnbull, D., J. Chem. Phys. 18 (1950) 768.

45. Melia, T. P., Moffitt, W. P., J. Colloid Sci. 19 (1964) 433.

46. Velazquez, J. A., Hileman, O. E. Jr., Can. J. Chem. 48 (1970) 2896.

47. Bempah, O. A., Hileman, O. E. Jr., Can. J. Chem. (1972) in press.

48. Bigg, E. K., Proc. Phys. Soc. B. 66 (1953) 688.

49. Carte, A. E., Proc. Phys. Soc. (London) B73 (1959) 324.

50. Gray, G. W., "Molecular Structure and the Properties of Liquid Crystals" Academic Press, New York, 1962.

51. Winsor, P. A., Chem. Rev. 68 (1968) 1.

52. Cameron, J. (1888) ref. 5 of Rosevear loc. cit. ref. 61.

53. McBain, J. W., Langdon, G. M., (1926) ref. 43 of Rosevear loc. cit. ref. 61.

54. Hartshorne, N. H., Stuart, A., "Crystals and the Polarizing Microscope" American Elsevier, New York, 1970 p. 503 ff.

55. Hartley, G. S., (1936) ref. 37 of Winsor loc. cit. ref. 49.

56. Clunie, J. S., Corkill, J. M., Goodman, J. F., Proc. Roy. Soc. (London) 285 (1965) 520.

57. Ostwald, W., (1931) ref. 43 of Clunie loc. cit. ref. 54.

58. Luzzati, V., Mustacchi, H., Skoulios, A., Disc. Faraday Soc. 25 (1958) 43.

59. Luzzati, V., Husson, F., J. Cell Biol. 12 (1967) 409.

60. Luzzati, V., Tardieu, A., Gulik-Krzywicki, T., Rivas, E., Reiss-Husson, F., Nature 220 (1968) 485.

61. Gilchrist, C. A., Rogers, J., Steel, G., Vaal, E. G., Winsor, P. A., J. Colloid and Interface Sci. 25 (1967) 409.

62. Brown, G. H., Dienes, G. J., Labes, M. M. "Liquid Crystals" Gordon and Breach, London, 1966.

63. Rosevear, F. B., J. Am. Oil Chem. Soc. 31 (1954) 628.

64. Brown, G. H., Shaw, W. G., Chem Rev. 57 (1957) 1049.

65. Shriner, R. L., Fuson, R. C., Curtin, D. Y., "The Systematic Identification of Organic Compounds", Wiley, New York, 1965.

66. Sears, G. W., J. Phys. Chem. 65 (1961) 1738.

67. Mocadlo, S. E., M. Sc. Thesis, Case Institute of Technology, 1968.

68. Velazquez, J. A. Ph. D. Thesis, McMaster University, 1970.

69. Wood, G. R., Walton, A. G., J. of Appl. Physics. 41 (1970) 3027.

70. Kuhns, I. E., Mason, B. J., Proc. Roy. Soc. A. (London) 302 (1968) 437.

71. Pochan, J. M., Gibson, H. W., J. Amer. Chem. Soc. 93 (1971) 1279.

72. Pochan, J. M., Gibson, H. W., J. Amer. Chem. Soc. 94 (1972) 5573.